NUREG/CR-1437
BNL-NUREG-51185
AN, R-2

TWO-PHASE FLOW MEASUREMENT TECHNIQUES IN GAS-LIQUID SYSTEMS

OWEN C. JONES, JR.

THERMAL HYDRAULIC DEVELOPMENT DIVISION
DEPARTMENT OF NUCLEAR ENERGY
BROOKHAVEN NATIONAL LABORATORY
ASSOCIATED UNVERSITIES, INC.
UPTON, NEW YORK 11973

PREPARED FOR THE UNITED STATES NUCLEAR REGULATORY COMMISSION
OFFICE OF NUCLEAR REGULATORY RESEARCH
UNDER CONTRACT NO. DE-AC02-76CH00016
NRC FIN NO. A-3045

ABSTRACT

A detailed summary of two-phase, gas-liquid measurement techniques is presented directed at the graduate engineer or practicing engineer as a refresher. Neither is expected to have any detailed knowledge of the mechanics of multiphase flows, but a working feeling for electromechanical methods is taken for granted. Starting with a brief description which places the field in perspective from a scientific standpoint as well as from an application viewpoint, both electronic and mechanical devices for taking internal diagnostic measurements and devices for obtaining measurements ments from outside the flow field are discussed. Recent advances which are expected to have significant impact on the use or interpretation of classical methods are also covered.

TABLE OF CONTENTS

TABLE OF CONTENTS (Continued)

LIST OF FIGURES

LIST OF FIGURES (Continued)

No. Page

LIST OF FIGURES (Continued)

LIST OF FIGURES (Continued)

LIST OF TABLES

1. INTRODUCTION

In the past 30 years, the advent of new chemical processing systems, modern power generation methods, and space propulsion devices have dealt increasingly with multiphase flows. This is especially true of nuclear reactor systems where off-normal and accident situations have been intensively studied to provide assurance of public safety under extreme conditions. In the future development of advanced energy systems, multiphase flows will play yet an increasing role due to the attractiveness of utilizing the latent heat of phase change to enhance the energy intensiveness of these systems. Currently, for instance, two-phase, gas-liquid flows are found in such diverse systems as ocean thermal energy conversion equipment, liquid metal magnetohydrodynamic generators, geothermal wells and turbine generating equipment, oil-gas pipelines, boilers, nuclear reactor systems, liquid metal blankets of fusion power systems, droplet combustors, distillation towers, turbomachinery, refrigeration systems, and coal liquifaction systems, to name just a few.

The overriding conclusion one draws from an examination of two-phase flow literature is that multiphase flow is such an exceedingly complex physical situation that practically no general analytical effort has had an impact on this field. Empiricism abounds. Experimental methods have been both borrowed from other fields and newly developed to allow examination of just one or two areas of the phenomena. Workers in general are in the position of the blind men attempting to describe an elephant by feel. One has hold of its trunk, another its leg, and yet a third the tail. Each arrives at a different conclusion due to his own vantage point, and none perceives the elephant as a whole.

In attempting to piece together the differing viewpoints, several facts come to mind. Like the experience of early workers in single-phase fluid mechanics, the overall picture remains elusive due to lack of insight into the intracies of the phenomena involved. When the experiments of J. Osborne Reynolds demonstrated the two major categories of single-phase flow fields, significant progress was then made in piecing together various conflicting results. Similarly, in two-phase flow, while people are cognizant of the vagaries of laminar versus turbulent conditions, few have paid more than lip service to other areas of demarcation. Flow regimes are of overriding importance. One would not expect the same equations to accurately describe pressure drop in both laminar and turbulent flow. No one would then expect a single equation to do the same for completely different two-phase regimes. And in fact virtually no distinction between two-phase flows of laminar or turbulent character has been seriously considered.

Many workers are still trying to treat this phenomenon as a single-phase fluid. It is not. Two-phase immiscible fluids are decidedly different. They behave differently. They are not generally microscopic intramixtures but are macroscopic conglomorations. Formulations and methodology based on single-phase technology can only be of limited utility. In the final analysis, new methods, new viewpoints, and new technology must be developed. We must view the entire field from as many points of view as possible in hopes of determining the true characteristics of two-phase flow.

Realizing that two fluids flowing together are different we must ask how they differ from a single fluid flowing in a pipe. First, one phase is usually lighter than the other, the result being diffusion of one fluid with respect to the other. This is due in part to Archimedes principal, a principal almost as old in concept as the study of fluid mechanics itself. This is basic. The relative movement of one fluid with respect to the other depends on the individual phase flow rates as related through the void fraction. No one would think of running a basic single-phase experiment without measuring the flow rates. But for two-phases, the void fraction is just as basic a parameter as the flow rates. No basic experiment in two-phase flow should be run without measuring the void fraction and phase flow rates where possible as an absolute minimum.

The need for determining the void fraction, that is the area or volume fraction of the flow occupied by the vapor phase, has beren widely recognized and has led to the development of numerous methods to obtain these measurements. Briefly, these methods may be divided into four general categories, depending on the spatial scale in relation to the duct size over which measurements are taken. The categories include:

a) Point average probe insertion techniques such as conductivity probes used by Neal [153], hot film anemometers used by Hsu, Simon, and Grahm [68], and impedance probes used by Bencze and Orbeck [63]. These will be discussed in Section 3.

b) Chordal average void measurements commonly obtained through the use of particle or photon beam attenuation techniques. These methods were used by Cravarolo and Hassid [154], Petrick [155], and Pike, Wilkinson, and Ward [156], and will be discussed in Section 5.

c) Area or small-volume average void fraction measurements by such means as impedance sensing devices similar to those employed by Orbeck [64], and Cimorelli and Premoli [66] (Section 3) or flow sampling devices (Section 4).

d) Large-volume average such as accomplished by Lockhart and Martinelli [151], and by Hewitt, King and Lovegrove [152], through the use of quick-closing valves at various points in a tube but not to be discussed hereing.

The methods listed above and the techniques employed are by no means exhaustive. Many will be discussed in what follows. The interested reader is directed to an excellent survey of the field of void fraction measurement compiled by Gouse [157] and published in April, 1964.

A second way in which two-phase flow differs from single-phase flow is due to the immiscibility of the phases, each separated from the other by interfaces. It can be shown that the existance of these interfaces, their number and location, are of fundamental importance in the analytical description of the movement of two-phase flows. Hydrodynamic and thermal transfer and relaxation phenomena in two-phase, gas-liquid flows, in addition to being dependent on the departure from equilibrium for phase interactions, are strongly dependent on the interfacial area density available for transfer to occur [1-3]. Such

interactions include mass, momentum, and energy exchange for which both the transfer coefficients and the areas available for transfer must be known accurately in order to specify transfers based on driving potential [4]. For instance, closure of a problem involving mass transfer between the phases requires specification of the volumetric vapor generation rate, Γ_v, in order to predict the vapor volume growth rates. Vapor generation rates are usually calculated in general terms by means of a constitutive relation given by [1]

$$\Gamma_v = \frac{1}{A\Delta i_{fg}} \int_{\xi_i} \sum_{k=\ell,v} \vec{q}''_k \cdot \vec{n}_k \frac{dA_i}{dz} \qquad (1)$$

where surface tension, shear, and relative kinetic energy effects are considered negligible. In this case the net heat flux to the interface is given by the summation of the normal phase fluxes $\vec{q}''_k \cdot \vec{n}_k$ at the point on the interface A_i having a density of dA_i/Adz. The interaction then sums the effects over all interfaces in A along the interfacial perimeter ξ_i. Similarly, specification of the momentum transfer between phases is important in prediction of the relative velocity between phases which is needed to couple void fraction to the quality in two-phase flows. The latter is especially important under low velocity situations such as with natural convective flows, or under conditions of countercurrent flows. The degree of momentum transfer and hence the relative velocity is very sensitive to the flow regime. In highly coupled flows such as bubbly and slug flows the transfer rates are high and relative velocities are low. Conversely, in weakly coupled flows such as in the annular or droplet regimes, momentum transfer is small and the relative velocities can be quite large [2]. In both cases, a knowledge of the interfacial area density is required. Thus basic experiments should also include some method of monitoring the passage and density of interfaces.

Is this sufficient? Certainly measurements of the gross flows in basic single-phase work were insufficient. Detailed velocity profiles were required as confirmation of theoretical models. It can be likewise assumed that both void and velocity profiles as well as interfacial area density profiles would be eventually required for analysis of two-phase flows. Likewise, different pressures are considered as essential measurements coupled with measurements relating to the frequency of void appearance. Lastly, as a minimum, certain characteristics of the flow must be identified as related to the structural behavior of the mixture, and levels of turbulance should be determined.

As in most other areas of scientific endeavour, purely theoretical analysis and prediction of the behavior of gas-liquid systems such as suggested above is clearly inadequate. Rather, experimental and analytical efforts must go hand-in-hand. While development of single-phase thermo-fluid measurement techniques has been intensively pursued during the last century, special problems are encountered in attempting to observe mixtures of fluids and it has been only over the last two to three decades that these problems have been considered. Measurements in two-phase, gas-liquid systems is very much still in the empirical stage. Researchers generally try to find something which "wiggles when tickled" and then try to calibrate and interpret the response. In short, it can be said that measurements in two-phase, gas-liquid systems carry all the

complexities of similar measurements in single-phase systems plus additional difficulties, some of which are itemized below.

a) Interface deformation due to sensor presence causes temporal distortion of the true pointwise behavior. Unequal distortions are generally observed in going from gas-to-liquid rather than from liquid-to-gas.

b) Inadequate transference from liquid-phase response to gas-phase response due to film retention, causes bias in resulting interpretation unless precautions are taken.

c) Destruction of metastability due to sensor presence, which, for instance, causes cavitation on a thermal probe which may then record saturation rather than superheat conditions.

d) Inaccurate response of pressure tap lines may result due to liquid vapor interfaces caused by gas entrapment or flashing. The former can occur in two component systems even in steady flow conditions due to the normal fluctuations while the latter can occur due to rapid decompression in heated lines during transients.

e) Improper averaging of nonlinear signals occurring due to fluctuations, with or without consideration of damping factors, causes intepretation errors.

f) Errors due to distortion of signals due to the transmitting medium environment such as the shunting effects in sheathed, high temperature thermocouples.

g) Simple lack of understanding of the physical phenomena affecting a sensor response mass lead to misinterpretation of the results.

There have been several excellent summaries of two-phase measurement techniques written previously for steady state measurements [5-8] and for transient or statistical techniques [9-10]. The purpose of this summary is to combine the techniques developed to date into a coherrent form suitable for a short, first graduate level, tutorial on modern methods.

This presentation will be divided into the following three sections:

1. Instream Electrical Sampling Techiques

2. Instream Mechanical Sampling Techniques

3. Global Sampling Techiques

2. TWO-PHASE, GAS-LIQUID FLOW PATTERNS

Since the entire thrust of this document is directed towards making measurements in two-phase flows, it is appropriate to briefly describe the basic configurations or patterns which these flows can attain.

Just as in single phase flows, there can be two different regimes within which different descriptions of momentum and heat transfer apply, so too in two-phase flows do we find laminar and turbulent situations. Unfortunately, at this stage, any distinctions made on the basis of these two classifications are purely qualitative. Rather, the major distinctions, which have been used, and which are probably the first order contributors to system behavior, are space-time phase distributions. These can probably be best described as a sequence of developing situations within a vertical tube evaporator.

As described by Collier [11] and shown in Figure 1, the changes with vertical upflow of an initially all liquid system are mainly due to "departure from thermodynamic equilibrium coupled with the presence of radial temperature profiles and departure from hydrodynamic equilibrium throughout the channel."

In the initial single-phase region the liquid is being heated to the saturation temperature. A thermal boundary layer forms at the wall and a radial temperature profile is set up. At some position up the tube the wall temperature will exceed the saturation temperature and the conditions for the formation of vapor (nucleation) at the wall are satisfied. Vapor is formed at preferred positions or sites on the surface of the tube. Vapor bubbles grow from these sites finally detaching to form a "bubbly flow."

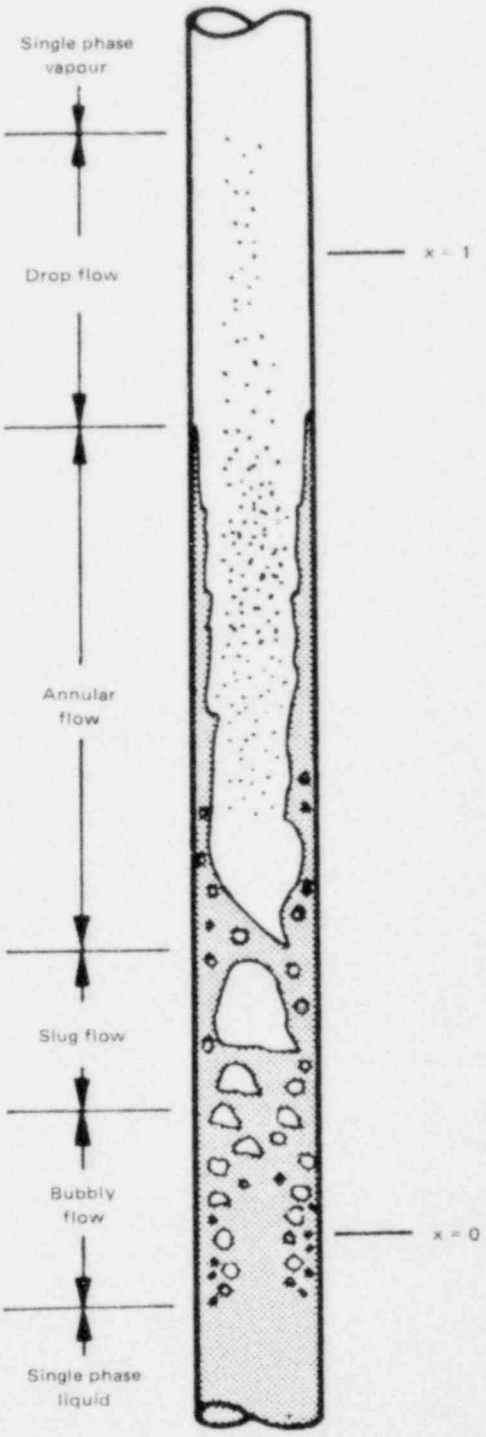

Figure 1 - Flow Patterns in a Vertical Evaporator Tube [11] (BNL Neg. No. 9-136-79)

With the production of more vapour due to continued heat addition, the bubble population increases with length and coalescence takes place to form slug flow which in turn gives way to annular flow as the elongated bubbles increase in length and merge further along the channel. Close to this point the formation of vapour at sites on the wall may cease and further vapour formation will be as a result of evaporation at the liquid film-vapour core interface. Increasing velocities in the vapour core will cause entrainment of liquid from the surface waves on the film which result in of droplets in the central vapor stream. The depletion of the liquid from the film by this entrainment and by evaporation finally causes the film to dry out completely. Droplets continue to exist, some of which may even be remnants of the upstream destructing of liquid slugs, and are slowly evaporated until only single-phase vapour is present. While this description presents a commonly perceived and encountered evolution of flow patterns in a heated duct, it should be kept in mind that these patterns may, in fact, be encountered in other situations and evolved differently.

From a researcher's viewpoint, then, for both analytical and experimental purposes, the phenomena of interest are generally associated with those detailed characteristics which distinguish one pattern from another. Of course, as in single phase flow, temperature, pressure, velocity and mass flow rates are of interest. In addition, specific items which deal with particular aspects include:

a) Bubbly flows: boiling inception, bubble size, bubble trajectory, bubble boundary layer thickness, liquid superheat, bubble agglomeration.

b) Slug flows: Slug lengths, bubble sizes, bubble spacings, film thicknesses, vapor entrainment, bubble velocity, slug velocity.

c) Annular flows: wave height, wave length, wave celerity, film thickness, film velocity, entrainment rate, de-etrainment rate.

d) Drop flows: dryout inception, drop size, drop trajectories, drop impingement.

In all cases, departures from mechanical or thermal equilibrium as evidenced by relative velocities of one phase with respect to the other and by differences between phase temperatures are important variables both for design and analysis as they can affect operating conditions of engineering equipment. Phase residence time fractions at a point in space and volume fractions at an instant in time as well as the distributions and alternate averages of each, are of overriding importance and interest. The balance of this report is devoted to describing methods of obtaining the measurements identified above.

3. INSTREAM SENSORS WITH ELECTRICAL OUTPUT

3.1. Conductivity Devices

The general principle of operation for conductivity sensing devices is for two electrodes to be immersed in a two-phase mixture. A potential difference is created between the two electrodes so that the current flow is a direct measurement of the conductivity of the fluid between the two electrodes. This

current flow may be measured by means of a voltage drop across a calibrated resistor connected to some steady state or transient measuring device, such as an oscilloscope, oscillograph, or recording voltmeter. Within certain limits, the relative amounts of conducting and non-conducting fluid, in other words the amounts of liquid and gas, will determine the amount of current flow between the two electrodes. In this manner, current may be calibrated as a function of the vapor fraction and/or phase distribution between the two electrodes. (These devices may also be used in the impedance mode where the capacitive reactance is the primary variable but they will still be called conductivity devices). Such devices may be used for indications or measurements of void fraction, liquid level, film thickness, flow patterns and, with some modifications, can be arranged to give quantitative information on wave frequencies, heights and velocities.

Level probe. Figure 2 shows an early liquid level transducer, designed and built by Kordyban and Ranov [12], for use in their air-water experiments. This probe consisted of a pair of insulated copper wires inserted through a hypodermic tubing coated with insulating paint. The wire ends were stripped of insulation and attached to the outside of the hypodermic needle tubing, thus being electrically insulated from themselves and from the tubing. When a potential was placed between the two wires, the amount of current flow was then a mea-sure of the percentage of the sensing element covered by the conducting fluid. These transducers were used in series along the test section to measure the time interval of slug travel between sensing stations in order to obtain the velocitiy of slugs and variations along the length of the tube. The authors were also able to use the transducer to make qualitative measurements of flow regime within their horizontal tube. Figure 3 shows a typical output trace from a pair of transducers located 20 inches apart in the horizontal tube during conditions of slug flow. Not only was the passage of slugs immediately evident from the trace, but also when the two traces are compared they show that the flow regimes retained their identity along the 20 inch length so that slug velocities could immediately be measured. Kordyban and Ranov mention that "the main difficulty with the transducers . . . was the fact that the exposed copper electrodes deteriorated gradually, affecting the range and linearity of output and require frequent cleaning and recalibration." In addition, 60 cycle noise on the transducer output made measurements difficult.

Needle probes. The needle type conductance probe as designed by Solomon [13] was further developed and used by Griffith [14], Neal and Bankoff [15] and by Nassos [16]. This needle probe, shown schematically in Figure 4, consisted of a single 0.8 mm diameter steel wire completely insulated and bent at an angle of 90°, giving a point of ~30 mm length. This needle formed the ungrounded conductor in a conductivity measurement system. The probe was inserted into a tube such that the point was aligned parallel to and opposing the flow streams. The non-insulated tip of the probe, when im-mersed in a conducting medium, would allow current to travel between the tip and a grounded electrode imbedded in the tube wall. Thus, the distribution of fluid between the probe tip and the

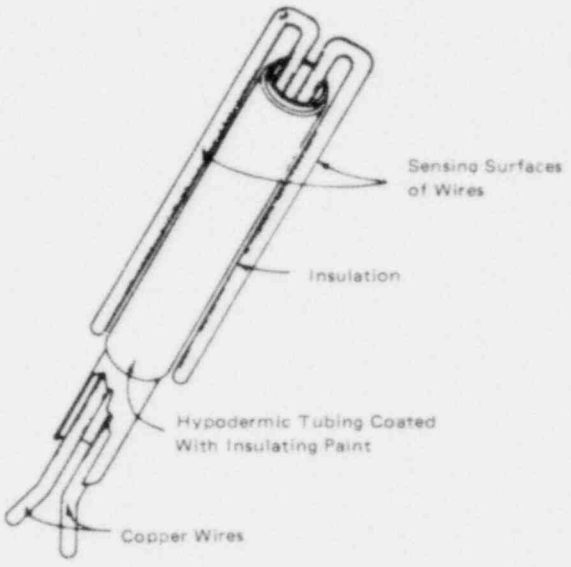

Figure 2 - Liquid Level Transducer of Kordyban and Ranov [12] (BNL Neg. No. 9-89-79)

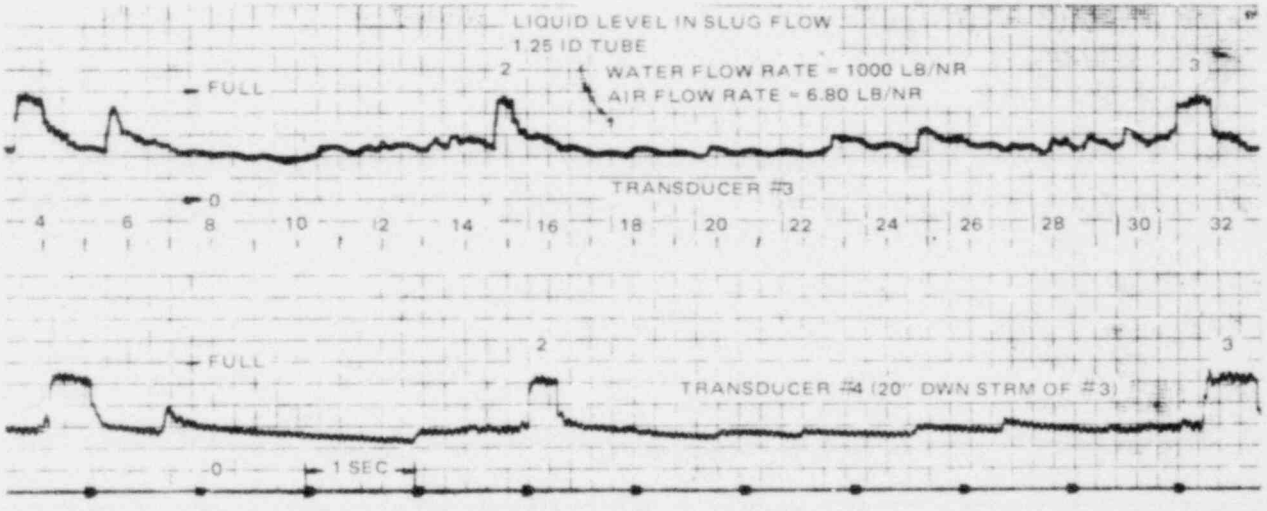

Figure 3 - Liquid Level Readings from Two Transducers at Different Axial Locations [12]. (BNL Neg. No. 9-93-79)

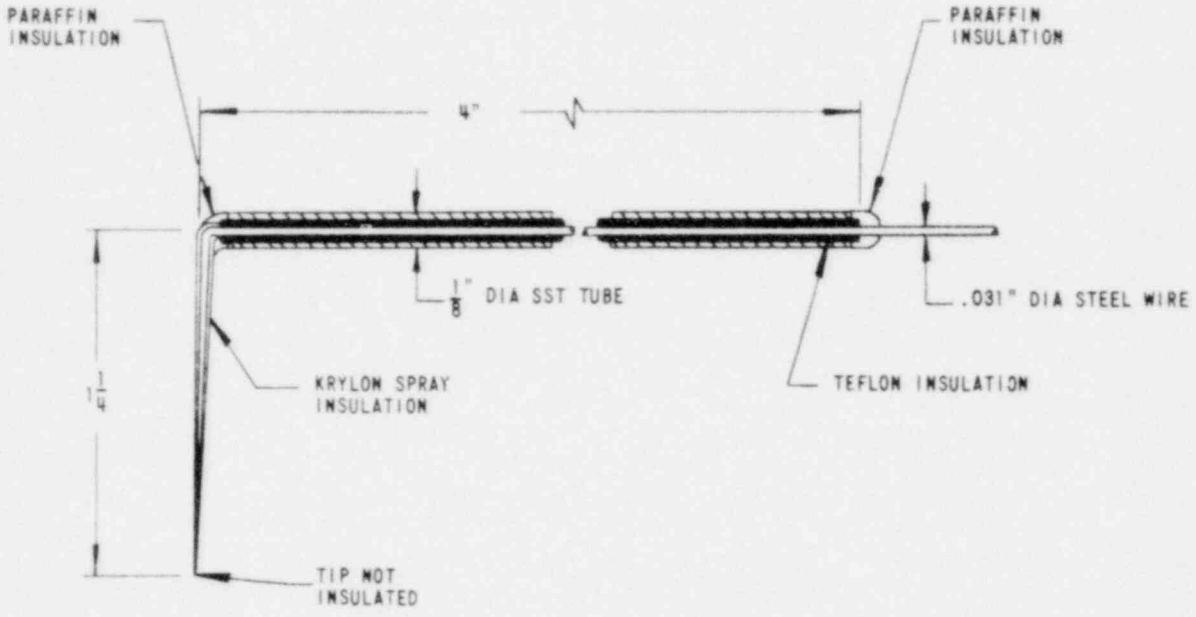

Figure 4 - Electrical Conductivity Probe Developed by Soloman [13]
(BNL Neg. No. 9-99-79)

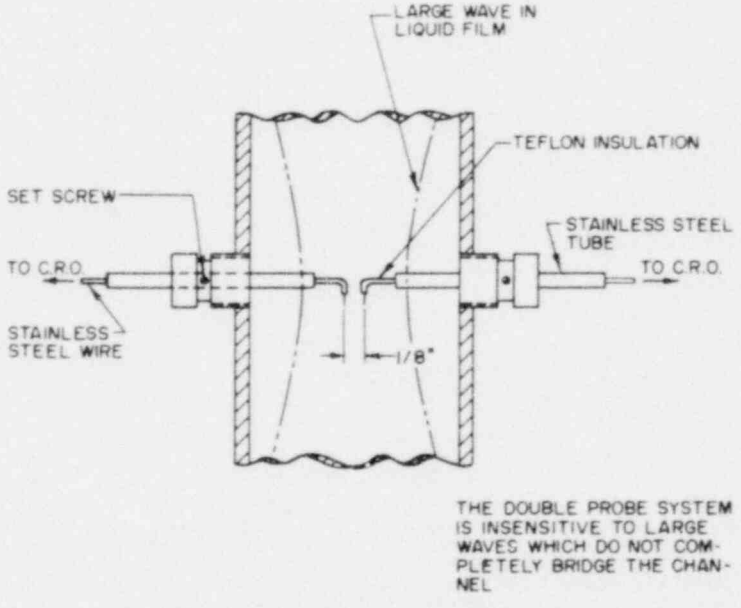

Figure 5 - Double Conductivity Probe Arrangement tried by Wallis [17]
(BNL Neg. No. 9-120-79)

grounded conductor on the wall determined the amount of electric current flow. In this manner, information on the distribution, number and velocity of bridges of liquid traveling in the tube, as well as qualitative information on flow regime, could be determined. This type of instrument seems also readily adaptable for the qualitative determination of the transition between slug flow and annular flow. Further, Neal and Bankoff describe a method of using this type of probe for the determination of local void fractions in mercury-nitrogen flow [15]. The non-wetting characteristics of mercury made nearly instantaneous make and break contacts possible, such that there was no surface tension effect on void fraction measurements. Nassos, on the other hand, when attempting to adapt this to an air-water system, experienced difficulty due to the surface tension effects at low temperature [16], which today are well accepted. In other words, when entering a small void, the gas phase would deform, keeping the probe tip within the conducting medium. Thus, the measurements for vapor fractions were low. Nassos stated that some improvement was obtained by means of a separate triggering device but the calculated vapor fractions were still somewhat lower when compared with gamma-ray attenuation measurements.

Wallis [17] used a similar mechanism where, instead of having the ground electrode attached flush to the inside tube surface, a duplicate probe was inserted from the opposite wall, as shown in Figure 5. The principle of operation was exactly the same as that used in the Nassos probe and in Kordyban and Ranov's probe except for the fact that the liquid bridge must be between the two electrodes which can be placed at any point covering any amount of the channel diameter. An interesting fact arose in Wallis' experiments. When he compared data on the transition between slug flow and annular flow with the Nassos-type probe on the one hand, and his double probe on the other hand, in all cases having similar conditions in the test assembly and the same transition criteria, he found a definite discrepancy between the two sets of data as shown in Figure 6. The discrepancy was due to the way in which the slug-annular transition was defined, both conceptually and implicitly through the type of instrumentation used. Certainly if a liquid conduction path exists between the tube centerline and the wall, and if the signal is a pure binary signal regardless of the path, then there should be no difference between transition from one probe and another. However, if large globules of liquid float down the core of the pipe in annular flow, these would appear to be bridges to the dual sensor but not be seen by the single probe. Conversely, if the conductance path for the single probe is tortuous, and the signal not truly binary in nature, then subjectiveness on the part of the observer and arbitrariness must result in variations in one's estimation of transition over another. In spite of these drawbacks, a number of other workers have used both the single wire probe [18-23] and the double probe [24-26], mainly due to its simplicity.

Considerable other information may be obtained from conductivity devices. If local velocity is obtained, bubble diameter distributions can also be measured [48-50] as well as gas and liquid slug lengths [48]. Uga [51] obtained histograms of bubble sizes in the riser and downcomer sections of a BWR. However, he used average values of bubble velocities rather than instantaneous values corresponding to the dewetting signals so that his size distributions were really normalized inverse dry-time distributions where a constant value of

velocity was the normalized factor. Similarly, Ibragimov et al. [52] used miniature traversing probes to obtain bubble frequency profiles in water-nitrogen flow similar to those obtained by Jones [53] with the anemometer. Sekoguchi et al. [49] reported histograms of bubble sizes using a double-tipped probe with tips 4 mm apart and 30 μm in dia. Using the transport time averaged over 10 observations, the bubble rise velocity was obtained which was then used to obtain the bubble size from the dewetting time. Similar to the method of Uga [51], this method requires the assumption that there is no correlation between bubble size and rise velocity. While this may be true for the > 1 mm bubble observed by Sekoguchi [49], it certainly is not in general. It is interesting to note, however, that these workers obtained excellent agreement between void residence time profile and the volume fraction profile calculated from the bubble diameter and frequency measurements, in agreement with the theoretical analysis by Serizawa [54] for long sampling times.

In their studies of thin film characteristics of annular two-phase flow, Telles & Dukler [55], Dukler [56], and Chu & Dukler [57] have used the straight electrical probe to determine information on wave structure. Such information has included probability density functions for wave height where the contributions due to the film substrate and due to large waves have been identified along with wave frequency. Also the spectral and cross spectral densities of film thickness fluctuations were determined.

Other statistical data can be obtained by using a double probe. Several authors tentatively described the granulometry of bubble flows with sophisticated models [51, 58, 54]. A bubble displacement velocity has also been looked for by the same authors and also by Lecroart & Porte [59], Kobayasi [40], and Galaup [50].

Transport methods have now begun to be utilized to obtain velocity information, although no author to date has specifically identified recognition that the correlated quantity is interfacial passage so that the velocities thus obtained are interfacial velocities. Serizawa [54], using a double-tip probe with tips 5 mm apart utilized both correlation and pulse-height methods to determine bubble velocity spectrums. Correlation of the outputs of the two probes after passing through Schmitt triggers provides a function which exhibits a well defined maximum at a time delay corresponding to the transport time between probes. Dispersion of the amplitude of the correlation function is representative of the probability distribution of this velocity, and hence of the fluctuations. Also, by using one probe signal as a starter and the other as a stopper, ramp functions are generated during the transport time which, when stopped and differentiated yield pulses whose heights are proportional to the transport time delay. Height analysis of this pulse train is assumed to yield the bubble velocity spectra.

Wall probes. A second type of conductivity instrument is a flush-mounted type developed at the Atomic Energy Research Establishment (AERE) at Harwell, England, and used in a number of studies in that Laboratory [27-32]. This device, which is shown in Figure 7, can be mounted for use in both tubes and rods. The operational principle is similar to that previously discussed, except for the fact that a high frequency alternating current (AC) carrier is used. Thus, when the probes are covered by a thin liquid film, the signal is

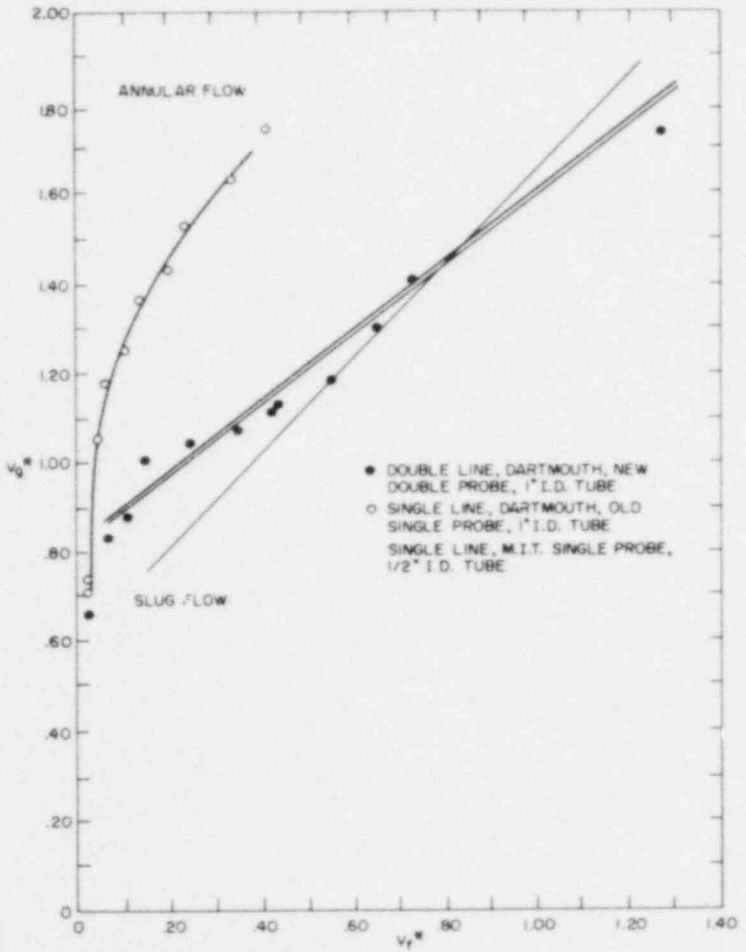

Figure 6 - Comparison of the Slug-Annular Flow Transition as Determined by the Single Conductivity Probe and by the Double Probe Method. (BNL Neg. No. 9-108-79)

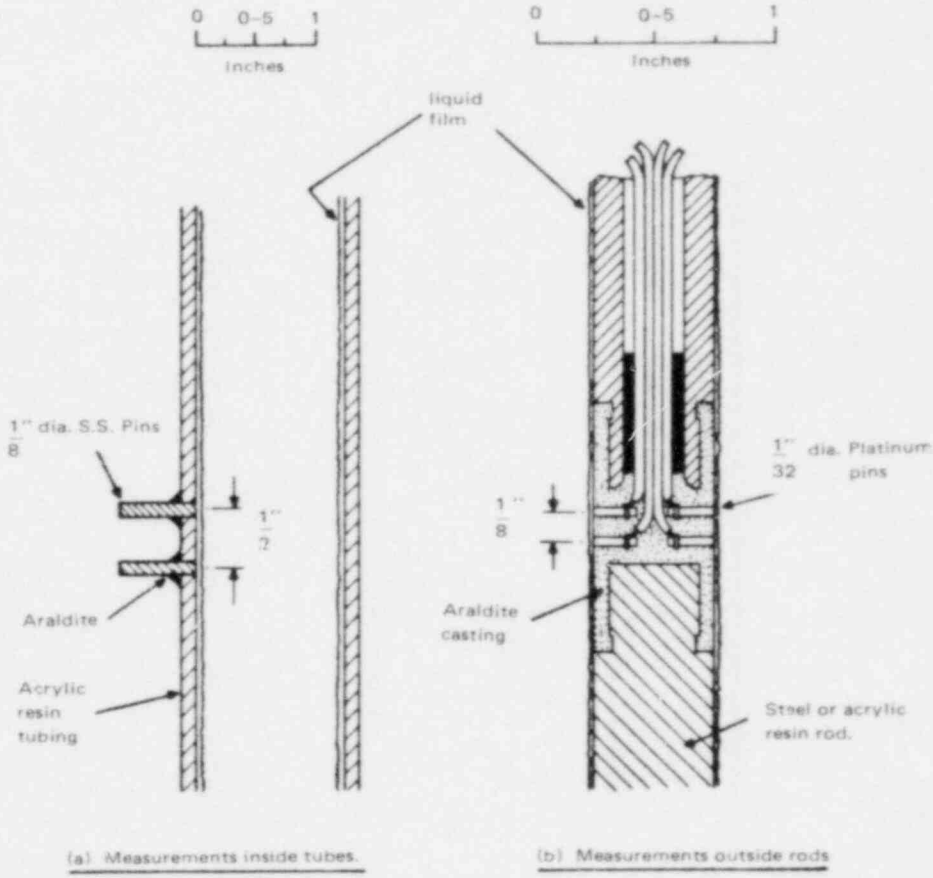

Figure 7 - Installation Characteristics of the Harwell Flush-Mounted Conductance Probes. (BNL Neg. No. 9-90-79)

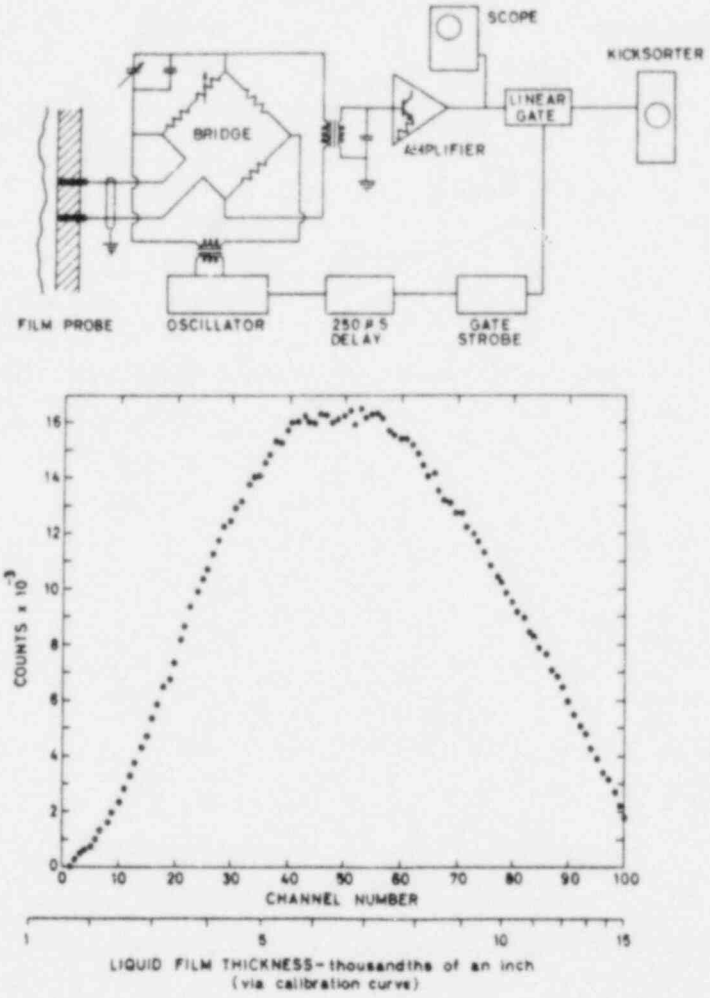

Figure 8 - Kicksorter Circuit and Representative Liquid Film Amplitude Distribution [33]. (BNL Neg. No. 9-97-79)

amplitude-modulated by the film itself, such that the output is related uniquely to the film thickness. This type of probe was used to determine the transition between slug and annular flow and to measure film thicknesses in annular flow when the probes are calibrated. A similar type of sensing device was also used at AECL in Canada [33, 34] where a kicksorter circuit, shown in Figure 8, was used to ignore all waves of thicknesses less than a predetermined value. In this manner, a wave thickness spectrum may be determined. The signal can also be halfwave rectified as shown in Figure 9 and combined as shown in Figure 10, such that the recordings from four separate measuring stations could be obtained simultaneously on, ray, a dual-beam oscilloscope [35]. Then, by comparing the outputs from probes at different stations, and keeping in mind that the flow patterns tend to retain their identity along the length of the tube, the velocities and frequencies of the waves may be determined.

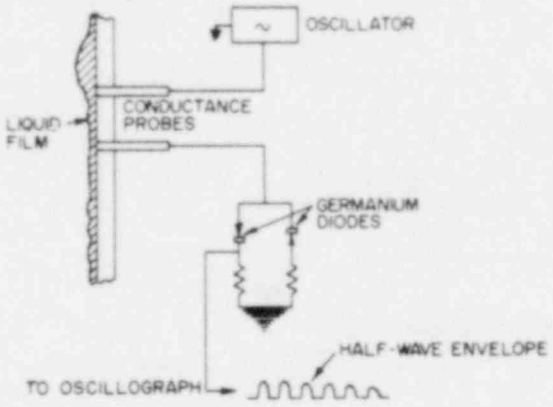

Figure 9 - Method of Half-Wave Rectification for Recording of Multiple Signals [35]. (BNL Neg. No. 9-113-79)

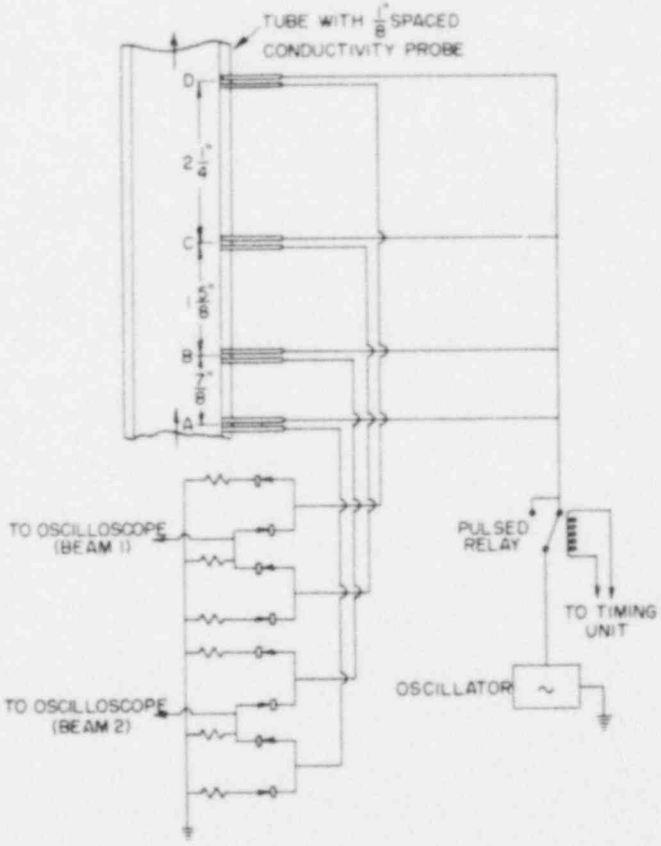

Figure 10 - Probes and Circuit for Multiple Probe Recording [35]. (BNL Neg. No. 9-105-79)

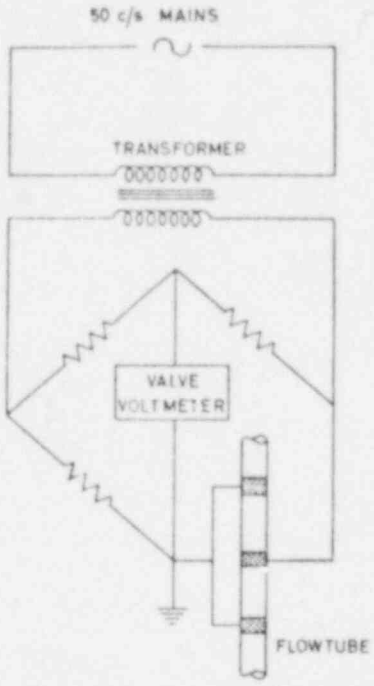

Figure 11 - Schematic of Film Conductance Method Developed at C.I.S.E. (Ref. 36) (BNL Neg. No. 9-86-79)

Another type of surface conductance probe was developed at Centro Informazione Studi Esperienze (CISE) [36]. As shown in Figure 11, the tube is entirely surrounded at various axial locations by metal rings flush with the inner tube surface. Whenever a potential is generated between any two rings, the conductance will be a function of the amount of fluid between the rings. However, this type of instrument is insensitive in annular flow to rapid changes in film thickness and high, sharply peaked waves. Reference 37 describes a test assembly shown in Figure 12 which was used to compare both the AERE and CISE type conductance probes. In addition to insertions of both the CISE and AERE conductance devices, the test assembly contained quick-acting, simultaneously operated valves on both ends which enabled the air water mixture to be completely isolated so that a measurement of the total amounts of each phase could be made. The results from these tests are shown in Figure 13. In this figure, several things are immediately evident. First, the CISE probe gave measurements definitely lower than those produced by the AERE instrument. This is probably due to the fact that the CISE probe is not sensitive to sharp or high wave peaks thereby underestimating the average film thickness. This is evidenced by the approach of the CISE data to the AERE data with increasing film thickness, i.e., where the wave peaks start to make less and less difference in the overall film thickness. Secondly, the holdup method appears to show film thicknesses which are larger on the average than the AERE measurements. This is

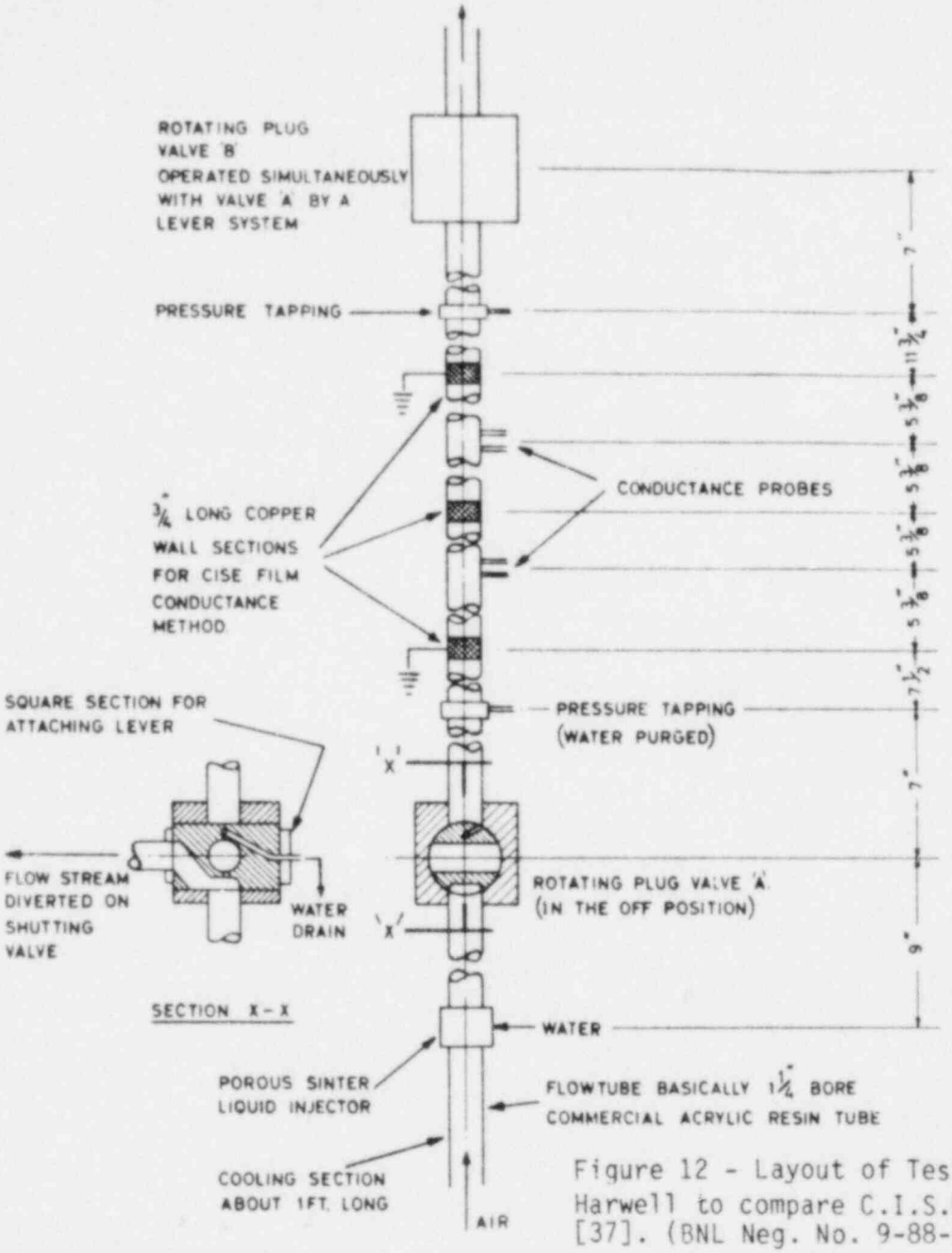

Figure 12 - Layout of Test Assembly used at Harwell to compare C.I.S.E. and Harwell Probes [37]. (BNL Neg. No. 9-88-79)

because the holdup method not only measures the liquid in the film itself, but also that the liquid which has been entrained in the gaseous core. In some instances, a large amount of the total liquid in the system is in the form of entrained droplets. Thus, any film thickness measurement which does not separate the entrained liquid from the film liquid must necessarily be overestimating the average film thickness. It is also probable that the AERE probes miss large waves thereby underestimating the average and instantaneous film thickness.

Problems encountered in the use of these instruments show that, as mentioned previously, wave peaks are not seen by the CISE instrument and, in some cases, not by the Harwell instrument. This may make the CISE instrument underestimate the average film thickness by as much as 40% in some cases. In addition, these instruments both require conducting mediums and as such may be difficult to use

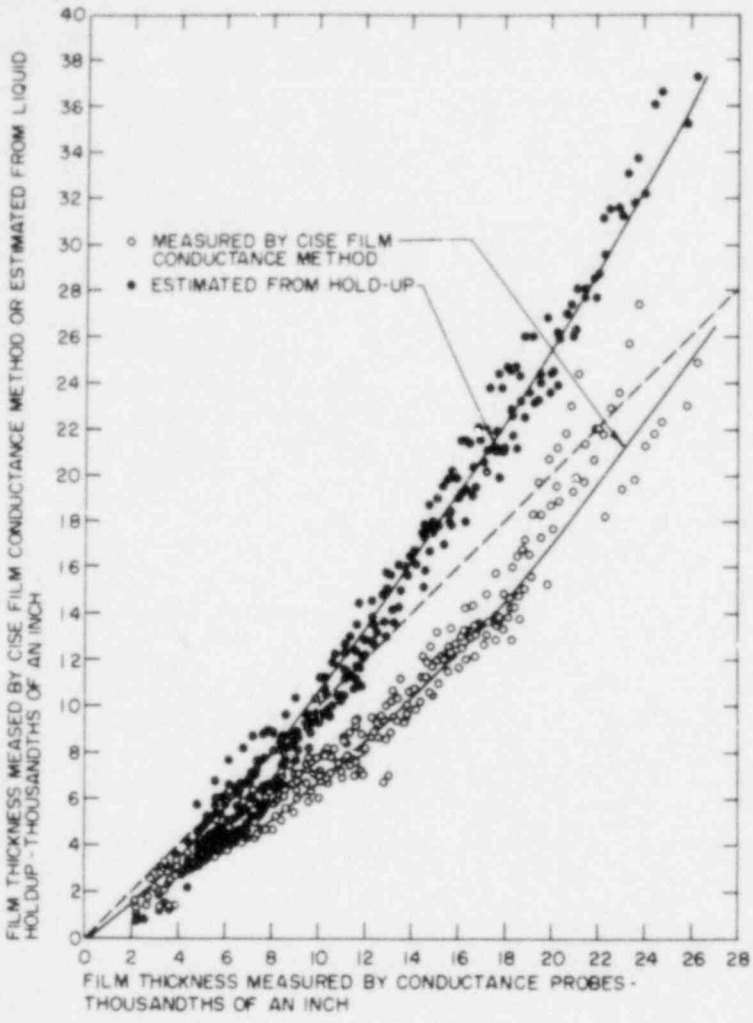

Figure 13 - Comparison of Data Obtained by C.I.S.E. and Harwell Conductance Probes [37]. (BNL Neg. No. 9-106-79)

in systems having high resistivity water chemistry requirements. The AERE method requires an extremely, well-designed geometry mockup for calibration of the instrument. Any misalignments or nonconcentricities in the calibration unit itself can have a significant effect on the calibration.

An excellent review of conductance measuring devices is given in Reference 37. In general, the characteristics of such devices have restricted their use to studies where the continuous phase is a conducting medium, their major application being in film thickness studies. Bergles and his coworkers at Dynatech had some success in the use of needle-type probes as flow regime-detectors [60] but the previous discussion seems to lend some uncertainty to this application.

Conductivity probe summary. Conductivity devices of both the probe-type and the wall type have been used for many years for various purposes including local void fraction (residence time fraction), flow regime indication, film thickness wave celerity, etc., and when coupled with a velocity indication, bubble size and slug length distributions. Two used in tandem can also be interpreted to

give a velocity indication. It should be understood that since the probe type device is basically a phase indicator, any transport information interpreted as a velocity between two points is really propagation of a phase delimiter or interface, ie.: interfacial velocity. As such, it is subject to all the effects which tend to produce errors at a single probe and may as well include selective distortion at one probe vs. another. In addition, interface velocities may or may not be a good indication of a phasic velocity, being subject to such things as biasing due to slip and evaporation.

General difficulties with electrical sensors include phase distortions due to probe insertion, electrochemical effects, nonrepresentative conductive liquid paths for electrical current, electrical field distortions, variable conductivity due to thermal or chemical effects, nonlinear response, and, if these aren't enough, inadequate physical interpretation of the results and resulting erroneous conclusions. Specifically, problems associated with this method include those due to probe wettability and surface tension, as well as bubble trajectory. Boundary contact times were noted by Sekoguchi et al. [45] to be 100-200 μs resulting in errors of up to 10% in void measurements and Jones [53] and Jones & Zuber [69] measured similar boundary times and errors with a 50 μm hot film anemometer. Generally speaking, more work is needed on this difficult problem, especially on the physical significance of the delay times measured with a double probe.

It has been seen that one of the principal features which differentiates the electrical circuits is the type of electrical supply, direct current or alternating current. With direct current supplies, electrochemical phenomena are encountered which obscure the desired signal unless low voltages are maintained. These, however, lead to complicated electronics and tend to yield poor signal-to-noise (s/n) ratio's. In addition, electrochemical deposits in low speed flows give alterations in the signals although at high velocities the sensors may remain clean. On the other hand, alternating current supplies generally eliminate electrochemical effects [38-40] while substituting stray capacitative effects. One must insure suitable separation of supply frequency from phenomena frequency. In some cases, very high frequencies over 1 MHz are required resulting in complex circuitry. It should be noted that Reocreux and Flamand [41] reported on a method using very low frequency, for high speed flows, to resolve this difficulty and yet eliminate electrochemical difficulties. Pseudo direct current behavior was obtained every half wave.

Finally, Tawfik [42] has shown that the interaction between the electrical field and the liquid field during bubble approach to a needle probe can affect the signal and hence the interpretation of the results. This points out the fact that a thorough knowledge of the interactive physics is very important in obtaining a good evaluation of experimental results.

In spite of the difficulties involved, the general simplicity of this class of measurement devices has resulted in their continued use in many fields, especially where qualitative diagnostic information is needed [43-46,54]. Continued development for improved understanding is, however, required and will no doubt be undertaken as the needs arise.

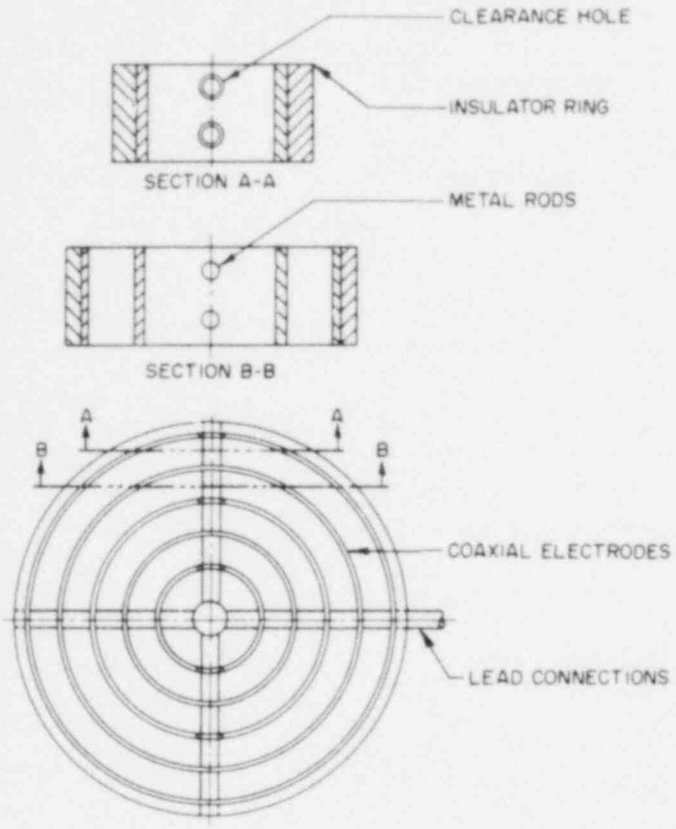

Figure 14 - Coaxial Impedance Void Meter [60]
(BNL Neg. No. 9-119-79)

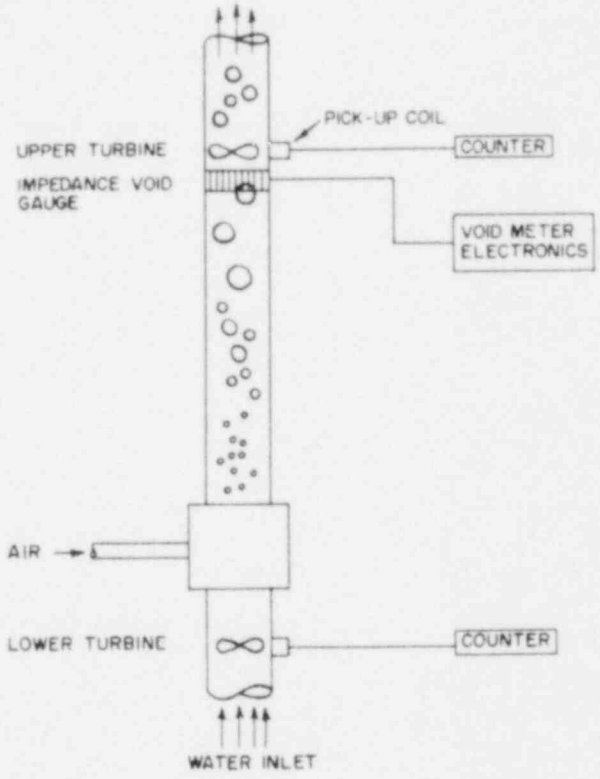

Figure 15 - System for Calibrating Impedance Void Meter [60]
(BNL Neg. No. 9-121-79)

3.2. Impedance Void Meters

The second type of instream electrical measuring instruments are the impedance type void sensors [60]. While these may be considered a subset of the previous types, significant differences in geometry exist, and these devices are usually always used in the impedance mode relying on phase variations of the capacitative reactance. Several types have been designed and used. The first type is a concentric cylinder meter which, shown in Figure 14, consists of concentric, thin-walled short cylinders which are alternately connected to one of two electrodes. When connected to an alternating current supply, the relative impedance may be measured as a function of the vapor fraction. The void meter may be calibrated by means of a system such as is shown in Figure 15. Measured amounts of water and air are injected into the base of a vertical section. The water velocity is measured initially by means of a turbine meter. In the upper portion of the channel, another turbine meter is placed immediately downstream of the impedance void gage. Thus, the mixture velocity, coupled with an accurate knowledge of the air and water flow rates, may be used to calculate the void fraction. This calculation is then compared with the impedance of the void meter and used as a calibration point. In this manner a curve of relative impedance versus vapor fraction can be easily obtained. There does, however, seem to be a sensitivity on the void distribution between the plates as shown in Figure 16. This is in accordance with established theory [61,62]. Here there

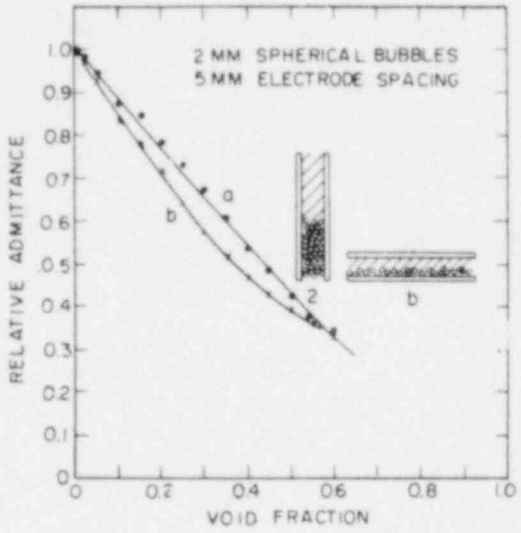

Figure 16 - Effect of Void Distribution on Impedance Void Meter Output [60] (BNL Neg. No. 9-122-79)

may be an effect amounting to as much as 15% or more depending on whether the voids are distributed horizontally or vertically with respect to the parallel plates of the void meter, and on the relative dielectric constants for the two phases.

Similar devices have been developed and used by a number of other investigators [63-67]. Marked effects due to void distributions at constant void fraction are also confirmed by Cimorelli and Premoli [66]. In general these sensors are bulky and the methodology unsuitable for adaptation for small volume measurements for use in small geometries.

3.3. Hot Film Anemometer

Hot wire and hot film anemometers have been widely used in gases. More recently, miniature cylindrical probes have been used for accurate velocity measurement in low velocity (for instance, in water, Ornstein [181], <0.5 m/s; Morrow & Kline [182] <0.25 m/s in mercury; Hollasch & Gebhart [183] <0.6 m/s, and Hurt & Welty [184] , <0.05 m/s. The larger and more sturdy wedge and conical probes has enjoyed greater success at velocities up to the region of 5 m/s (Rosler & Bankoff [185], <3.7 m/s; Bouvard & Dumas [186], <5 m/s; Resch & Coantic [187], <4 m/s; Resch [188], <4 m/s). It has been found that hot-wire or hot-film anemometry can be used in two-component two-phase flow or in one-component two-phase flow with phase change. In the first case, an air-water flow, for example, it is possible to measure the local void fraction, the local

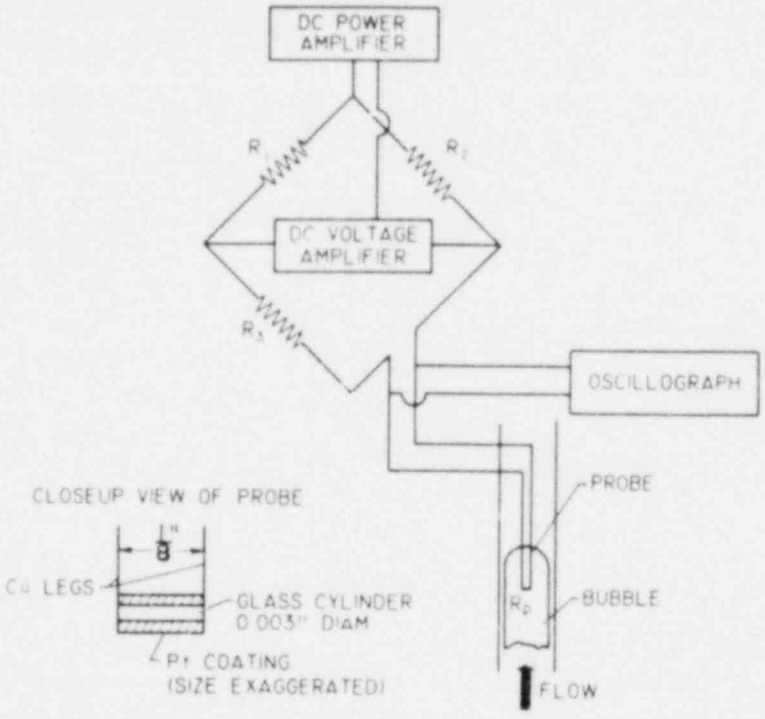

Figure 17 - Hot Film Anemometer System Used by Hsu, Simon, and Grahm [68] (BNL Neg. No. 9-104-79)

liquid volume flux or instantaneous velocity and the turbulence intensity of the liquid phase in conjunction with the arrival frequency of bubbles or droplets. In the second case, a steam-water flow for example, it has been so far impossible to obtain consistent results on calibrated liquid velocity measurements.

The hot film anemometer was tried as a two-phase flow indicator device by Hsu, Simon, and Grahm [68], Jones [70], and later by Jones and Zuber [69]. The study by Hsu et al. indicated that this instrument could be useful in measuring all the parameters measurable by the previously described instruments and, additionally, provide both temperature and phase velocity measurements as well. The reason why this instrument has not received wide acceptance to date is because of its extreme fragility and short life time. To explain the principles of operation of this instrument, Figure 17 is used. The close-up view of the probe shows that it consists of a small diameter glass cylinder covered with a platinum coating and connected on either end to a copper lead wire. In operation, the resistance of the probe was set by means of an electrical current at a value corresponding to a desired probe temperature. If the probe resistance began to change from the preset value due to a change in temperature, the control unit would respond with a change in current to maintain a constant probe resistance. This setup is shown schematically in Figure 17 where the probe is one arm of a four-arm bridge. The output of the transducer was measured as a voltage drop across a calibrated resistor by an oscillograph.

A typical output trace for this instrument in different flow regimes taken from Reference 68 is shown in Figure 18. Here it is possible to compare the traces from bubbly flow, slug flow, and mist flow with low droplet concentration. As seen in this figure, the different flow regimes are readily discernible one from the other. The only possible conditions that might cause confusion are bubbly flow with large bubble concentration as opposed to mist flow with very rich droplet concentration. As seen in Figure 18, these two traces could look quite similar; however, one distinguishing feature would be the relative point on the scale at which the trace occurs. In bubbly flow, there would be expected to be a larger power dissipation on the probe than there would be in the mist flow due to the smaller void fraction.

Figure 19 shows the typical trace of a bubble as it passes the probe. From bottom to top in this figure, as the bubble approaches the probe, the vanguard consists of locally increased velocity as shown by increasing power dissipation. The entrance of the probe into the void is shown by a sharp decrease in power dissipation followed almost immediately by an increase as it enters the wake. The same effect happens again with another bubble and then, as the probe exits from the effect of the wake, the power dissipation decreases corresponding to the decreasing local velocities. In addition, since there is apparently a relatively rapid response of the transducer when entering a void, this instrument was expected to give good quantitative information on local vapor fractions.

Measurements in two-component two-phase flow without phase change. Hot-wire anemometry has been used for measuring the concentration flux and the diameter histogram of liquid particles moving in a gas stream. Goldschmidt & Eskinazi [189,190] measured the arrival frequency of liquid droplets, 1.6 to 3.3 μm in dia, with a constant temperature anemometer and a cylindrical probe, 4.5 μm in dia. When the impaction frequency of the droplets is different from the energetic frequency range of the turbulent gas stream, the signal fluctuations due to impacts can be distinguished from the fluctuations due to turbulence. In experiments by Goldschmidt & Eskinazi [189,190], results showed that the ratio of the impaction frequency to the maximum impaction frequency was insensitive to the threshold amplitude of a discriminator used to produce a binary chain of pulses due to droplet impactions. This fact has also been observed by Lackme [191] for void fraction measurements with a resistive probe. Ginsberg [192] used the same technique to study liquid droplet transport in turbulent pipe flow. Goldschmidt [193] determined that the measured impaction rate is lower than the true value but proportional, and should thus be calibrated against another technique.

In determining droplet diameter histograms, Goldschmidt & Householder [72,194] theoretically found a linear relationship between particle diameter and cooling signal peak value which was verified experimentally for droplet diameters lower than 200 μm. Bragg & Tevaarverk [73], however, contradicted these results and concluded that the hot wire was unsuitable for this purpose. This conflict has yet to be resolved.

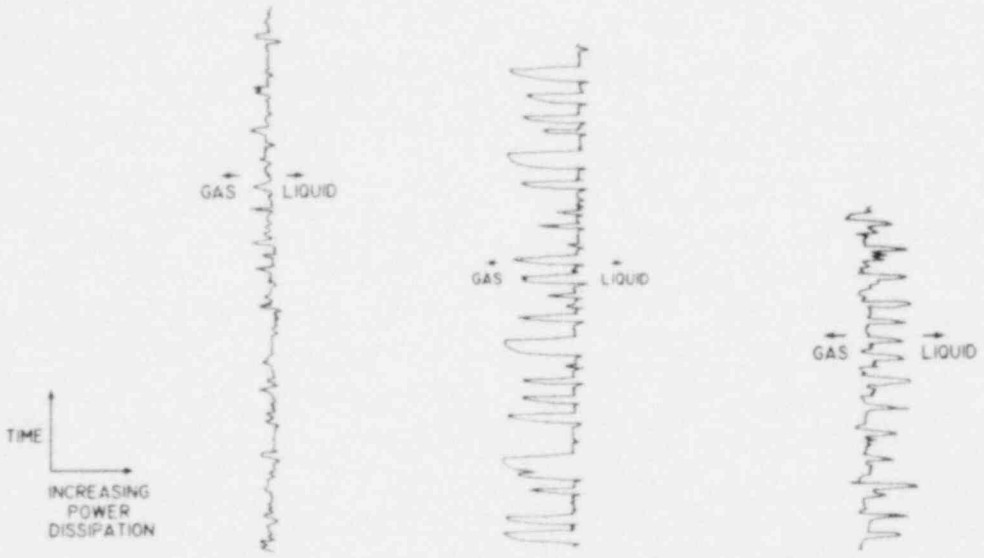

a) bubbly b) slug c) mist

Figure 18 - Typical output from the Hot Film Anemometer [68]
(BNL Neg. No's (a) 9-103-79; (b) 9-85-79; (c) 9-84-79

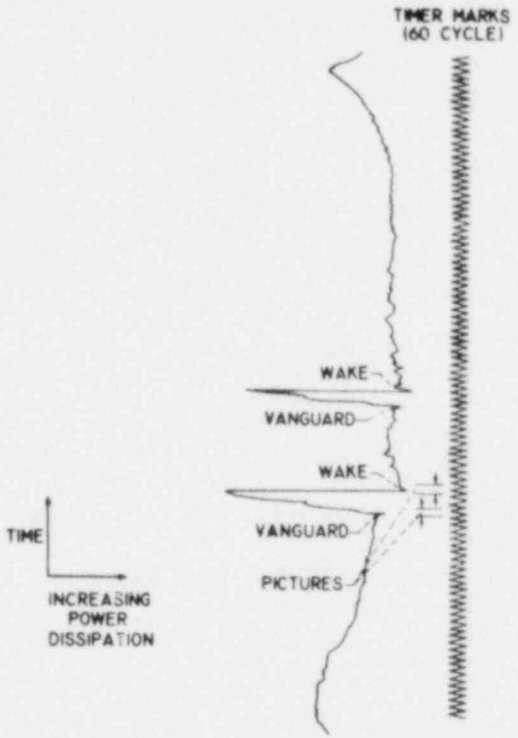

Figure 19 - Wake and Vanguard Effects Due to Bubble Passage by a Hot Film Anemometer [68] (BNL Neg. No. 9-96-79)

Time-averaged gas velocities as well as gas turbulent intensities were measured by Hetsroni et al. [204] in low concentration mist flow. The spikes due to the impingement of the liquid droplets on the hot-wire were eliminated with the help of an amplitude discriminator and a somewhat simpler electronic circuit than that of Goldschmidt & Eskinazi [189,190]. The resultant signal was used to obtain time averaged gas velocity and turbulent intensities. Chuang & Goldschmidt [195] employed the hot-wire as a bubble size sampler by theoretically investigating the nature of the signal due to the traverse of an air bubble past the sensor.

Despite several difficulties arising in droplet granulometry determination, the hot-wire has successfully been employed for studying the turbulent diffusion of small particles suspended in turbulent jets by Goldschmidt et al. [196]

Following the studies done by Goldschmidt in aerosols and by Hsu et al. [68] in steam-water flow, and the preliminary work of Jones [70], a thorough investigation of the hot-film anemometry technique in two-phase flow was carried out by Delhaye [77,78] using a conical constant temperature hot-film probe which has three major advantages over the cylindrical hot-film sensor: small particulate matter carried with the fluid does not attach to the tip, bubble trajectories are less disturbed, and the relatively massive geometry is less

susceptible to flow damage at higher velocities. The maximum overheat resistance ratio of the probe of 1.05, (ratio of operating resistance to the resistance at ambient fluid temperature), was suggested by Delhaye [77,78] to avoid degassing on the sensor. This corresponded to a difference of 17°C between the probe temperature and the ambient temperature, significantly below saturation temperature. Jones [53], and Jones & Zuber [69] found little difference between resistance ratios of 1.05 and 1.10 insofar as degassing on their 50 μm dia cylindrical sensor was concerned, and chose the latter for increased sensitivity. Degassing in their system was found to occur in operation following failure of the 8000 Å thick quartz coating over the platinum film. This failure occurred during forced resonant vibration of the sensor caused by vortex shedding at velocities over 1.5 m/s. Degassing caused the calibration to be unstable only at velocities less than ~30 cm/s.

Delhaye [74-77] developed some rather sophistical anemometry techniques for measuring void fraction in large tubes with the rugged, conical, hot film probe. Using a multichannel analyzer, he obtained amplitude histograms of the voltage signal produced for a constant temperature sensor control system in a two-phase mixture. Referring to Figure 20, one may see that in the ideal case, (a), the anemometer voltage is either at the voltage corresponding to the presence of liquid at a given velocity, E_ℓ, or at the voltage corresponding to all gas, E_g, at the given gas velocity. The multichannel analyzer periodically determines the amplitude of the signal voltage. A block of memory locations is allocated where each location represents a different voltage level range of width ΔE. The first memory location represents the voltage range E_{min} to $(E_{min} + \Delta E)$ while the last in the block represents $(E_{max} - \Delta E)$ to E_{max}. At the time the voltage level is determined by the analyzer, one count is added to the memory location representing the voltage range within which the current amplitude was found to be. In this manner, each location or channel, will contain a count proportional to the fraction of the total sampling time during which the voltage level was within the range assigned to that channel. For the ideal case, then Figure 20 shows that the histogram on the right would contain N_ℓ counts for liquid voltage amplitude and N_g counts for gas voltage amplitude. The percentage of time the probe "sees" the gas would then be

$$t_g = \frac{N_g}{N_g + N_\ell} \qquad (2)$$

and could be taken as a measure of the local void fraction, α .

In the somewhat less ideal case where each voltage level has some fluctuations associated with it but still the switching from all one-phase to the other occurs instantaneously, (b). The amplitude histogram would show a cluster of vertical lines centered about E_ℓ and another cluster about E_g, the height of each line being the number of times the particular voltage level was encountered during periodic sampling. Thus, if all the lines clustered about E_g are associated with the gas, and all the lines clustered about E_ℓ associated with the liquid, the void fraction would be

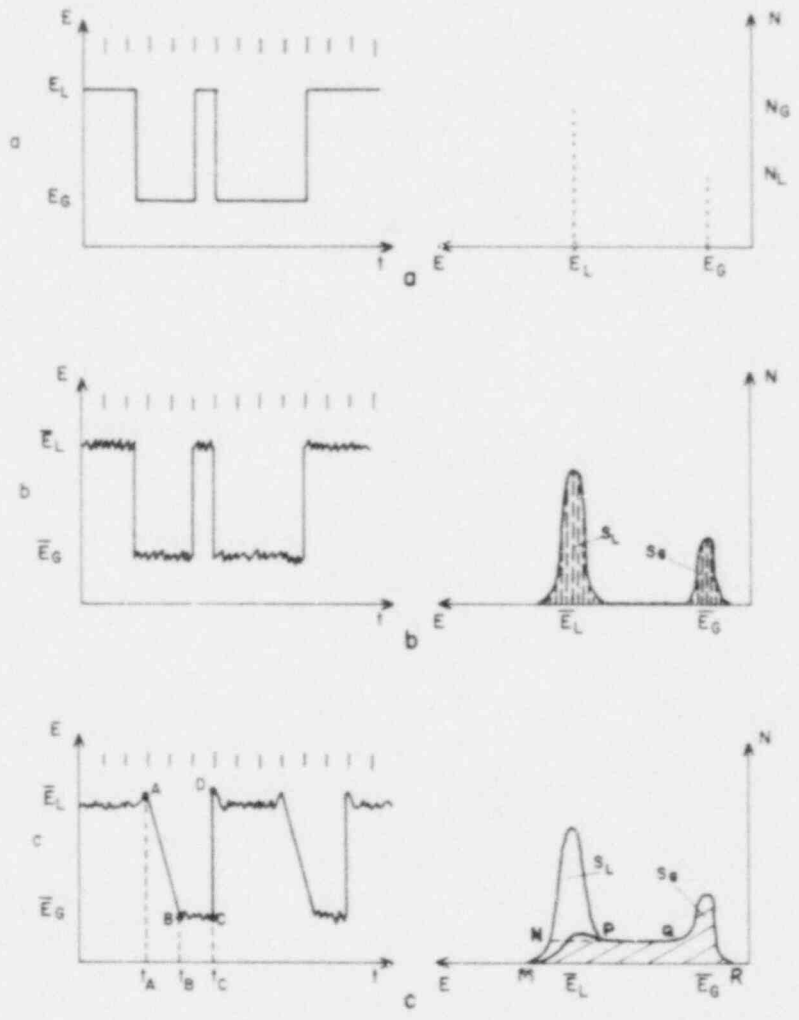

Figure 20 - Delhaye's Method for Local Void Fraction Using Multi-Channel Analysis [76] (BNL Neg. No. 9-94-79)

$$\alpha = \frac{\sum N_{gi}}{\sum N_{gi} + \sum N_{\ell i}} \tag{3}$$

For this case it becomes convenient to begin thinking in terms of a continuous amplitude spectrum, N(E), such that in the limiting case where the voltage intervals vanish (3) becomes

$$\alpha = \frac{\int_{A_g} N(E)dE}{\int_{A_T} N(E)dE} = \frac{S_g}{S_g + S_\ell} \tag{4}$$

where the void fraction becomes the ratio of the gas histogram area to the total histogram area.

In the real case, the anemometer signal is more as shown in Figure 20 (c) where a finite time is required for the sensor to dry out (A-B) before becoming characteristic of all gas (B-C). In some instances the gas residence time may be shorter than the dry out time and the gas voltage is never reached before the liquid appearance forces the voltage back to E_ℓ. Thus, the region between S_g and S_ℓ will contain some counts and the voltage amplitude histogram will appear as shown at the right of 20 (c). Thus, the gas-caused area of the histogram would be the cross-hatched area shown in the figure having some counts for all voltage levels up to approximately the maximum for all liquid.

Delhaye calculated the void fraction locally by application of Equation (4) where in practice

$$\alpha = \frac{A_{MNPQR}}{A_T} \tag{5}$$

To a first approximation, then, the local void fractions were calculated as the ratio of the hatched area to the total area which then compared favorably with radiation absorption methods (γ-rays). Notice that trigger levels for S_g and S_ℓ affect the result. Delhaye adjusted both to get accurate comparison between the resulting line-averaged void fraction and an independent γ-ray measurement but developed no specific formula governing these settings. The liquid time-averaged velocity and the liquid turbulent intensity are calculated with the nonhatched area of the amplitude histogram (Figure 20c) and the calibration curve of the probe immersed in the liquid. The same method has extensively been used by Serizawa [54] for measuring the turbulent characteristics and local parameters of air-water two-phase flow in pipes.

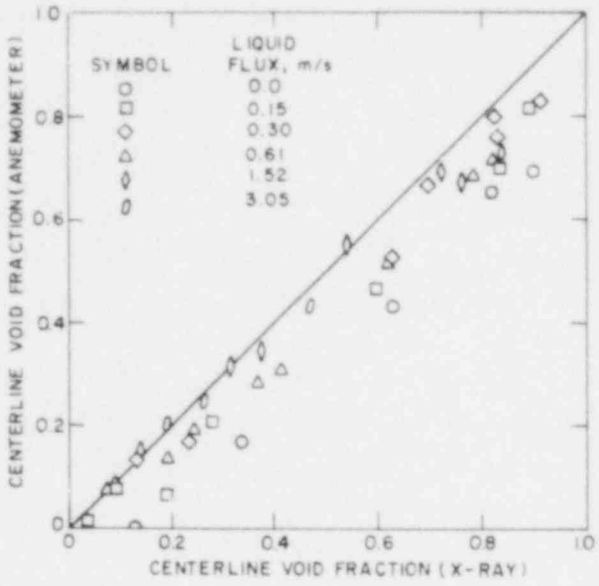

Figure 21 - Uncorrected Anemometer for Averaged Void Fraction (Jones [69]) (BNL Neg. No. 9-128-79)

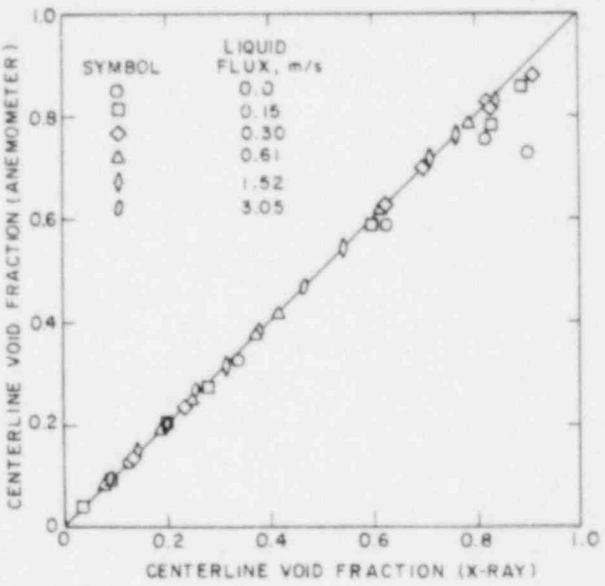

Figure 22 - Corrected Anemometer for Averaged Void Fraction per Equation (6) (Jones [69]) (BNL Neg. No. 9-129-79)

A different processing method was proposed by Resch & Leutheusser [197] and Resch et al. [198] in a study of bubble two-phase flow in hydraulic jumps. The nonlinearized analog signal from the anemometer is digitally analyzed. A change of phase is recognized when the amplitude between two successive extremes of the signal is higher than a fluctuation threshold level ΔE. In this way the liquid mean velocities and turbulence levels were obtained along with bubble size histograms. ΔE was chosen to be in a plateau region of ΔE versus measured void fraction.

Jones [53] and Jones & Zuber [69] used a discriminator applied to the raw anemometer signal to obtain a binary signal representative of local void fraction but found the cutoff level needed to be adjusted depending on the local velocity to a point just below the minimum value for a liquid. Even though the threshold value was set at every point in the traverse, errors in averaged void fraction were encountered when calibrated against an X-ray measurement. These errors were found to be dependent on the liquid volume flux and the mean void fraction.

Comparisons as shown in Figure 21 show significant errors exist, especially at low liquid throughput rates. By choosing a relationship between the corrected and measured void fraction as

$$\alpha_c(y) = \{1 + f_c(y)\}\, \alpha_m(y) + \alpha_{zc} \tag{6}$$

where

$$f_c(y) = C_1\, (1 - \alpha_m)\, \left(1 - \frac{4y^2}{s^2}\right) \tag{7}$$

and

$$\alpha_{zc} = \frac{C}{K_\alpha + j_\ell}\, (1 - \alpha_m)\, \left(1 - \frac{4y^2}{s^2}\right) \tag{8}$$

and averaging in y, a relationship between C_1 and the averages could be obtained as

$$C_1 = \frac{\bar{\alpha}_c - \bar{\alpha}_m - \bar{\alpha}_{zc}}{\overline{f_c \alpha_m}} \tag{9}$$

Note that C and K_α for all data were found to be 0.0055 m/s and 0.028 m/s respectively, while the averages in (8) were found from the data. Good results were obtained as shown in Figure 22.

By counting the number of times the output of the discriminator changed from one level to another, Jones [2] also obtained local values for interface frequency. He also measured the liquid-volume flux directly by time averaging the linearized signal equal to the liquid velocity when the sensor was in liquid, and zero when the sensor was in gas. Liquid velocities were obtained by pointwise division of the measured liquid flux by the measured void fraction. The results were somewhat questionable, however, due to the cracking of the 8000 A-thick, quartz coating mentioned previously. No attempt was made to measure the turbulent fluctuations.

Serizawa [54] used a conical probe of much more sturdy construction and larger size, similar to that of Delhaye [77,78]. In bubbly and slug flow in air-water mixtures he used multichannel analysis techniques to obtain the frequency spectrum of the velocity signal including fluctuations up to ∿2 m/s. Ishigai et al. [199] used an anemometer to measure liquid film thicknesses.

Measurements in one-component, two-phase flow with phase change. The earliest paper on hot-wire anemometry in two-phase flow seems to have been published by Katarzhis et al. [200]. This preliminary and crude approach was followed by the work of Hsu et al. [68]. These authors, by comparing the signal with high-speed movies concluded that hot-wire anemometry was a potential tool for studying the local structure of two-phase flow, in particular for determining the flow pattern and for measuring the local void fraction. Hsu et al. [68] specified that in steam-water flow the only reference temperature is the saturation temperature. If water velocity measurements are carried out, the probe temperature must not exceed saturation temperature by more than 5°C to avoid nucleate boiling on the sensor. Conversely, if only a high sensitivity to phase change is desired, then the superheat should range between 5°C and 55°C causing nucleate boiling to occur on the probe when the liquid phase is present, and a resultant shift to forced-convective vapor heat-transfer when the vapor phase is present.

The low electrical conductivity of Freons enables bare wires to be used instead of hot-film probes. Shiralkar [201] used a 5 μm, boiling tungsten wire with a very short active length (0.125 mm) so that the whole active zone would generally be inside a bubble or droplet. Local void fraction was determined by an amplitude discriminator with an adjustable threshold level. For void fraction lower than 0.3 the threshold was set just under the liquid level whereas for high void fraction (0.8), it was set just above the vapor level. For void fractions ranging from 0.3 to 0.8 the threshold was set half-way between the liquid and vapor levels. The method was subsequently applied by Dix [202] and Shiralkar & Lahey [203].

Anemometer summary. The major advantages of the hot film sensor over the needle-type conductivity probe is that the sensor is self-contained not requiring a secondary electrode and is, therefore, not limited to use in specific flow regimes. This type of sensor appeared to be responsive to all flow conditions and apparently provides information on velocities and temperatures as well as void fractions. The major drawback with this type of sensor seemed to be the high initial cost for electronics and probes, and the general fragility of the sensing elements. In addition, an independent method must be utilized for calibration purposes which to date has been a chordal X-ray measurement of the void fraction. The line-averaged value obtained from the anemometer may then be compared with the X-ray measurement and parameters adjusted to yield suitable agreement.

3.4. Radio Frequency Probe

A relatively new development is the use of separate, small, transmitting and receiving antennas with radio frequency signals amplitude nodulated by the dielectric coefficient of the surrounding media [50,80-82]. The r-f probe developed at Brookhaven National Laboratory is shown in Figures 23 and 24 and consists of two 0.25 mm diameter insulated wires, with each wire encased in a 1 mm outside diameter stainless steel tube which were electrically connected to a common ground and acted as an electrical shield. The two shielding tubes

themselves were encased in a larger stainless steel tube, which acts as a holder and provides rigidity. The sensitive part of the probe, the probe tip, was formed by extending the two insulated wires by ~3 mm from the end of the shielding tubes. To prevent water from entering into the stainless steel tubes, each of the end connections were covered with a thin layer of epoxy including the tip of the two insulated wires which were also covered to insulate them from the surrounding media, water or air. When a d-c voltage was applied across one of the wires and the common ground, zero voltage was measured across the second wire and the ground. In operation of the probe, one of the wires was used as an emitter to which a sine wave was applied from a function generator. The second wire was used as a receiving antenna, and its output was fed directly to an oscilloscope or to a magnetic tape recorder after amplification. Similar r-f probes were previously described in the literature [50,81] but a systematic study of the response characteristics was not undertaken.

When a sine wave was applied to the transmitting antenna (input), the amplitude of the received signal (output) varied with the signal frequency of the input (from 100 Hz to 10^7 Hz) both in air and in water, Figure 25. Depending on the input frequency, the signal amplitude in water can be higher than the signal in air or vice versa . The r-f probe seems to act as a band pass filter. For a 500 kHz, 22.7 peak-to-peak sine wave input, the output voltage of the r-f probe was also observed to be dependent on the static immersion depth of the insulated nonshielded portion of the probe tip into the water. The output increased linearly with the immersion depth, reached a maximum and then decreased and leveled off at the all water signal level. An additional fact observed was that the output vs. input curve as presented in Figure 25 depends on the tube or pipe diameter in which the probe is immersed. Thus before undertaking any application of this probe for a specific geometry, a careful signal optimization with input frequency should be performed.

The probe with a 500 kHz, 22.7 v peak-to-peak sine wave input was also checked during the passage of bubbles with known velocities and lengths. Figure 26 presents the detailed output of the r-f probe during the passage of a bubble (obtained digitally with 20 μsec resolution). The output decreases from its water level to the air level with the penetration into the bubble and stays almost constant during the passage of the bubble. When the water impinges on the probe tip again, the signal increases, passes through a maximum, decreases, and then levels off at the steady air level. A possible explanation for this maximum was proposed by Fortescue [83] as being due to the additional capacitance of the water surrounding the insulated unshielded wires. Grounding the water close to the tip by a separate copper wire was shown to eliminate this maximum.

In Figure 27, bubble velocities determined by the r-f probe are compared with velocities determined from the output of the two light-source detectors. Two penetration time intervals were measured from the r-f probe output (Figure 26), at t_1, and t_2. By considering a typical characteristic length of the sensitive part of the tip (3 mm and 2.75 mm), a bubble velocity was calculated. The actual dimension of the sensitive part of the tip was around 3 mm, (see Figure 24), but was difficult to determine exactly due to the geometry and construction. The bubble velocities determined by the two independent methods agree with each other within ~10 percent. Thus with an r-f probe, the average

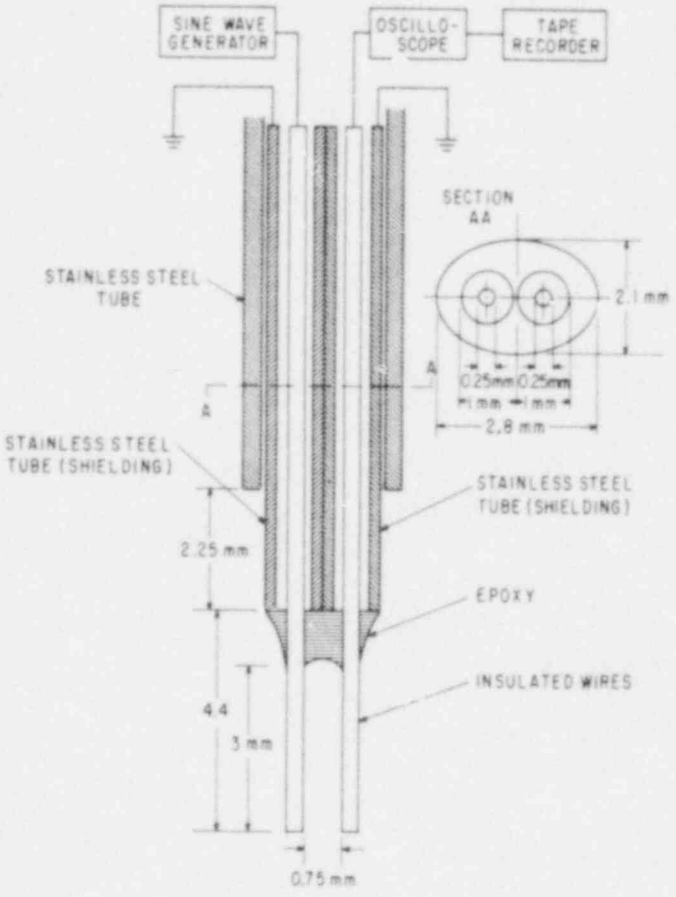

Figure 23 - Schematic representation of the r-f probe. (BNL Neg. No. 9-1493-78)

Figure 24 - r-f probe. (BNL Neg. No. 3-524-79)

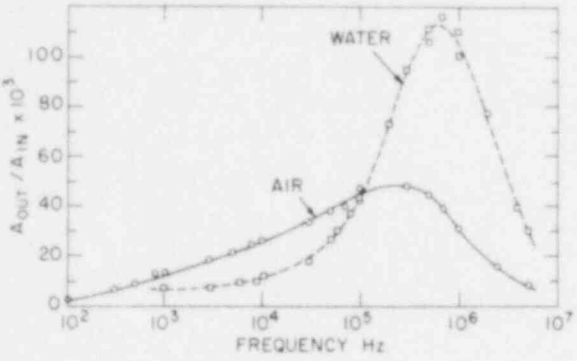

Figure 25 - Ratio of r-f probe output to input voltage level as a function of input sine wave frequency, for the probe tip in air and in water. (BNL Neg. No. 3-529-79)

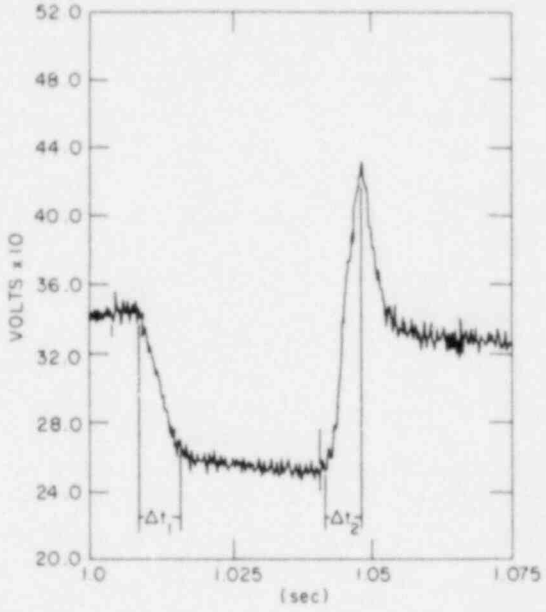

Figure 26 - Expanded output of the r-f probe during passage of the bubble. (BNL Neg. No. 3-526-79)

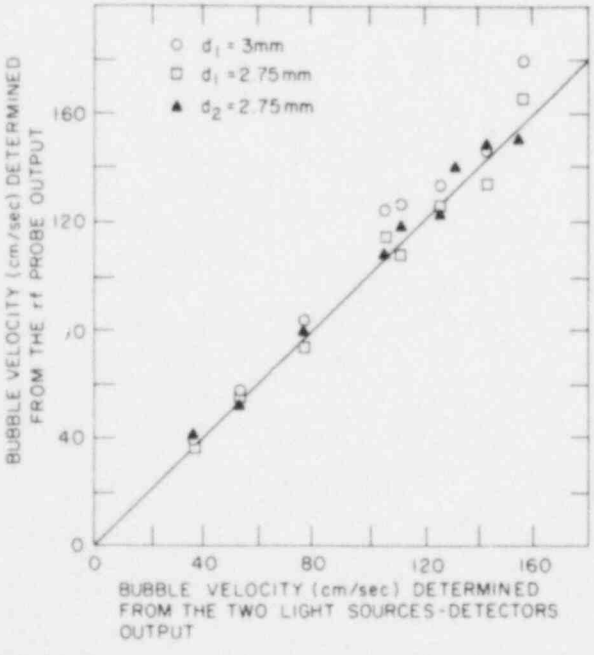

Figure 27 - Comparison of bubble velocity as determined by two independent methods, i.e, r-f probe and two light sources and detectors. (BNL Neg. No. 3-527-79)

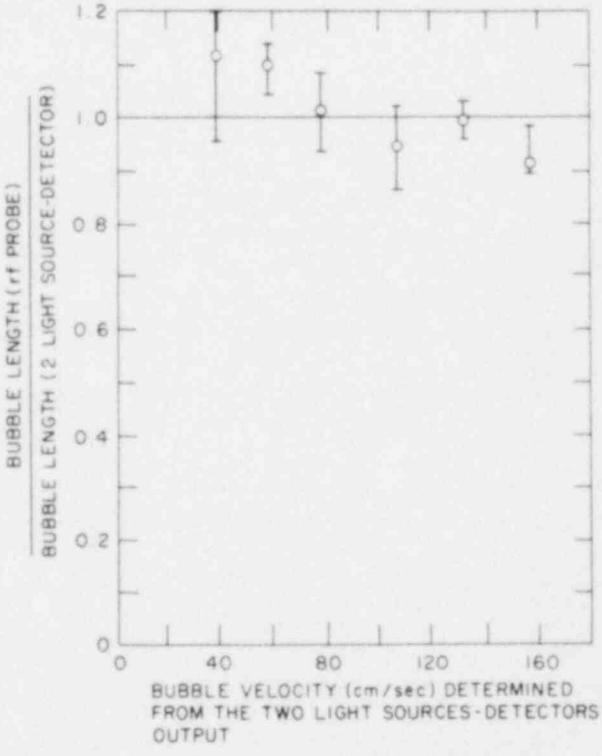

Figure 28 - Ratio of bubble length as determined by the r-f probe and the two light source detectors as a function of bubble velocity. (BNL Neg. No. 3-525-79)

bubble velocity can be determined from the passage time of either interface, air-water or water-air, along the insulated wires. This is true irrespective of the amplitude of the signal which may change with fluid state, purity, or test geometry.

The probe output levels for water and air did not change with the bubble velocity in the range considered (up to 160 cm/sec). Figure 28 depicts that the bubble sizes as determined by the two independent methods agree with each other with a maximum deviation of ~10 percent. The bubble lengths recorded by the r-f probe are 10 percent higher at the low bubble velocities around 30 cm/sec. This fact may be due to surface tension effects during the penetration which become important at these low bubble velocities.

In summary, the r-f probe investigated has a relatively simple construction, and once tuned properly to the test geometry seems to provide information on both bubble sizes and velocities. More work, however, is needed to check the response of the probe in complex two-phase pipe flow conditions.

3.5 Microthermocouple Probes

The classical microthermocouple enables one to determine both steady and some statistical characteristics of the temperature. If combined with an electrical phase indicator, data regarding the local void fraction may also be obtained. Both are discussed below although the latter seems more appropriate in boiling two-phase flows.

Experiments on boiling heat-transfer include studies of temperature fluctuations near a heated surface with either pool boiling or forced convection.

A microthermocouple probe using wires 50 μm in diameters was used by Marcus and Dropkin [84] in measuring mean and fluctuating temperatures to evaluate the thickness of the superheated liquid layer in contact with a heated wall. The results, although timely, were somewhat inaccurate.

Bonnet and Macke [85] reported results obtained with a microthermocouple imbedded in a resin block in such a way that only 20 μm of the hot junction was in the flow. Unfortunately the size of the probe, 80 μm, produced a disturbance in the flow and its thermal inertia led to extra vaporization of the liquid on the sensor so that the significance of the signal was not clear.

Temperature profiles using a 125 μm diameter, chromel-alumel junction were measured by Lippert and Dougall [86] in the thermal pool boiling sublayer. According to the authors, this large diameter thermocouple data was shown to be reasonable by the results of tests in water, Freon-113 and methyl alcohol.

The interaction between bubbles and a microthermocouple, 25 μm in diameter was examined by Jacobs and Shade [87]. These authors, and also Van Stralen and Sluyter [88] were primarily concerned with the thermocouple response time.

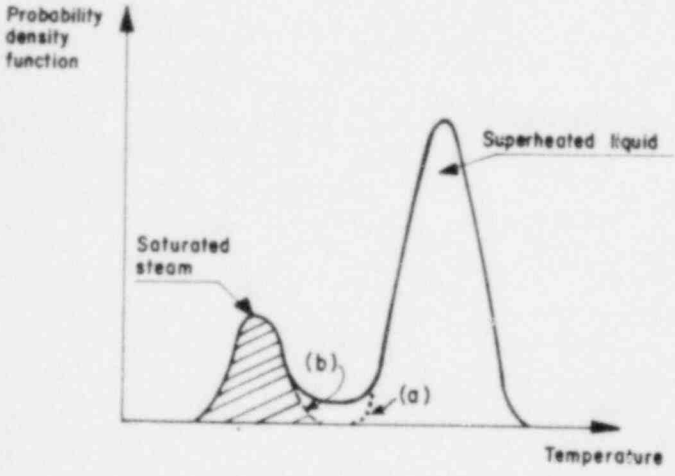

Figure 29 - Separation of steam and water distributions: (a) according to Stefanovic et al. [90,91]; (b) according to Barois [96]. (No BNL Neg.)

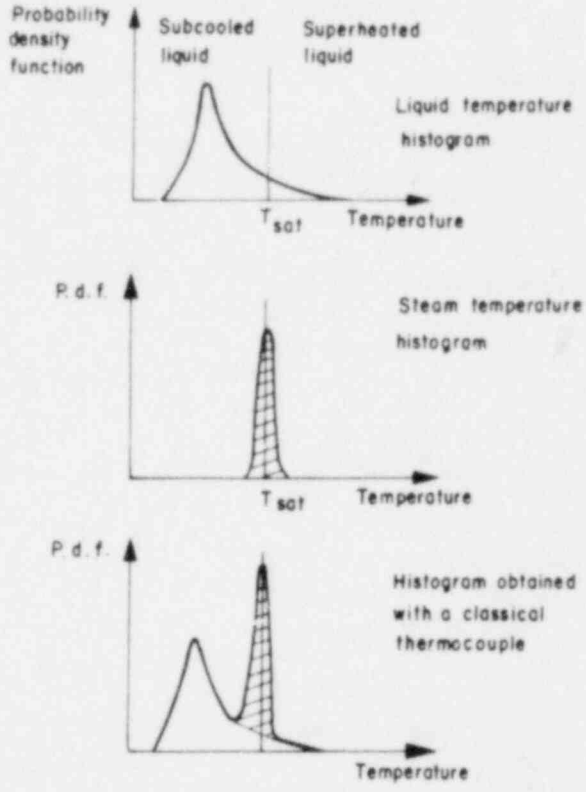

Figure 30 - Subcooled boiling Temperature histograms according to Delhaye et al. [98,99] (a) liquid temperature; (b) steam temperature (c) coupled classical temperature histogram. (No BNL Neg.)

These investigations of the response time were augmented by Subbotin et al. [205] who examined the behavior of bubbles hitting different types of thermocouples.

Stefanovic et al. [89] verified the adequacy of a signal from a 40 μm diameter thermocouple by recording the impact of a bubble on the hot junction using high-speed movies. Amplitude histograms were obtained in pool boiling and in forced convection boiling. The authors separated steam and water temperature histograms by assuming that the predominant phase had a symmetrical distribution of temperature (Figure 29). The identical assumption was used by Afgan et al. [90,91].

Superheat layer thickness measurements were conducted in saturated and subcooled nucleate boiling by Wiebe and Judd [92] employing a 75 μm, chromel-constantan, microthermocouple. A time-average temperature was determined by integrating the temperature signal.

One of the first investigations into temperature profiles in forced convection boiling was carried out by Treschov [93]. The results appear less interesting than those obtained by Jiji and Clark [94] with a chromel-

constantan thermocouple, 0.25 mm in diameter. Despite the large size of their sensor, these authors succeeded in measuring an average temperature and average values indicative of the temperature extremes.

Local subcooled boiling, characterized by important nonequilibrium effects, was studied by Walmet and Staub [95] with the help of several local measurements: pressure, void fraction, and temperature. For temperature measurement the authors used a large, 0.15x0.2 mm copper-constantan thermocouple, and analytically related the measured value to the liquid temperature through the void fraction obtained using X-rays.

In his study of flashing flow of water, Barois [96] proposed to separate the distributions of steam and water by assuming that the steam temperature histogram was symmetrical (Figure 29), rather than the predominant phase as done by Stefanovic et al. [89] and Afgan et al. [90,91].

Although all the preceding works have contributed to a large extent to the understanding of the local structure of two-phase flow with change of phase, they have not provided any reliable statistical information on the distribution of the temperature between the liquid and the vapor phases.

The work done by Delhaye et al. [98,99] is based on the possiblity of separating the temperature of the liquid phase from the temperature of the vapor phase, and of giving the statistical properties of the temperature of each phase as well as the local void fraction. These workers used an insulated 20 μm thermocouple both as a temperature measuring instrument and as an electrical phase indicator (see section on electrical probes) by using a Kohlrausch bridge to sense the presence of a liquid conductor between the noninsulated junction and ground. The phase signal is used to route the thermocouple signal to two separate 1000 channel subgroups of a multichannel analyzer thus providing separate histograms of liquid and vapor tempratures as shown in Figure 30 for a subcooled boiling case. Comparison of these histograms with those in Figure 29 clearly shows the inconsistency in the assumptions of Stefanovic et al. [89], Afgan et al. [90,91], and of Barois [96].

Van Paassen [97] did a detailed study of the microthermocouple as a droplet size sampler, showing good agreement between theory and experiment in determining droplet sizes between 3 and 1188 μm. Detection frequencies of up to 1 kHz were obtained for small droplets.

3.6. Optical Probes

An optical probe is sensitive to the change in the refractive index of the surrounding medium and is thus responsive to interfacial passages enabling measurements of local void fraction or interface passage frequencies to be obtained even in a nonconducting fluid. By using two sensors and a cross-correlation method, information may be obtained on a transit velocity (Galaup [50]). A major advantage of such systems over others is the extremely high frequency response, limited electronically only by photoelectric electronics and photon statistics. The next best seems to be the conductivity probe having frequency response reported as high as 100-200 kHz [50].

Glass rod system. (Miller and Mitchie [100,101]; Bell et al. [102]; Kennedy and Collier [103].) This probe (Figure 31) consists of a glass rod 2 mm in diameter reduced to 0.3 mm at one end. The small tip of the rod is ground and polished to the form of a right-angled guide. The light from a quartz-iodine lamp is focused on one of the branched ends of the light guide. A phototransistor is located at the other branched end of the light guide.

Light is transmitted parallel with the rod axis towards the tip of the probe. When light beam strikes the surface at an angle of 45°, it emerges from the probe or is reflected back, depending upon the refractive indices of the surrounding material n and of the probe material n_o according to Snell's law. Thus for a glass rod when $n_o = 1.62$, if the incident internal angle between the light and the polished tip is 45°, light is reflected back along the rod if $n < 1.15$ and exists from the rod if $n > 1.15$. Table 1 gives possible combinations in which this probe can be successfully used.

Table 1. Liquid vapor systems where $n_g < 1.15$ and $n_\ell > 1.15$. Adequate for use of a 45°-tipped optic probe rod.

System	n_g	n_ℓ
Steam-water	1.00	1.33
Air-water	1.00	1.33
Freon-Freon Vapor	1.02	1.25

For signal processing, all the cited authors used a discriminator to transform the actual signal into a binary signal. A trigger level is set at a value above the background level corresponding to the case where the probe is immersed in the liquid. Miller and Mitchie [100,101] arbitrarily set the trigger level 10% of pulse amplitude above the all-liquid level obtained by comparing the value of the local void fraction at a given point to the volume void fraction measured with quick-closing valves. Bell et al. [102] set the trigger level half-way between the all-water and all-gas signal levels, while in a study of droplet jet flow, Kennedy and Collier [103] related the trigger level and the droplet time fraction with the sizes of the probe and of the droplets. It should be noted that significant variations in the results can sometimes be obtained with variations in the trigger level.

Fiber bundle system. (Hinata [104].) The basic element of this probe is a 30 μm diameter glass fiber which consists of a central core and an outer cladding. Several hundred such elements are tied together in a Y-shaped bundle similar in appearance to that shown in Figure 31, with a light source and a phototransistor. The active end of this bundle is glued to a glass rod, 0.5 mm in diameter, 1 mm long, itself coated with a glass of lower refractive index

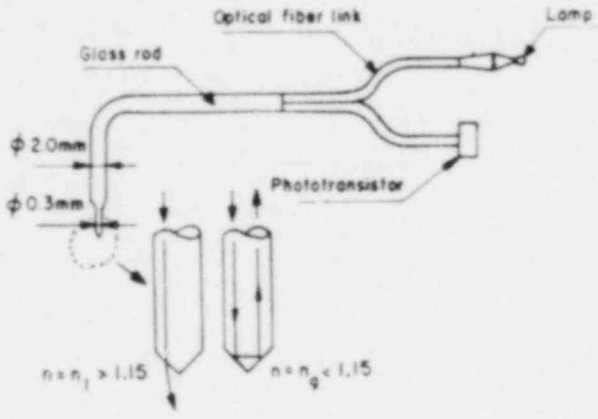

Figure 31 - Typical optical probe system. Miller & Mitchie [100,101] (BNL Neg. No. 9-127-79)

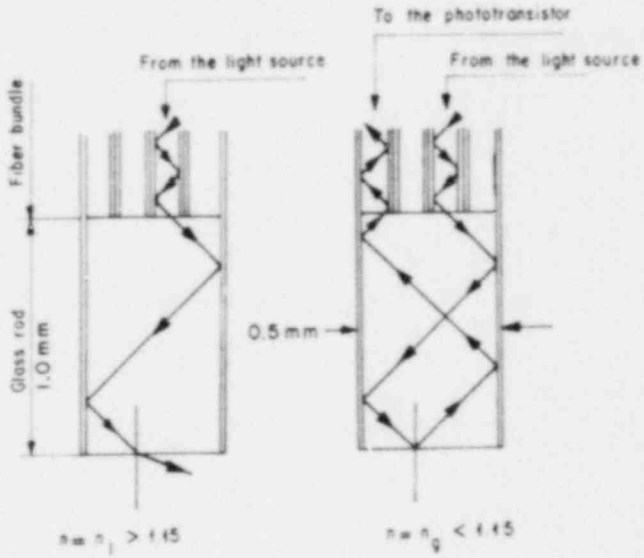

Figure 32 - Fiber bundle optical sensor. Hinata [104]. (ANL Neg. 900-5431)

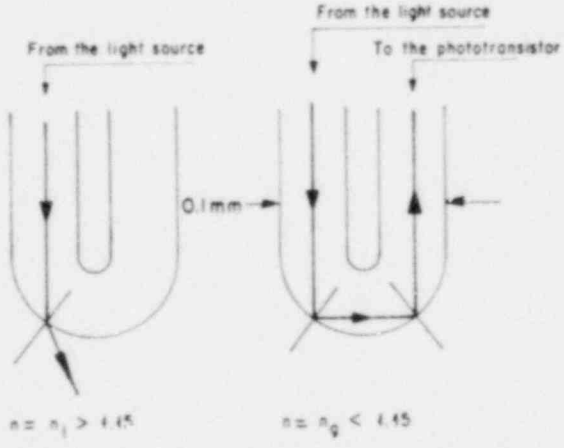

Figure 33 - U-shaped fiber optical sensor. Danel & Delhaye [105] (ANL Neg. 900-5430)

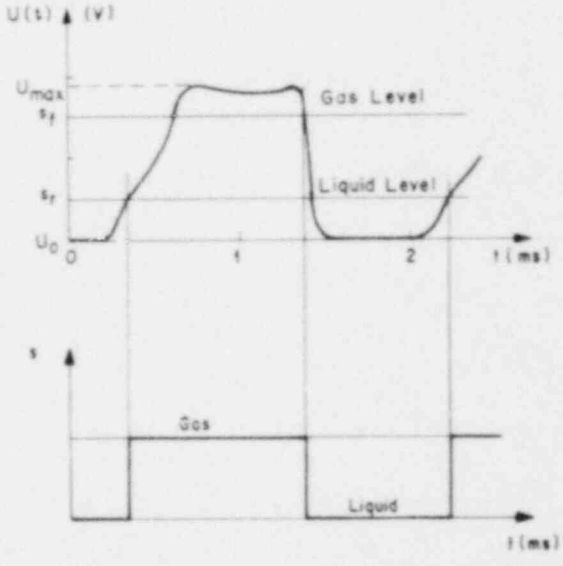

Figure 34 - Typical optical probe signal and discrimination method. Delhaye [107]. (ANL Neg. 900-5418)

(Figure 32). The extremity of the glass rod is ground and polished. The operation of this device is similar to that of the glass rod system. Hinata [104] obtained S-shaped curves of local void fraction measurement versus trigger level, with a plateau corresponding to a given value of the void fraction. He used the trigger level value corresponding to this plateau.

U-shaped fiber system. (Danel and Delhaye [105]; Delhaye and Galaup [106].) One of the major drawbacks of the glass rod and fiber bundle systems is the large dimension of the sensitive part of the probe (respectively, 0.3 and 0.5 mm). An alternative sensor configuration developed by Danel and Delhaye [105] has a distinct size advantage. This probe consists of a single coated optical fiber, 40 μm in diameter. The overall configuration is similar to that shown in Figure 33 with a miniaturized lamp and a phototransistor chosen for its high sensitivity. The active element of the probe is obtained by bending the fiber into a U-shape and protecting the entire fiber, except the U-shaped bend, inside a stainless steel tube, 2 mm in diameter. The active part of the probe has a characteristic size of 0.1 mm as shown in Figure 33.

Signal processing for this system was taken one step further. A typical signal delivered by the probe is shown in Figure 34. The voltage U can be divided into a static component U_0 which was reported to vary with local void fraction, and a fluctuating component u.

Since U_0 corresponds to a sensitive part of the probe completely immersed in the liquid, the change in U_0 can be due to (a) the response time inherent in hydrodynamic and optoelectronic phenomena when the interface is pierced by the probe, and (b) the scattering of light by the bubbles surrounding the probe.

The fluctuating component constitutes the interesting part of the signal while the maximum value U_{max} corresponds to the sensor completely immersed in the gas and does not depend on the local void fraction. Signal analysis is accomplished through two adjustable thresholds, S_r and S_f which enable the signal to be transformed into a square-wave signal (Figure 34). Consequently, the local void fraction α is a function of S_r and S_f which are adjusted and then held fixed during a traverse in order to obtain agreement between the profile average and a γ-ray measurement of void fraction. Since the signal shape varies with void fraction, and since changes in S_r and S_f alter the result, local measurement of void fraction can be quite in error. This is true due to the compensating errors even though the average is in agreement with an independent measurement.

Wedge-shaped fiber system. All previously described methods suffer from difficulties associated with signal processing, hydrodynamic response time uncertainties, and fragility to which the U-shaped fiber system is especially susceptible. Signal processing at best seemed dependent on a global reference. The variable signal levels described by Delhaye and his coworkers [50,105,106] can only yield an accurate local result at a specific void fraction. At other values of void fraction corresponding to different physical locations, values will be distorted due to differences between probe wet and rewet response characteristics. The overall effect is a distortion in the void fraction profiles measured in a flowing mixture.

To circumvent these difficulties, a new design optical probe was developed by Abuaf, Jones, and Zimmer [107,108].

A schematic of the probe as developed is depicted in Figure 35, with the light source and amplifier circuit diagram used in the apparatus. Two .125 mm fibers were inserted into a 0.5 mm-O.D. stainless-steel tube. The two fibers were fused together at one end by means of a minitorch, forming a slightly enlarged hemispherical bead similar to that shown in Figure 33. This fused end of the fibers was then pulled into the tube and epoxied in place. The fibers were separated at the opposite end and encased in two pieces of stainless-steel tubing (0.25 mm O.D.). The ends of the fibers and the bifurcation were then epoxied for strength. The tip of the probe containing the fused end of the fibers was ground and polished at a 45° angle to the axes of the fibers, thus forming an included angle of 90° at the finished probe tip. The resultant probe geometry is extremely rugged, capable of withstanding considerable abuse without altering its characteristics, even to the extent of being dropped on its tip.

After grinding and polishing the free ends of the two fibers flat, one of them was placed in front of an incandescent light source (3 V), and the other in front of a Hewlett-Packard PIN photodiode (5082-4024). An amplifier with a design rise time of 20 μs [109] was used to enhance the output before going into the readout device (Figure 35). The electronic response of the system was checked by means of a light-emitting diode (LED) placed in front of the probe tip. The LED output was modulated by using a signal generator so that rectangular light pulses of different spacings and widths were emitted, simulating the passage of bubbles. The rise time of the output was thus verified to be 20 μs as specified. The amplitude of the probe output did not change with the frequency of the input signal of the LED.

The hydrodynamic response of the probe to the passage of an interface or bubble was investigated as described in References 107 and 108, where single bubbles could be generated and forced past the probe while independent methods were used to determine the velocity. Typical oscillograms of the probe output during the passage of the bubble are presented in Figure 36. Here the probe output in mV is shown as a function of time for two cases where the bubble velocities were 19 and 74 cm/s, respectively. It was observed that when the tip was immersed in water the probe output was always zero without any artificial bias representing a significant improvement over previous optical probes. As the bubble hit the probe, the output was seen to increase, and after an overshoot, to level off to a certain steady value. At the end of the passage of the bubble the signal dropped to its original water level of zero. The bubble penetration time was clearly observed to be larger than the time it takes the probe tip to be immersed in water, Figure 37. Also the signal amplitude decreased with increasing bubble velocity, although both bubbles had almost the same length (void fraction), Figure 38. These two effects were investigated in some detail. Results obtained with two different probes are presented in Figure 38 as a function of bubble velocity. Although the two probes had a steady air signal amplitude of 125 and 600 mV, respectively, the ratio I/I_0 follows the same consistent pattern.

A similar observation was noted by Miller and Mitchie, "With smaller bubbles and higher velocities. . . . The probe signal generated under these conditions. . . never reached maximum amplitude." [101]

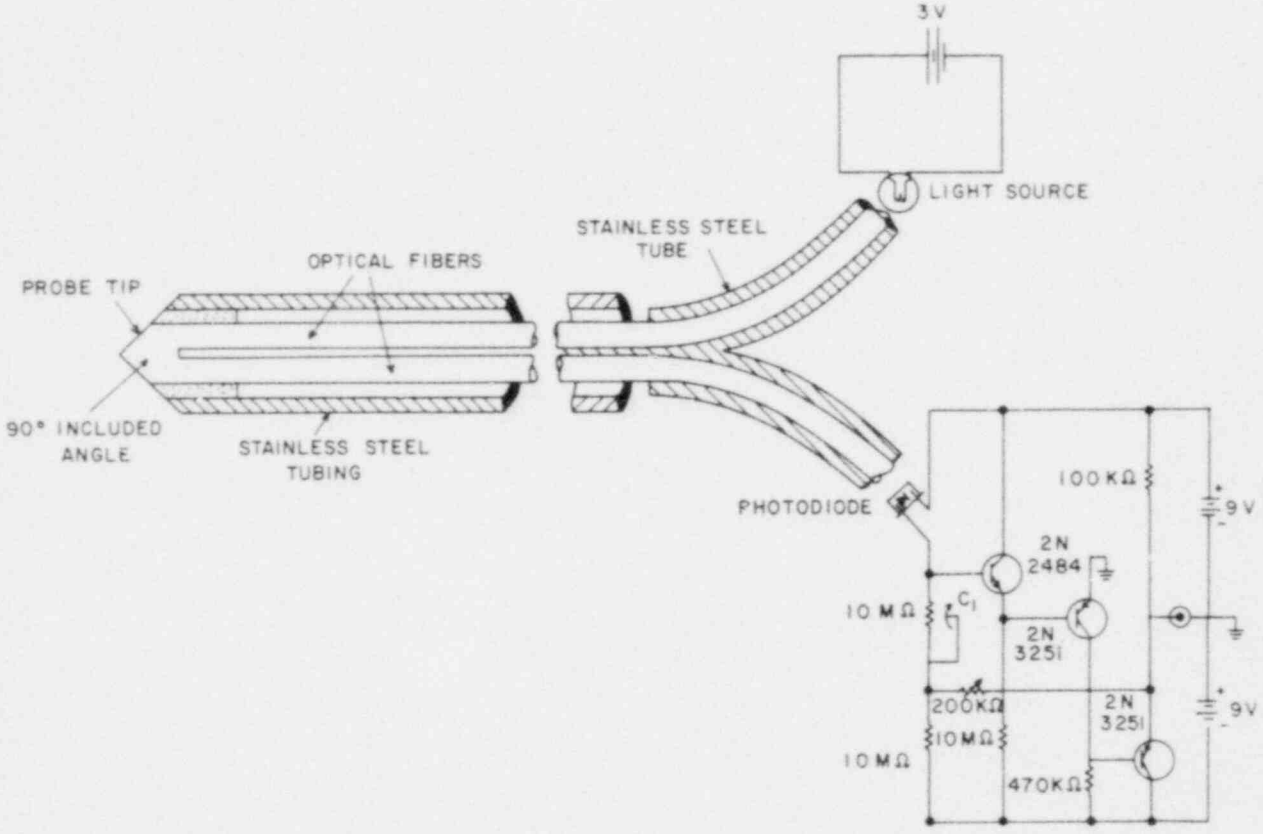

Figure 35 - Schematic representation of the optical probe.
(BNL Neg. No. 1-641-78)

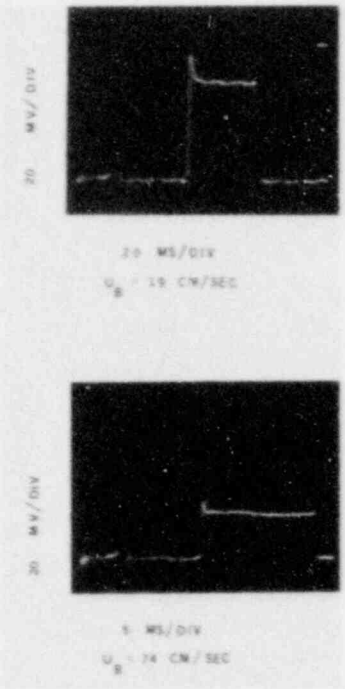

Figure 36 - Typical oscillograms of the output. (BNL Neg. No. 9-111-77)

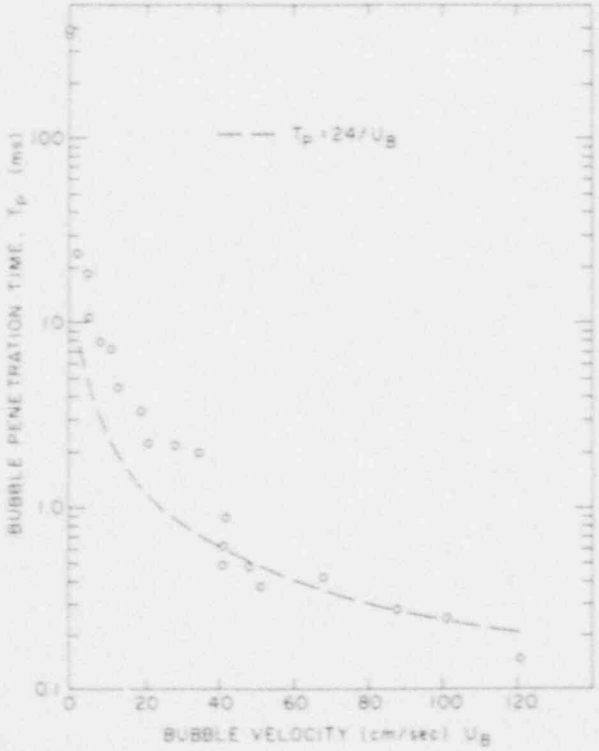

Figure 37 - Bubble penetration time vs. bubble velocity.(BNL Neg. No. 1-643-78)

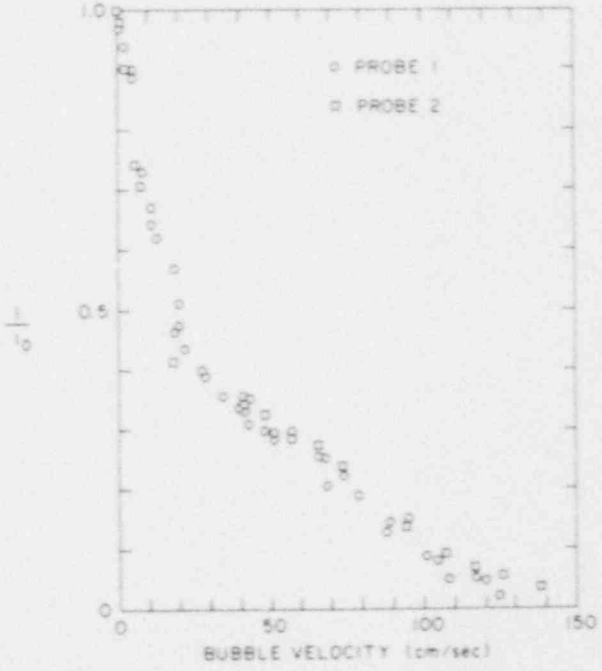

Figure 38 - Probe signal at a given bubble velocity, I, divided by the steady air signal, I_0, vs. bubble velocity. (BNL Neg. No. 1-650-78)

An important conclusion that can be drawn from Figure 38 is that the optical probe is able to measure the local interface velocity as well as the local void fraction, after proper calibration within the velocity range observed.

A computer program was written to study the theoretical response of the output to hydrodynamic conditions at the tip of the probe by tracing individual rays of light from their source to the detector. The effects of varying liquid film thicknesses on the the probe tip was included. Comparison of the geometric effects for the probe of Danel and Delhaye[105] and the new design are shown in Figure 39 where the new geometry is seen to be dependent on probe tip angle.

For a possible explanation for the optical probe output behavior for various bubble velocities, it was proposed that a water film thickness left on the probe tip and increasing with the bubble velocity could explain the decrease in the signal intensity that was observed experimentally

Computer calculations were thus extended to study the signal attenuation that would be experienced when a variable film thickness is present at the probe tip. The water layer was assumed to increase linearly along the flat face. β_w is defined as the angle between the outside face of the water layer in contact with the air and the glass face of the probe tip in contact with the water layer. The attenuation of the rays during their passage from one media to another was not taken into account. Although the 52° half tip angle gave a higher signal in air when compared to the 45° half angle probe tip, the large angle tip (52°) was found to be strongly dependent on the water layer thickness left on the probe tip. In order to show this strong dependence of the probe output to the water layer left on the probe tip, we plot in Figure 40 the maximum angle β_{max} that can be sustained on a probe tip angle before the coherent light rays are refracted out and the signal is zero. Within the tip angle range of interest, $37° < \beta_t < 65°$, (Figure 39), the maximum angle β_{max} increases, and the sensitivity of the probe to the water layer thickness decreases for the lower values of tip angle.

It is known that when a cylinder is withdrawn from a liquid that the film thickness remaining on the cylinder increases with withdrawal velocity (White and Tallmadge [110]). This theoretical prediction was also checked experimentally for various liquids. The dimensionless film thickness (Tallmadge and White [111] was related to a Capillary Number,

$$N_{Ca} = \frac{\mu U_w}{\sigma} \tag{10}$$

and a Goucher Number,

$$N_{Go} = \frac{R}{a} \tag{11}$$

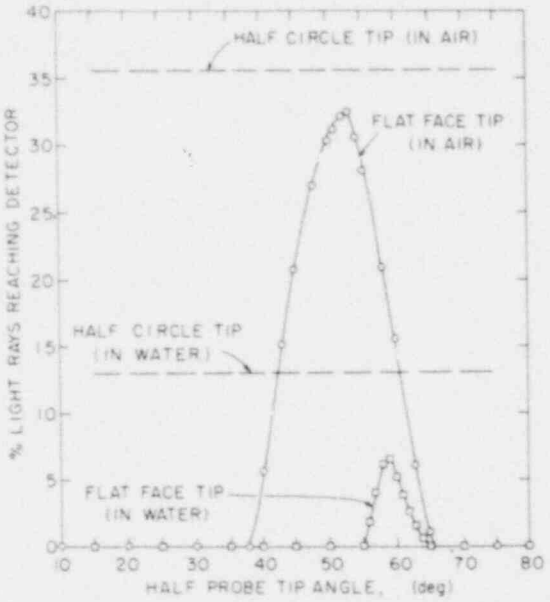

Figure 39 - Percent of light rays reaching the detector as a function of the half probe tip angle for the cases of the probe tip in air and in water. Comparison between the half circle and the flat face probe tips [108] (BNL Neg. No. 1-646-78)

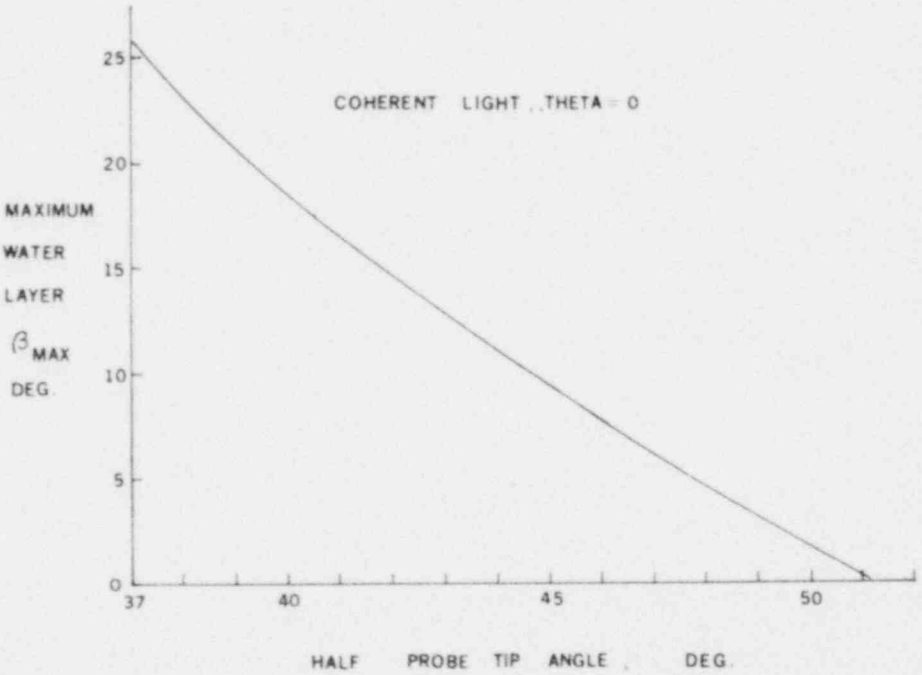

Figure 40 - Maximum thickness of water layer on the flat face probe tip for zero output [108] (BNL Neg. No. 3-1722-78)

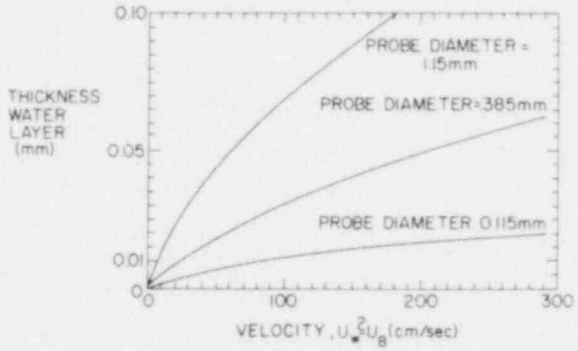

Figure 41 - Plot of water layer thickness vs. wire withdrawal velocity (Tallmadge and White [111]). (BNL Neg. No. 3-1723-78)

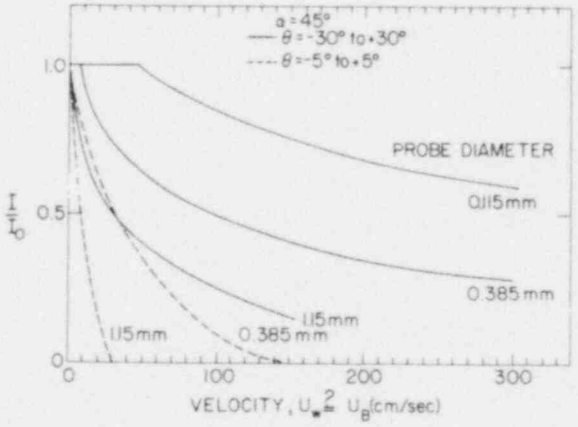

Figure 42 - Cross plot of normalized probe signal, I/I_0, vs. wire withdrawal velocity for three probe diameters and two values of the acceptance angle [108] (BNL Neg. No. 31-1719-78)

where μ and σ are the viscosity and surface tension of the liquid, u_w is the withdrawal velocity, R is the wire radius, and a is the capillary length defined as $a = (2\sigma/\rho g)^{1/2}$. In addition to this, White and Tallmadge [112] observed that experiments conducted with distilled water provided film thicknesses almost twice those predicted by the theory. This fact is still unexplained. In any event, the results may be used to obtain Figure 41 showing the increase in film thickness with increasing velocity.

The two parts of the theory explaining the probe behavior thus include:

a) Amplitude of signal vs. water film thickness;

b) Water film thickness vs. interface passage velocity.

A combination of the two will thus yield the predicted variation of signal amplitude with interfacial velocity as shown in Figure 42, in good qualitative agreement with the observed behavior. Differences may perhaps be explained by the presence of nonlinear films, slanted optical surfaces instead of surfaces colinear with the probe direction, etc.

4. INSTREAM SENSORS WITH MECHANICAL OUTPUT

A large class of devices developed for taking measurements in two-phase flow have been designed for use primarily in annular flow. The single needle conductance probe when traversed toward a film has been used for measuring film thickness. The dual, flush mounted Harwell conductivity [27] probe and the ring-type CISE probes [36] were also designed to measure film thicknesses. Likewise, a number of devices with mechanical output have also been designed for measuring specific properties of annular flow. The major impetus is the general idea that the critical heat flux phenomena is predominantly an annular flow phenomena caused by dryout or disruptured of the liquid film.

In all of these sensors, the general principle is to remove from the flowing stream a certain portion of the fluid to determine the flow rate of either one phase or the other, usually the liquid phase. The sensor may be either stationary or may be designed with traversing mechanisms to determine the transverse distribution of the particular parameter under study. In some more intricate designs, the amount of suction is determined by matching the probe inlet static pressure with the channel static pressure in order to have minimum effect on the flow stream lines. The main development of these instruments may be attributed to the Atomic Energy Research Establishment (AERE) at Harwell, England, and the Centro Informazioni Studi Esperanzi (CISE) in Milan, Italy.

4.1. Wall Scoop

The wall scoop device was developed at CISE and was reported by Cravarolo and Hassid [113], and Adorni, et al. [114]. This device, shown in Figure 43 consisted of a movable scoop built into the wall of the tube being investigated. In their 2.5-cm diameter tube, the scoop could measure the integrated flow rates in the film region from 0.13mm to 2mm from the wall. To obtain a sample, the valve was opened until the static pressure just inside the scoop was identical to the static pressure at the same axial location on the opposite side of the

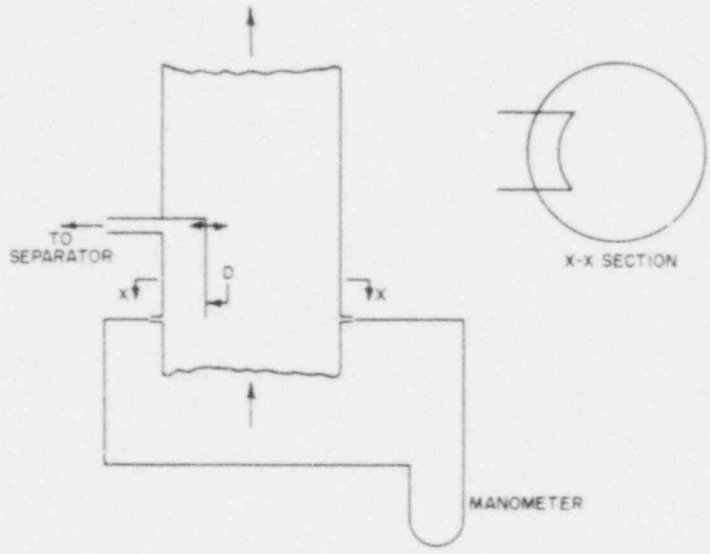

Figure 43 - Schematic of Wall Scoop used at C.I.S.E. [113]
(BNL Neg. No. 9-114-79)

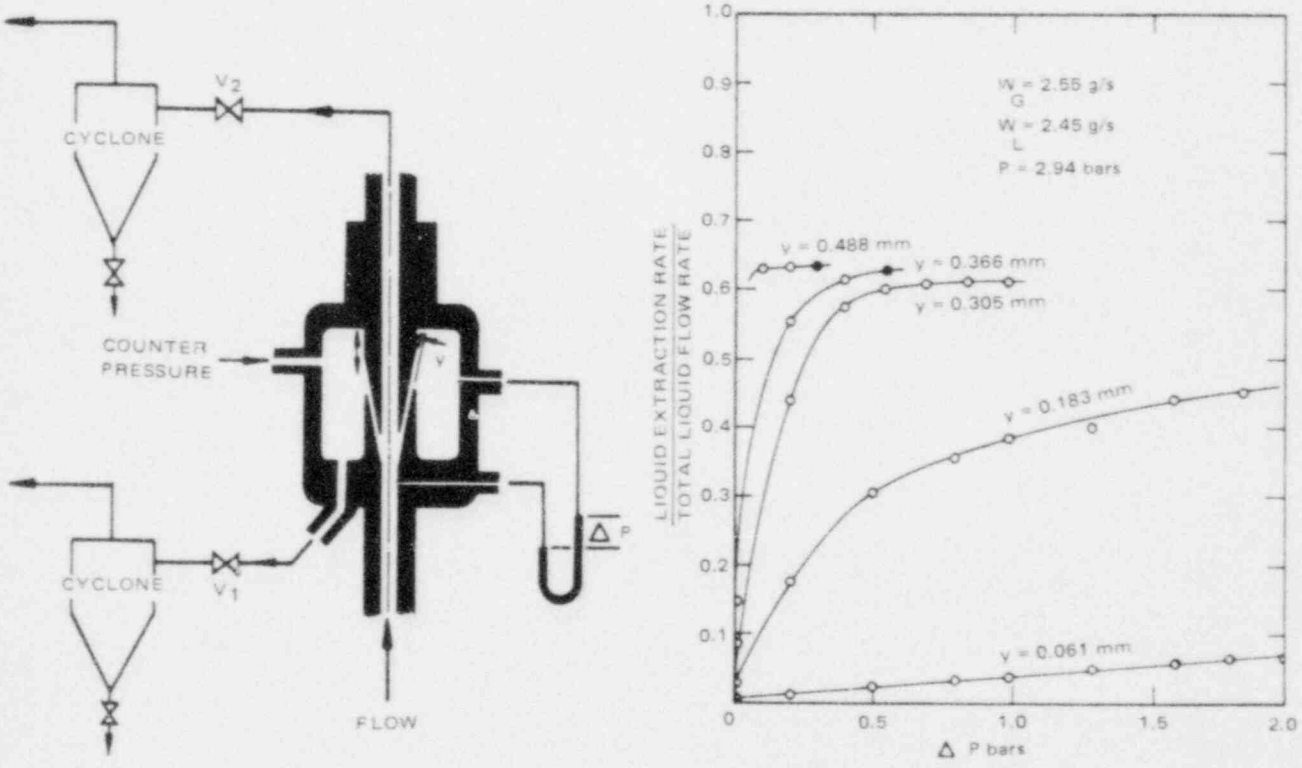

Figure 44 - Film Suction Device used by Truoug Quang Minh and Huyghe [115]
a) left; b) right. (BNL Neg. No. 9-101-79)

tube. The theory is that by matching the static pressures, only minimal disturbance to the flow stream occurs and the sample is thus taken at the undisturbed, "or "isokinetic" conditions. In reducing the data to obtain local values of void fraction an assumption regarding the slip ratio must be made. Cravarolo and Hassid [113] assumed that gas in the film region would occur as small bubbles and that the slip ratios would thus be close to unity. The flow rates, coupled with the known area, also provided information regarding the velocities once the assumption of unity slip was been made. In any event, if the flow rates are accurately known, the phase volume fluxes may also be readily calculated without further assumptions.

One basic disadvantage of this type of instrument is that it disturbs the flow regime irrevocably. In other words, once the film is removed from the wall there is no method of putting it back in the same distribution. Other disadvantages are its limited size which tends to give erroneous readings for very thin or very thick films. In addition, while the method provides reasonable results in two-component flows, single component flows are more difficult to determine accurately due to phase change effects caused by heat losses and pressure drops, and under nonequilibrium conditions become virtually impossible to determine accurately.

Truoung Quang Minh and Huyghe [115] used a somewhat similar device wherein a circumferential slit was provided at a point in a tube. The axial width of the slit could be varied as shown in Figure 44(a). They found that the film flow rate measured would become almost independent of both slit width and differential pressure for widths over a certain minimum, and for differential pressures above some minimum. This behavior is shown in Figure 44(b). As discussed by Moeck [116] both this device and that designed at CISE can underestimate the film flow rate when large waves are present.

4.2. Porous Sampling Sections

Another device which has been used for annular flow studies is the porous sampling section, sometimes fabricated from a sintered porous plate and sometimes from a fine-mesh screen [117-127]. The purpose of this porous sample section is to remove the film of water selectively in annular or dispersed annular flow in order to measure the film flow rates. Typical of the devices used is that used at General Electric's Atomic Power Equipment Department [117] in an annular test section shown in Figure 45(a). Pressure is decreased in the plennum chamber behind the porous plate by opening of a sampling valve. In two-component flow the phases are usually separated and measured separately while the single-component flow the mixture is condensed in a calorimetric device and a heat balance is applied to calculate the mass flow rates of the separate phase. In the case of two components, the liquid flow rate is usually plotted as a function of the pressure drop across the plate and curves similar to those for the wide gap slit sampling device shown in Figure 44(b) are usually obtained; that is, beyond some nominally small differential pressure the sample flow rate does not change for a wide range of differential pressures. The concept of this behavior is that if the sintered plate is sufficiently long, the entire film is removed with little pressure drop and thereafter only additional amounts of core gas are pulled through the porous plate. If sufficient pressure

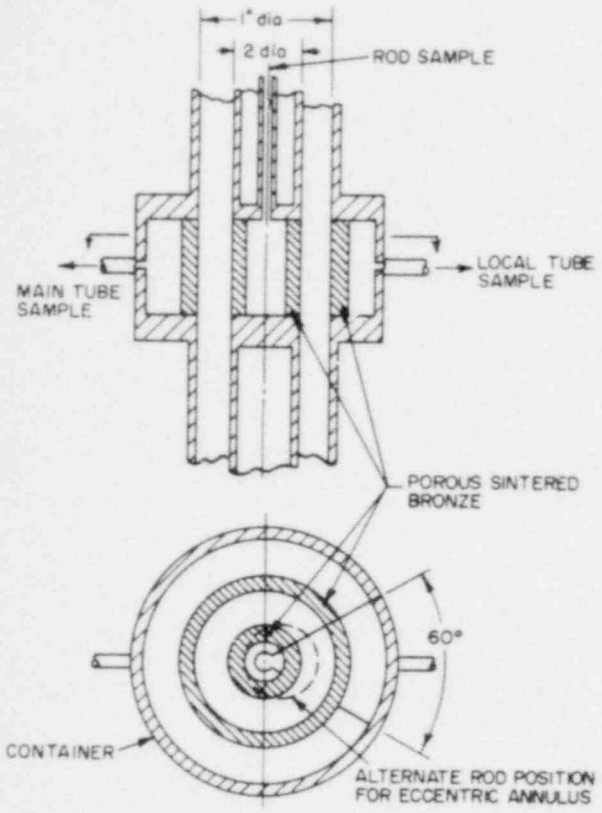

Figure 45(a) Porous plate
(BNL Neg. No. 9-109-79)

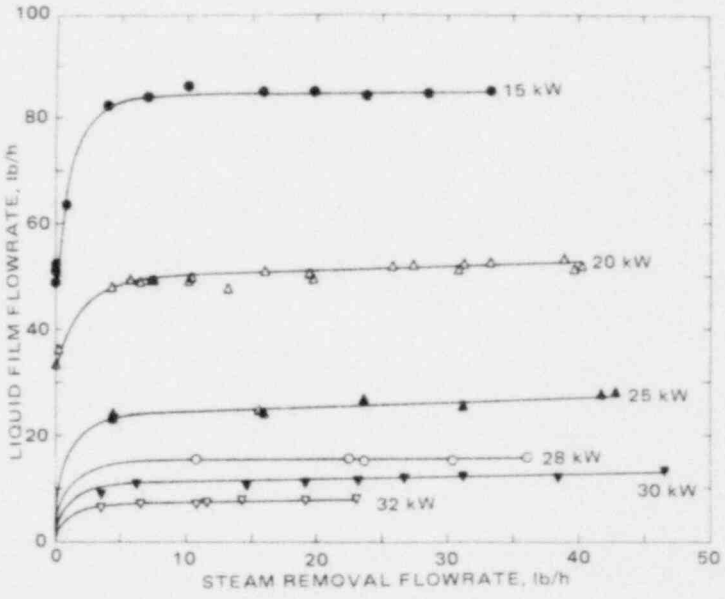

Figure 45(b) Flow data
(BNL Neg. No. 9-92-79)

Typical Design and Results for a Porous Plate Film Flow Sampling Device
(References 117,118)

drop is applied, however, core-borne liquid would also begin to be extracted causing the liquid sample flow rate to increase again. The film flow rate in these cases is defined as the liquid flow rate independent of the pressure drop, the plateau value.

A second method of determining the film flow rate is to plot the liquid flow rate verses the gas phase flow rate. This method has also been the predominant method of determining the film flow in single component fluids. As shown in Figure 45(b), the liquid removal rate becomes quite insensitive to the vapor rate with increasing total sample flow [118]. The plateau in this case can also be quite flat. In some instances such as low quality or where the annular core is highly laden with liquid, the determination of the film flow rate is not so clean cut and various extrapolation schemes must be applied as shown in Figure 46. In addition to uncertainties, Singh et al. [125] showed that in single component flow, similar to two-component cases, the experimentally determined film flow rate was dependent on the length of the porous section due to deposition of core-borne droplets and due to increasingly more efficient capture of the liquid in large roll waves with longer plates.

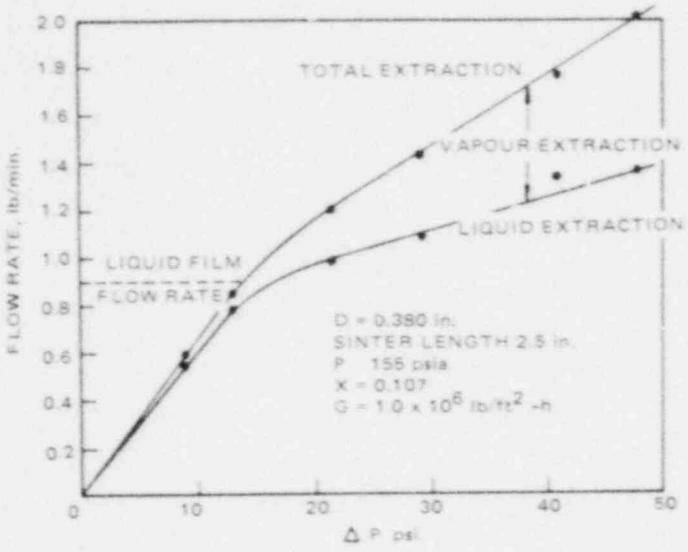

Figure 46(a) - Data of Staniforth et al. [127] (BNL Neg. No. 9-83-79)

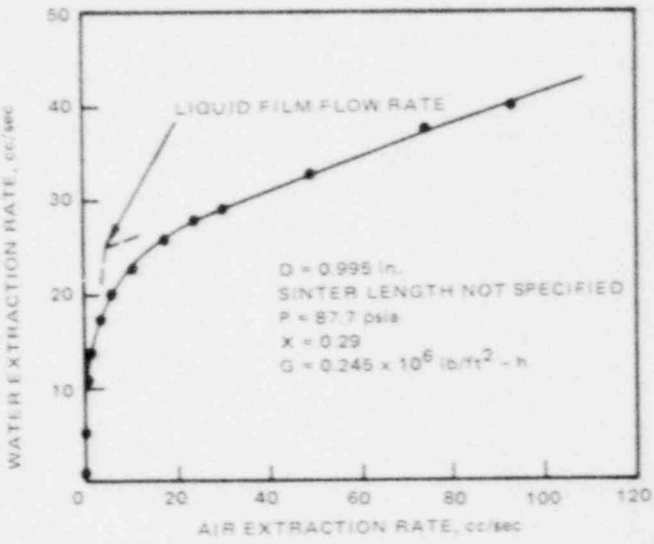

Figure 46(b) - Data of Schraub et al. [126] (BNL Neg. No. 9-82-79)

4.3. Isokinetic Sampling Probe

Where the two previously described mechanical sampling devices have been stationary or slightly moveable and restricted to measuring film flow quantities, a device was developed by CISE [128] for measuring component flow rates and, with the aid of a suitable assumption regarding slip, the void fraction at various locations of a tube cross section. This device has subsequently been used by Lahey, Shiralkar, and Radcliff [129], by Schraub [126,130], Adorni et al. [128], Todd and Fallon [131], and Jannsen [132]. All of these designs are similar in that they resemble a small Pitot-static probe as shown in Figure 47. In general, this probe is used in either of two distinct manners. The first manner is quite similar to the wall scoop in that flow is

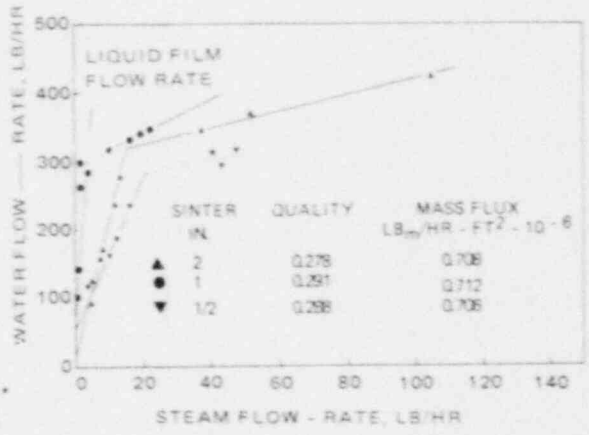

Figure 46(c) - Various Film Sampling Results of Different Investigations (BNL Neg. No. 9-87-79)

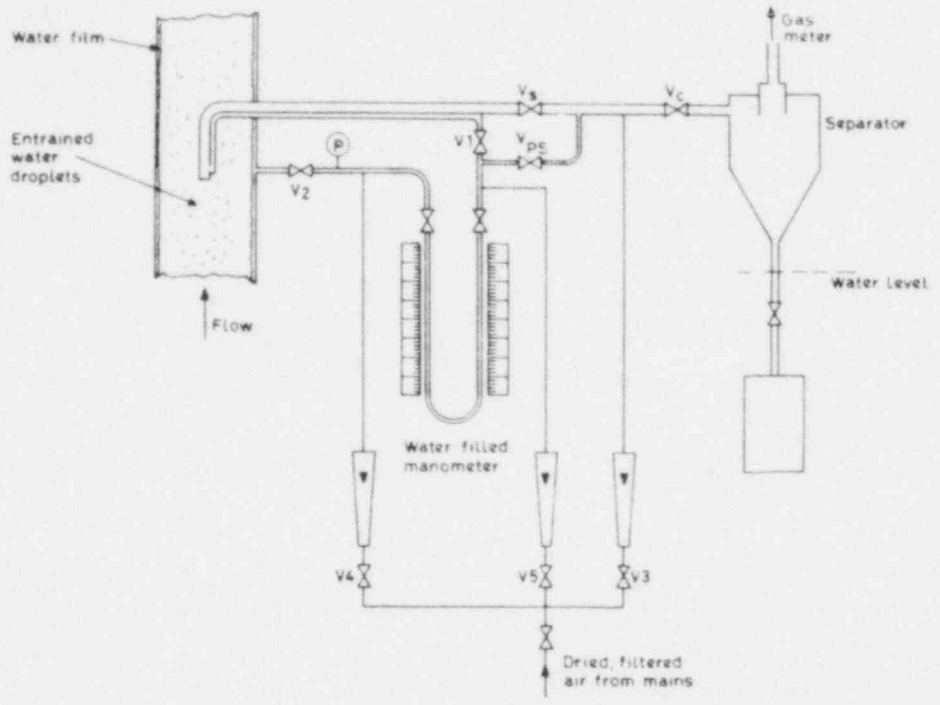

Figure 47 - Isokinetic Probe System as Designed by C.I.S.E. [128]
(BNL Neg. No. 9-102-79)

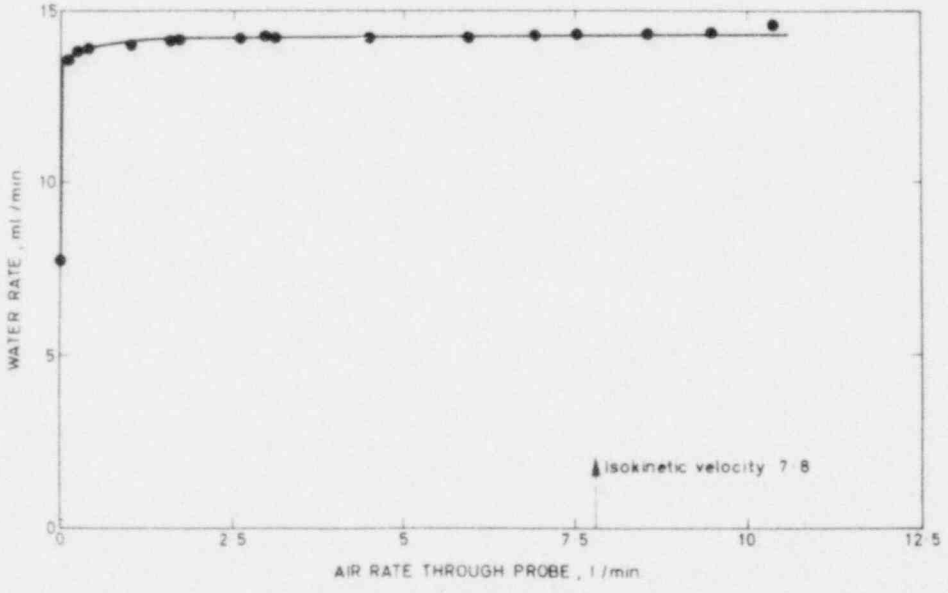

Figure 48 - Typical Results from an Isokinetic Sampling Probe When Used in an Air-Water System. Data of Gill, et al. [139]
(BNL Neg. No. 9-98-79)

drawn off through the main body of the probe until the static pressure near the interior tip of the probe just equals the static pressure in the tube adjacent to the probe opening. Various degrees of sophistication can be employed in the design of such a probe from the very simple device used by Wallis and Steen [133], to that used by Burick, Scheuerman and Falk [134] based on a design by Dussord and Shapiro [135]. Ryley and Kirkman [136], in fact, added a momentum deflector with a floating impulse cage to combine momentum flux measurements with measurements of the mass flow rates of saturated steam and liquid in the exhaust section of a steam turbine. The second method of isokinetic probe operation simply utilizes the probe as a stagnation pressure metering device where reverse purging of one phase or the other, usually the gas, is used to provide a metering reference.

A number of problems exist with the use of the isokinetic probe, not the least of which is the necessity to compensate for the pressure losses between the probe tip entrance and the static pressure port. For small probes Schraub [130] outlines a method to sample at various conditions around the isokinetic condition and then to iterate on the proper conditions by checking the integrated flow profiles against the known values. This is good for two component systems with axisymmetric geometries and perhaps would also work in equilibrium single component systems where this check is possible. In planar or grossly two dimensional geometries, such a system would be extremely difficult. In addition, since the corrections are flow dependent, virtually every reading requires a different correction and profile distortion of measured results would occur.

Another problem lies with the fact that different assumptions lead to different results for the void fraction. The Italians [128] assumed a constant slip in the fluid approaching the probe whereas Schraub [130] assumed variable slip. Schraub [137] mentions, however, that only slightly differing results are obtained with different assumptions. In addition, Shires and Riley [138] show that if the probe is much larger than the dispersed phase, the vapor volume flow fraction is measured whereas if the reverse is true, the vapor volume fraction itself, α, is measured. In spite of these various problems many workers have used this instrument with varying degress of success, mainly because it appeared to be the only general class of instrument capable of providing the desired combination of measurements of phase velocities and void fraction.

A variation on the isokinetic probe has been used by Gill et al. [139] who demonstrated that for two component, slightly laden flows, the measured liquid flow rate is practically independent of sampled gas flow rate as shown in Figure 48. Thus, if only gas core liquid content in annular flow is desired, it is simply sufficient to have a slight amount of gas to obtain a representative liquid flow rate measurement.

4.4. Wall Shear and Momentum Flux Measurement Devices

Various mechanical or electromechanical devices have been designed or adapted for the measurement of skin friction in two-phase flow. The latter type are included herein because these instruments are basically mechanical in nature, using ancillary electrical methods for readout purposes only.

Perhaps the most widely used device for directly measuring wall shear in single-phase flow is the Preston [140] tube which is simply a small right angled total pressure probe which is used when the mouth rests against the wall with its opening directed upstream. Preston's calibration as corrected by Patel [141] relates the dimensionless wall shear stress to the dimensionless dynamic head. This device was used successfully by King [142] with condensing annular-dispersed flow in a 1-inch tube, and by Jannsen [143] in a nine-rod bundle.

Cravarolo et al. [144] devised a null-balancing wall sensor (shown in Figure 49) for measurement of the skin friction within an accuracy in non-fluctuating flows of ~2%. In slug flow, however, they were unable to balance their device. By noting the pressure drop required to just begin to move the sleeve off the lower support, then doing the same to drive the sleeve down off the top support, the average value provided the shear stress without the effects of friction and inertia. Similar to the Preston tube, this device can give the wall shear for a relatively small area of a tube.

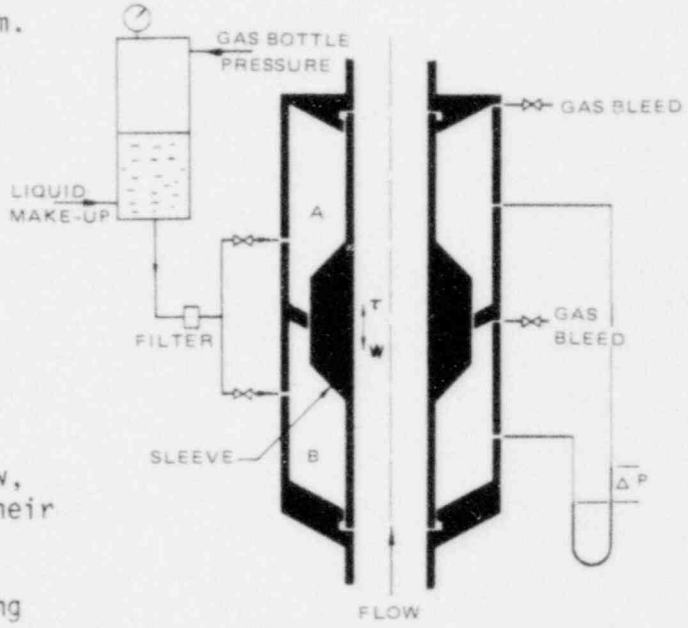

Figure 49 - Schematic Drawing of the Device Developed by Cravarolo et al. for Measurement of Shear Stress on the Wall of a Conduit. [144]
(BNL Neg. No. 9-91-79)

Rose [145,146] suspended his test section between two rubber connectors which allowed it to more freely in the vertical direction (Figure 50). Attached somewhere to the vertical section was a linear, variable, differential transformer (LVDT) assembly which detected small changes in position of the test section itself. The channel was first balanced in an equilibrium position and then deflected by known forces in order to obtain a calibration. Then, starting at the equilibrium position, flow of two-phase mixture is passed through the tube. The deflection of the tube is then due only to the shear stress on the wall and the difference in pressure between the inlet and the outlet of the test section acting on the end areas of the tube. A similar device was designed by King [142] but, because of hardware difficulties was never actually put into service although the method appears promising.

A device for measuring exit momentum flux was built and used by Rose, and subsequently by Andeen and Griffith [147]. This instrument, shown in Figure 51, is simply a device to change by 90° the direction of flow at the annular channel and measure the force required to do this. With an LVDT apparatus, similar to that described for his wall shear-stress instrument, Rose measures the forces needed to deflect the flow stream. Thus, the measurement of exit

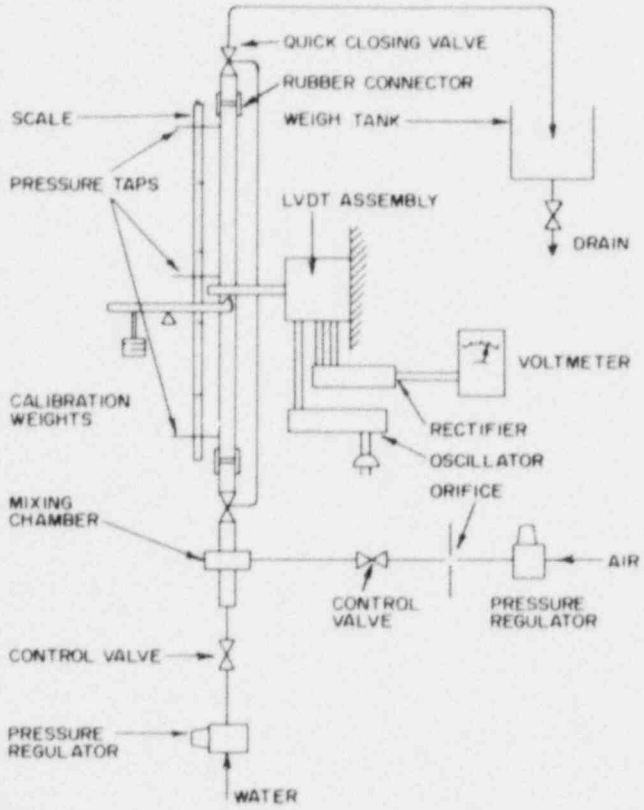

Figure 50 - Diagram of the Vertical Tube Apparatus Used by Rose. (Reference 146) (BNL Neg. No. 9-110-79)

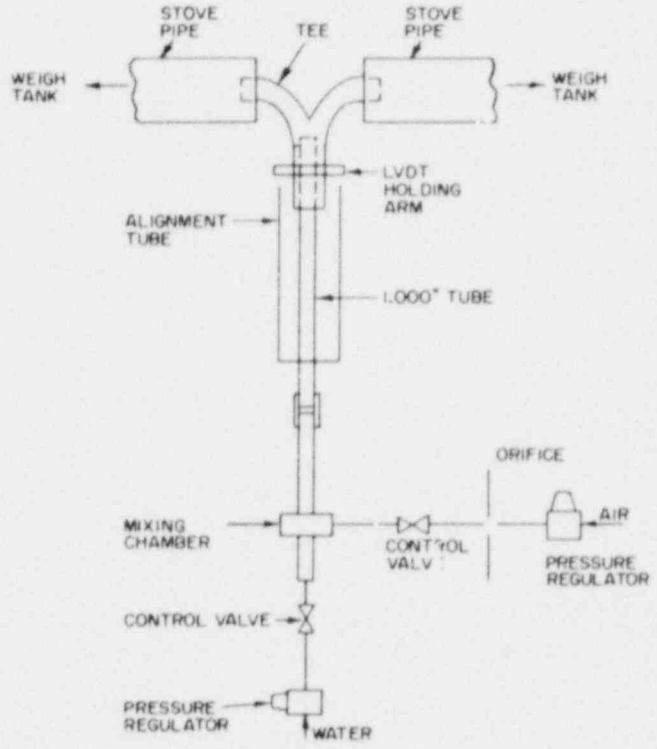

Figure 51 - Schematic Diagram of the Exit Momentum Efflux Measurement System Used by Rose and by Andeen (References 146 and 147) (BNL Neg. No. 9-117-79)

momentum flux, combined with a knowledge of the inlet momentum flux, and the integrated wall shear stress can result in accurate values for the component or pressure drop due to elevation and average channel vapor fraction.

5. OUT-OF-STREAM MEASURING DEVICES

This class of instruments consists of those whose measurement ability depends on the attentuation or reflection of electromagnetic radiation or atomic particles. Excellent reviews of light photography methods are given by Arnold and Hewitt [148], Cooper et al., [149] and by Hsu et al. [150], and will not be discussed herein. The majority of those methods are aimed at obtaining qualitative information. Indeed, visual examination of photographs has been one of the major methods of flow pattern determination to date. On the other hand, the attenuation of non-visable radiation has come to be the most widely used method of obtaining quantitative measurements of void fraction to date.

Of all the methods used, the most popular involves the attenuation of the strength of a concentrated beam of photons (γ- or X-rays). This method is popular mainly because measurements may be made of space averaged void fraction along a chord length without disturbing the fluid to a noticeable degree. This attentuation technique has generally been used to obtain average measurements of void fraction in steady systems [154-156] or systems with slowly varying transients (< 10 HZ). Schroch [158], however, has had some success with more rapidly varying signals, and Jones [53,157,159] has reported a system capable of measuring transients in the millisecond range. More recently, high intensity, high energy systems have been developed and used for rapid transients in large pipes, driven by the emphasis on large scale nuclear safety tests [171,172].

There are basically four types of void measurement systems using attenuation techniques:

a) X-ray systems where a source of electromagnetic radiation in the general range of 25 - 60 kev is provided by an X-ray tube.

b) γ-ray system where the source is a radioisotope which emits photons with energies usually between 40 and 100 kev.

c) γ-ray systems which obtain a stream of electrons from a radio-isotope with energies up to 10 mev.

d) Neutron systems where neutrons are supplied by a source in the range up to about 1 mev.

The general problems of attenuation methods are similar for all four systems and shall be discussed shortly. The basic differences between these systems lie in the differences in the attentuation laws and the hardware required to accomplish the measurement. Otherwise, the overall concepts are similar as discussed by Schrock [160]. The choice of a method then usually is dependent on the experimental constraints, cost, hardware availability, etc., rather than on the desirability of one system over another for reasons of accuracy or ease of application.

5.1. X-Ray and Gamma Ray Methods

From a source standpoint, only the X-ray system does not require a nuclear or radioisotopic source. Instead, X-rays are generated in a vacuum tube where a high potential is applied between a target of a specific material, and a heated filament. Electrons which are "boiled" off the filament are accelerated in the potential field toward the target. Target material may be of any element but is usually of high melting temperature and high atomic number such as Tungsten or Molybdenum. Since a large amount of heat is usually generated, these targets are sometimes made hollow to permit circulation of cooling water. About 99% of the electrons striking the target simply give off their energy in the form of heat upon being decelerated. The remaining 1% will give off a spectrum of electromagnetic radiation, X-rays, having energies from zero up to the maximum energy of an incident electron. In addition, since some electrons will knock bound electrons from atoms of the target material, other electrons will fall back into these vacancies giving off particular quanta of X-radiation characteristic of the material and the energy level vacated. This latter effect tends to produce a localized maxima in the X-ray energy spectrum at these characteristic energies. Filtering of the emitted X-ray beam may be used to remove lower energy radiation, producing a beam of X-ray of nearly monoenergetic characteristics near the characteristic energy.

The advantage of using X-rays lies in the lack of bulky source holders and the repeatability and long term stability of the source strength. The disadvantages lie in the short term unsteadiness in the source due to the alternating portion of the applied voltage. This problem has severely limited the capabilities of transient systems such as those used by Schrock [158] and Zuber et al. [161]. Jones, [157,159], however, used special filtering techniques in the high voltage side of his X-ray transformer supply to reduce the induced thermal ripple in the beam strength [160-162] to a negligible amount. In an attempt to minimize the effects of short term unsteadiness, many users have employed dual beam X-ray tubes where one beam was used for the test while the other served as a reference. In theory, then, the ratio of the intensities of the two beams removes the original source from consideration.

A schematic of such a system is shown in Figure 52 as taken from Reference [160]. This is a typical dual-beam system where, in this case, Schroch used a tungsten target operated at 100 kv with a tungsten filter. The result was a sharp resonant peak in the 50-70 kev range, corresponding

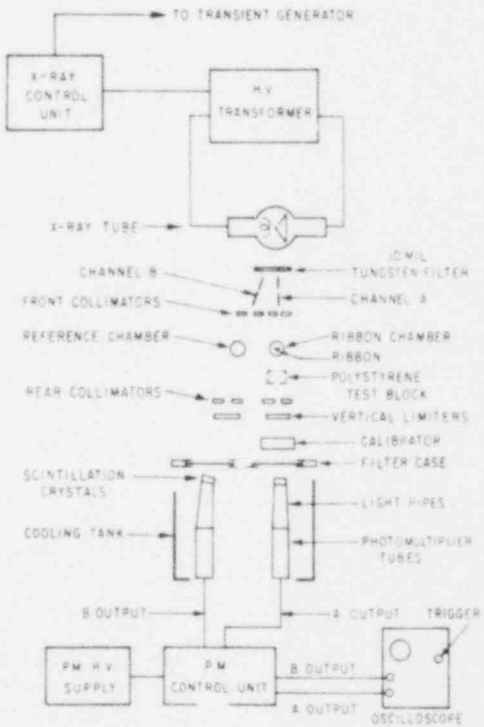

Figure 52 - Schematic of X-ray Densitometer System [160] (BNL Neg No. 9-100-79)

to the lowest electron quantum level, K_α, of 58.5 kev, and the second, K_β, level of 68 kev. Detection and measurement of each beam intensity was by means of a Thallium-activated, sodium-iodide crystal which absorbs X-rays wave length radiation and gives off radiation in the visible range in its place. While the crystal has some self absorption, the emergent intensity of the visible light is proportional to the incident X-radiation intensity. Light-piping was employed to direct the scintillated light to photomultiplier tubes which produced an electrical current proportional to the incident light intensity. The output from the two photomultipliers was then differentially amplified, and recorded. Additional problems in such a system include the inability to obtain well-matched photomultiplier tubes, differences in the fatigue or short term aging characteristics of the tubes, and problems in maintaining a stable excitation voltage for the pair of detectors.

For both X- and γ-rays, the intensity of a beam, I, of original intensity, I_0, is given by

$$I = I_0 e^{-\mu x} \tag{12}$$

where μ is the linear absorption coefficient and is dependent both on the material and the energy of the photons, and x is the thickness of the absorber. The major difference between the X-ray and γ-ray systems is the source. γ-rays are identical in nature to X-rays. Historically, however, γ-rays were usually extremely energetic, being obtained from radioisotopes and having wave lengths much shorter than those generally associated with X-rays. In general usage, however, the term now applies to any photons originating from a nucleus while the term X-ray is reserved for similar but extra-nuclear radiation. Since γ-rays are obtained from nuclear disintegration, the source strength is time-dependent. Thus, the half life of the source material becomes as important a consideration as the strength of the beam. Since the uncertainty (1 standard deviation) in a measurement of beam intensity is equal to the square root of the number of events measured, an intense beam from a highly radioactive source must be used to minimize observation time. The level of radioactivity measured in curies, (1 ci = 2.22×10^{12} disintegrations/min), is dependent on the half life, (time to disintegrate 50% of the material), and the mass of the element, (total number of atoms available for radioactive decay). A short half life material requires frequent recalibration whereas a long half life material of acceptable disintegration rate must be massive and necessarily hazardous to handle. In addition, most systems have been concerned with measuring voids in water-metal or freon-metal systems. Since the linear absorption coefficient for photon attenuation decreases more rapidly with increasing energy for water than for most metals, energies less than 100 kev are desirable from a sensitivity standpoint. The three radioisotopes which have found the most use are compromises based on the above factors and include Thulium-170, Samarium-145, and Gadolinium-153. The table below taken from Reference [160] gives the half life and γ-energies of these materials.

Table 2 - Popular isotopes for void measurements

Isotope	Half Life (days)	γ-Energies kev
Samarium-145	240	39-61
Gadolinium-153	240	42-72
Thulium-170	170	52-84

The advantages of γ-sources over X-rays are principally in cost, short term stability, and simplicity. Since short term stability is not a problem, dual beam systems become unnecessary. In addition, high voltage supplies and regulating systems are not required.

In general, X- and γ-ray systems have been the most popular void measuring technique used to date. Extensive discussion of the errors associated with these techniques was presented by Hooker and Popper [162], with exception of errors due to the fluctuations in nonlinear signal [157,159,163-166]. In the system described by this reference, a one-shot method was designed to measure the voids for the entire cross section of a 0.5 x 2.175-inch rectangular channel by collimating a thulium-170 source parallel to the wide plates of the channel. They identify errors due to the following sources:

a) Errors in the electronics system due to such characteristics as amplifier drift, photomultiplier gain sensitivity to small changes in the supply voltage, and temperature sensitivity of the sodium-iodide crystal.

b) Errors in measuring technique due to measurement of γ's which reach the detector by some path other than through the test section, strip chart reading errors, and errors due to calibration at non-test conditions.

c) Errors due to decay of the source.

d) Errors due to Preferential Phase Distributions

For a uniform distribution of voids, Hooker and Popper concluded that the maximum absolute errors in such a system is about 2.5% voids over the entire range of 0-100% voids. Similar conclusions have been reached for X-ray systems as well, and, in References 157, 159, 160, and 163 an estimate was given of absolute error of 1.7% voids is given for stationary measurement of local void fraction and 2.3% voids for local measurement during a transverse void profile scan.

The errors indicated above do not take into consideration additional errors due to void streaming effects in preferential void distributions, nor errors due to linear averaging of a nonlinear, fluctuating quantity. Hooker and Popper discuss the former errors associated with nonhomogeneous phase distributions. Basically these errors arise when liquid and vapor phases are separate, the

limiting geometry possible being layers of liquid and gas whose planes are parallel to the beam of photons. In this case, the attentuated beam can be considered as two separate beams, one having passed through the gas and the other having passed solely through the liquid. The total intensity is, then, the sum of the individual intensities, each of which has been separately attentuated. The result is not the ideal exponential attenuation law normally employed in data reduction. Petric and Swanson [206] verified this source of errors and showed that typical one-shot measurement techniques could be off by up to 40%. Errors of the same order or larger were also predicted by the writer [159,163] to arise due to the fact that two-phase flow is by nature a nonstationary phenomena. Thus time averaging of a quantity nonlinearly related to the desired quantity, in this case void fraction, leads to significant errors when the void fraction is calculated from the average. These errors were verified by Harms and his co-workers [164-166] in consideration of their neutron experiments.

In the case of void streaming errors, these errors may be significantly reduced or eliminated by reduction of the beam size with respect to the voids, and also by reducing the length of the measurement path, thereby reducing the magnitude of the fluctuations in intensity. Problems associated with the fluctuation source of errors may be eliminated by linearizing the signal with respect to the desired quantity, or by sampling on time scales smaller than the fluctuation periods of interest. Many workers have used fine collimation to reduce photon streaming errors [161, 156, 167-169]. One has used linearlization to eliminate fluctuation errors [157,159] and, to the writer's knowledge, only one group has attempted to use alternative methods [164-166] (i.e., short term sampling), to circumvent this problem. In the latter case, however, sampling periods were not judged by this writer to be sufficiently short to eliminate all errors.

Quite recently, the γ-ray or X-ray methods have been extended to multibeam techniques where multiple beams, spreading radially from a single source or in parallel from separate sources, to individual detectors are used. These methods have been utilized most recently in the large scale testing programs being undertaken for nuclear safety studies. Single-source systems have been described by many workers such as Smith [170] who used five beams in a vertical plane plus two references to characterize phase distributions in a horizontal pipe during blowdown experiments. Cut-metal windows, (sometimes Berillium filled), were used for high pressure access while otherwise standard scintillation crystal and photomultiplier instrumentation methods were used. Similarly, Yborrando [171] utilized a γ-ray system having a single source. Lassahan et al. [172] recently summarized the technology of X-ray and γ-ray techniques. Such devices are useful compromises for discerning cross-sectional flow variations where flow stratification exists under transient conditions, but their usefulness where a high degree of accuracy is required is limited.

All but one multi-beam system to date have been static, non-traversing, systems usually Cs-137 or Co-60. As such, except in high water-to-metal mass thickness ratio systems, sensitivity tends to be limited and parasitic attenuation high. In a newly described system, however, Ahuaf et al. [173], describes instead a parallel 5-beam, traversing system utilizing 5 separate Thulium-170 sources. The solid state detection and readout system has been

previously described [174] utilizing Cd-Te crystal detectors requiring no elaborate thermal stabilization techniques and using standard nuclear instrumentation. The 84-kev resonance is used since it has the highest activation efficiencies of ~3%, requiring only 30-35 Ci total source activity for each effective Curie at 84-kev. 84-kev source strengths of 1-5 Ci have been reported with activation up to 30 Ci or more expected. The major difficulty encountered was impurity activation, here-to-fore unencountered by other isotope researchers. It was found that any impurity having a highly efficient, high decay energy resonance would lead to difficulties necessitating unwieldy shielding. If impurity levels were maintained at less than 100 ppb, than 2.5 cm of lead would be sufficient at 30 Ci (84-kev) activation level to keep radiation levels at one foot at 3 mr/hr or less except in the beam. At high source strengths, however, the low energy edge yields an extremely sensitive beam with good transient response capabilities.

5.2. Beta-Ray Methods

In 1961, Perkins, Yusuf, and Leppert [175] made the following assessment of γ-attentuation methods:

> "...the γ-method is reasonably accurate for the determination of void volumes under the following conditions: (1) the voids are distributed in a homogeneous manner; (2) the test section offers a radiation path of greater than about 2500 mg/cm^2 (equivalent to one inch of water); and (3) the void fraction is greater than 25%. For smaller void fractions, smaller channels, or preferential distributions, the gamma technique may not offer sufficient accuracy."

While methods and accuracy of β-ray techniques have improved considerably since then, the methods they outlined are worthwhile as representative of the β-ray method of void measurement. Specifically, β-rays are really made up of a stream of electrons emitted at high energy from a radioisotope. The basic method of attenuation for electrons is different than for photons. Attenuation of X-rays and γ-rays is caused by photoelectric effects where X-rays are completely absorbed by ejecting electrons from the absorbing material, and by Compton or recoil scattering where only partial energy loss of a photon occurs with the electron ejection and a new photon of longer wavelengths is emitted. In both cases the electron density of the abosorbing medium is important because interaction is primarily with material electrons. Likewise, the electron density is important for the absorption of β's or free electrons. Just as when electrons decelerating in a target of an X-ray tube generate X-rays, so do they decelerate in any absorber. This loss of energy is caused by both electron interaction and nuclear interaction. The result is some X-ray production in a continuous spectrum of wavelengths called bremstrahlung. Up to a certain thickness of a material this absorption is exponential, similar to photon attenuation. However, over a certain thickness the absorption coefficient is nearly the same for all absorbing materials. The mass per unit area required to produce a given beta absorption is nearly independent of material type and is called the stopping distance or range of the material. The thickness required to stop a β-particle is then the range divided by the material density. The range of an electron, as seen in Figure 53, is necessarily dependent on the initial energy since absorption is mainly by collision. Thus, for water density of 1 gm/cc, a 2 mev electron will be stopped by about 1 cm of water.

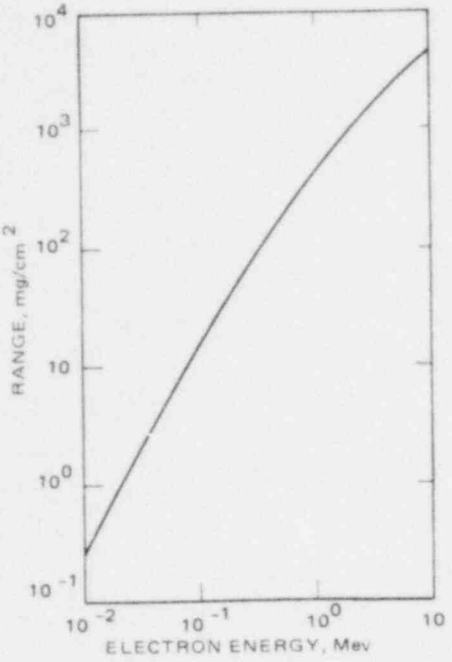

Figure 53 - Range of Beta Particles in Water [160]
(BNL Neg. No. 9-95-79)

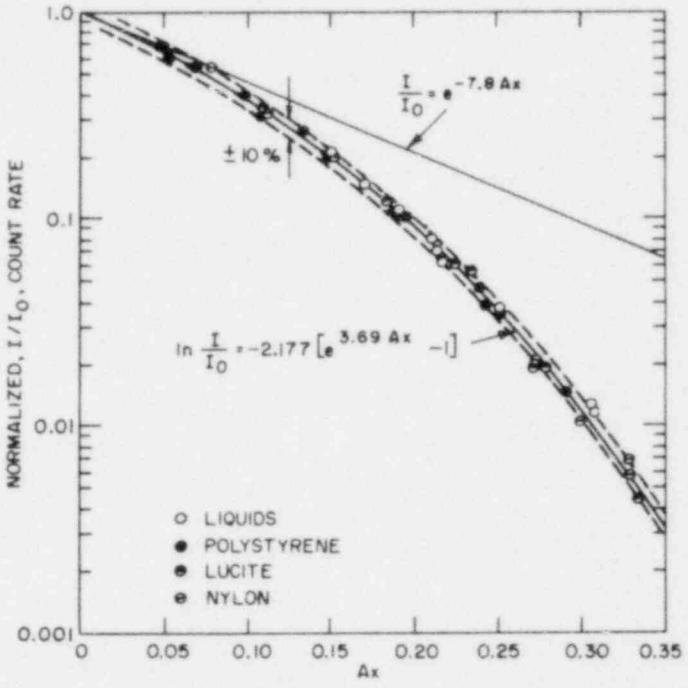

Figure 54 - Experimental Results for Absorption of Betas [175] (BNL Neg. No. 9-118-79)

While β-absorption is exponential for thin absorbers, Perkins, Yusuf, and Leppert [175] found that a more general law for β's was

$$\ln \frac{I}{I_0} = -2.177 \left\{ e^{3.69Ax} - 1 \right\} \qquad (13)$$

where A is proportional to the equivalent linear absorption coefficient.

For small thickness (13) degenerates to

$$I = I_0 \, e^{-7.8Ax} \qquad x \sim 0 \qquad (14)$$

These two equations are compared in Figure 54 and it is seen that exponential-like absorption occurs for values of Ax up to about 0.05.

There are two major advantages in using betas for void measurements where complete absorption doesn't occur. First, the sensitivity is greater. Perkins et al. [175] using a Strontium-90 source producing 2.26 mev betas found a sensitivity ratio between the full and empty case of 82:1 whereas for photons of about 60 kev the ratio would have been about 1.15:1. In addition, shielding is not a major obstacle since β's are absorbed readily in most dense materials. A major disadvantage however exists due to the advantage of high sensitivity. That is, due to the high attenuation rates, massive sources are required to obtain event rates at a test detector which would allow accurate transients to be measured. Since electrons are absorbed in the source itself, (self shielding), use of betas becomes impractical for this application.

5.3. Neutron Methods

Lastly, neutron attenuation has been used occasionally to measure void fraction in high pressure channels. Sha and Bonilla [176] employed a Sb-Be neutron source to measure voids within 3% in simulated rod bundle geometry. Sensitivities of over 20 times that of Tm^{170} gammas was obtained. More recently Moss and Kelly [177] measured film thicknesses in a heat pipe to an accuracy of 0.006 inches out of 0.125 inches while Harms and company [178-180] measured void fractions by the one-shot method to an accuracy of 6.5% between 3% and 70% voids. Neutrons being uncharged are not subject to coulomb scattering as are the charged particles including beta rays. If elastic scattering is the predominant mode of neutron slowing down, the lightest elements will tend to take on the largest percentage of the neutron current energy. Thus, in any given collision, neutrons are attenuated much more rapidly by the hydrogen atoms in water than by metallic atoms in, say, a test section wall, and so the sensitivity of void measurement approaches that of the β-ray equipment unhindered by the metal walls of a test section. For a water system it was found [180] that the attenuation law obtained was

$$I = I_0 B(x) e^{-\mu x} \tag{15}$$

where

$$B(x) = 1 + 1.011\ x^2 - 0.475\ x^4 + 0.488\ x^6 \tag{16}$$

Currently, however, the use of neutrons as a test vehicle is extremely limited due to the inaccessibility and general unavailability of nuclear reactors and the high cost of intense alternative sources.

6. SUMMARY

This summary has attempted to outline the basic methodologies used in making two-phase flow measurements today. Rather than provide an up-to-date research synopsis and critique carefully including every latest reference in characteristic sophisticated scientific manner, the writer has instead tried to review the fundamental methods which have found wide acceptance and utilization, and which have provided workers with insight into the mechanics of two-phase, gas-liquid flows. The difficulties of using each approach have been identified and important advances which are expected to lead to significant improvements listed. For the beginning researcher or for the engineer wishing to gain an overview, this is probably already too much.

Specifically, this summary has discussed the design, use, interpretation, and difficulties associated with the following techniques.

A) Instream Sensors with Electrical Output Including:

1) Conductivity Devices

a) Level Probe

b) Needle Probes

c) Wall Probes

2) Impedance Void Meters

3) Hot Film Anemometer

4) Radio Frequency Probe

5) Microthermocouple Probes

6) Optical Probes

a) Glass Rod System

b) Fiber Bundle System

c) U-Shaped Fiber System

d) Wedge-Shaped Fiber System

B) Instream Sensors with Mechanical Output Including:

1) Wall Scoop

2) Porous Sampling Sections

3) Isokinetic Sampling Probe

4) Wall Shear and Momentum Flux Measurement Devices

C) Out-of-Stream Techniques including:

1) X-ray and Gamma-ray Methods

2) Beta-ray Methods

3) Neutron Methods

7. ACKNOWLEDGEMENTS

This manuscript was originally prepared for the Minnesota Short Course on Fluid Mechanics Measurements, given at the University of Minnesota's Department of Mechanical Engineering during the week of September 10-13, 1979. Certain portions of this manuscript were extracted from the author's prior publications, especially Reference 9. This work was performed under the auspices of the U.S. Nuclear Regulatory Commission.

8. NOMENCLATURE

8.1. English

a	Capillary length
A, A_i	Area, Interfacial area
C, C_1	Coefficients (Eqn. 7-9)
d_1, d_2	r-f probe tip dimensions (Fig. 27)
E, E_{max}	Anemometer probe voltage, (maximum)
f_c	Correlation function (Eqn. 7)
g	Gravitational acceleration
i	Enthalpy
I	Photon intensity
j	volume flux
K	Correlation coefficient (Eqn. 8)
n	Index of refraction
N	Count
N_{Ca}	Capillary number
N_{Go}	Gocher Number
q	heat flux
R, R_p	Radius, probe resistance
S	Area of PDF
t	Time
$\Delta t_1, \Delta t_2$	Time delays associated with d_1 and d_2.
U	Optical Probe Signal, velocity
x	Thickness
y	Distance from wall
z	Streamline coordinate

8.2. Greek

α	Vapor volume or area fractions
β	Vapor volume flow rate fraction
β_w	Water layer angle (optical probe)
μ	Viscosity or linear atenuation coefficient
Γ_v	Rate of vapor generation per unit volume
ξ_i	Interfacial perimeter in A
σ	Surface tension
ρ	Density

8.3. Subscripts

B	Bubble
c	Computed
g	Gas
i	Initial or interfacial
ℓ	Liquid
m	Measured
max	Maximum
v	Vapro
w	Withdrawal

9. REFERENCES

1. Jones, O. C. Jr. and Zuber, N., "Slug-Annular Transition With Particular Reference to Narrow Rectangular Duct," presented at the 1978 International Seminar for Momentum Heat and Mass Transfer in 2-Phase Energy and Chemical Systems, Dubrovnik, Yugoslavia, September 4-9, 1978.

2. Jones, O. C. Jr. and Zuber, N., "Interfacial Passage Frequency for Two-Phase, Gas-Liquid Flows in Narrow Rectangular Ducts," presented at The Institution of Mechanical Engineers Conference, September 13-15, 1977, and published in Heat and Fluid Flow in Water Reactor Safety, 5-10, I Mech E, London, 1977.

3. Jones, O. C. Jr. and Saha, P., "Non-Equilibrium Aspects of Water Reactor Safety," Thermal and Hydraulic Aspects of Nuclear Reactor Safety: Vol. 1. Light Water Reactors, O. C. Jones and S. G. Bankoff, Ed., ASME, 1977.

4. Jones, O. C. Jr. and Zuber, N., "Post-CHF Heat Transfer: A Non-Equilibrium, Relaxation Model," presented at the AIChE-ASME Heat Transfer Conference, Salt Lake City, Utah, August 15-17, 1977.

5. LeLourneau, B. W., and Bergles, A. E., Ed., Two-Phase Flow Instrumentation, ASME, (1969).

6. Hewitt, G. F., and Lovegrove, P. C., "Experimental Methods in Two-Phase Flow Studies," EPRI Report NP-118, (1976).

7. Delhaye, J. M. and Jones, O. C., "A Summary of Experimental Methods for Statistical and Transient Analysis of Two-Phase Gas Liquid Flow," Argonne Report ANL-76-75, (1976).

8. Hewitt, G. F., Measurements of Two-Phase Flow Parameters, to be published by Academic Press, (1978).

9. Jones, O. C., and Delhaye, J. M., "Transient and Statistical Measurement Techniques for Two-Phase Flows: A Critical Review," Int. J. Multiphase Flow, 3, 89-116, (1976).

10. Hsu, Y. Y., Ed., "Two Phase Flow Instrumentation Review Group Meeting," NUREG-0375, (1977).

11. Collier, J. G., Convective Boiling and Condensation, McGraw-Hill, New York (1972).

12. Kordyban, E. S., and Ranov, T., "Experimental Study of the Mechanism of Two-Phase Slug Flow in a Horizontal Tube," Winter Annual ASME Symposium on Multiphase Flow, Philadelphia, November, 1963.

13. Solomon, V. J., "Construction of a Two-Phase Flow Regime Transition Detector," MS Thesis, Mechanical Engineering Department, MIT, June, 1962.

9. REFERENCES (Continued)

14. Griffith, P., "The Slug-Annular Flow Regime Transition at Elevated Pressure," ANL-6796, November, 1963.

15. Neal, L. G., and Bankoff, S. G., "A High Resolution Resistivity Probe For Determination of Local Void Properties in Gas-Liquid Flow," AIChE J., 9. 4, 490, (1963).

16. Nassos, G. P., "Development of an Electrical Resistivity Probe for Void Fraction Measurements in Air-Water Flow," ANL-6738, June, 1963.

17. Wallis, G. B., "Joint US - Euratom Research and Development Program," Quarterly Progress Report, July, 1963.

18. Jannsen, E., "Two-Phase Flow and Heat Transfer in Multirod Geometries," GEAP-10214, April, 1970.

19. Haberstroh, R. E., and Griffith, P., "The Slug-Annular Two-Phase Flow Regime Transition," ASME Paper No. 65-HT-52, 1965.

20. Chevalier, H., Lakme, C. and Max, J., "Device for the Study of Bubble Flow within a Pipe," English Patent Application No. 36315/65, August, 1965.

21. Gardner, G. C., and Neller, P. H., "Phase Distributions in Flow of an Air-Water Mixture Round Bends and Past Obstructions at the Wall," Paper No. 12, IMechE Conference, Bristol, 1969.

22. Yu, H. S., and Sparrow, E. M., "Experiments on Two-Component Stratified Flow in a Horizontal Duct," ASME Paper No. 68-HT-14, August, 1968.

23. Jannsen, E., "Two-Phase Flow and Heat Transfer in Multirod Geometries, Eighteenth Quarterly Progress Report January 1 - March 31, 1970," GEAP-10214, April, 1970.

24. Akagawa, K., "Fluctuations of Void Ratio in Two-Phase Flow," Bul. JSME, 7, 25, 122, (1964).

25. Lafferty, J. F., and Hammitt, F. G., "A Conductivity Probe for Measuring Local Void Fraction in Two-Phase Flow," Nuc. Appl., 3, 317, (1967).

26. Jannsen, E., "Two-Phase Flow and Heat Transfer in Multirod Geometries," Fourth and Fifth Quarterly Progress Reports," GEAP-5056, January, 1966.

27. Collier, J. G., and Hewitt, G. F., "Film Thickness Measurements," ASME Paper 64-WA/HT-41, (1964).

28. Hewitt, G. F., and Lovegrove, P. C., "Comparative Film Thickness and Holdup Measurements," AERE-M-1203, April, 1963.

9. REFERENCES (Continued)

29. Hall-Taylor, N., and Hewitt, G. F., "The Motion and Frequency of Large Disturbance Waves in Annular Two-Phase Flow of Air-Water Mixture," AERE-R-3952, June, 1962.

30. Hewitt, G. F., and Wallis, G. B., "Flooding and Associated Phenomena in Falling Film Flow in a Tube," AERE-R-4022, May, 1963.

31. Hewitt, G. F., Kearsey, H. A., Lacy, P.M.C., and Pulling, D. J., "Burnout and Film Flow in the Evaporation of Water in Tubes," AERE-R-4864, March, 1965.

32. Butterworth, D., "Air-Water Climbing Film Flow in an Eccentric Annulus," AERE-R-5787, May, 1968.

33. Moeck, E. O., "The Design, Instrumentation, and Commissioning of the Water-Air-Fog Experimental Rig (WAFER)," APPE-1, Atomic Energy of Canada Ltd., January, 1964.

34. Wickhammer, G. A., Moeck, E. O., MacDonald, I.P.L., "Measurement Techniques in Two-Phase Flow," AECL-2215, October, 1964.

35. Hewitt, G. F., King, R. D., and Lovegrove, P. C., "Techniques for Liquid Film and Pressure Drop Studies in Annular Two-Phase Flow," AERE-R-3921, March, 1962.

36. Adorni, et al., "Experimental Data on Two-Phase Adiabatic Flow; Liquid Film Thickness, Phase and Velocity Distribution, Pressure Drop in Vertical Gas-Liquid Flow," EURAEC-150, (CISE Report R35) (1961).

37. Hewitt, G. F., and Lovegrove, P. C., "Comparative Film Thickness and Holdup Measurements in Vertical Annular Flow," AERE-M-1203, April, 1963.

38. Iida, Y., and Kobayasi, K., 1969, "Distributions of Void Fraction Above a Horizontal Heating Surface in Pool Boiling," Bull. J.S.M.E., 12, pp. 283-290.

39. Iida, Y., and Kobayasi, K., 1970, "An Experimental Investigation of the Mechanism of Pool Boiling Phenomena by a Probe Method," Heat Transfer, Vol. 5, pp. 1-11, Elsevier, Amsterdam.

40. Kobayasi, K., 1974, "Measuring Method of Local Phase Velocites and Void Fraction in Bubbly and Slug Flows," presented at the Fifth Int. Heat Transfer Conf., Round Table RT-1.

41. Reocreux, M. and Flamand, J. C., 1972, "Etude de l'utilisation des sondes resistives dans des ecoulements diphasiques a grande vitesse" CENG, STT, Rapport interne No. 111.

42. Tawfik, H., Alpay, S.A., and Rhodes, E., "Resistivity Probe Error Study Using a Two-Dimensioonal Simulation of the Electrical Field in a Two-Phase Media," Proc. 2nd Multiphase Flow and Heat Transfer Symposium-Workshop, Miami Beach, Florida, April 16-18, 1979.

44. Sheppard, J., private comnmunication.

45. Sekoguchi, K., Fukui, H., and Sato, Y., "Flow Characteristics and Heat Transfer in Vertical Bubble Flow," Proc. Japan-U.S. Seminar on Two-Phase Flow Dynamics, 107--127, Kobe, July 31-August 3, (1979)

46. Block, J., private communication.

47. Gouse, S.W. Jr., "Void Fraction Measurement," AD-600524, April, 1964.

48. Neal, L. S., and Bankoff, S. G., "A High Resolution Resistivity Probe for Determination of Local Void Properties in Gas-Liquid-Flow" A.I.Sh.E. J. 9, 49-54, (1963).

49. Sekoguchi, K., Fukui, H., Matsuoka T., and Nishikawa, K., "Investigation into the Statistical Characteristics of Bubbles in Two-Phase Flow," Trans. J.S.M.E., 40, 336, 2295-2310,(1974).

50. Galaup, J. P., "Contribution a l'etude des methodes de mesure en ecoulement diphasique." These de docteur-ingenieur, Universite Scientifique et Medicale de Grenoble, Institute National Polytechnique de Grenoble, (1975).

51. Uga, T., "Determination of Bubble Size Distribution in a BWR," Nucl. Engng Design, 22, 252-261, (1972).

52. Ibragimov, N., KH., Bobkov, V. P., and Tychinskii, N. A., "Investigation of the Behavior of the Gas Phase in a Turbulent Flow of a Water-Gas Mixture in Channels." Teplofiz. Vysok. Temp., 11, 1051-1061. Also High Temperature, 11, 935-944, Consultants Bureau, New York, (1973).

53. Jones, O. C., Statistical Considerations in Heterogeneous, Two-Phase Flowing Systems, Ph.D. Thesis, Rensselaer Polytechnic Institute, Troy, N.Y., (1973).

54. Serizawa, A., "Fluid-Dynamic Characteristics of Two-Phase Flow," Institute of Atomic Energy, Kyoto University, Ph.D. thesis, (1974).

55. Telles, A. S., and Dukler, A. E., "Statistical Characteristics of Thin, Vertical Wavy Liquid Films," I/EC Fundamentals, 9, 412-421, (1970).

56. Dukler, A. E., "Characterization, Effects, and Modeling of the Wavy Gas-Liquid Interface," Progress in Heat and Mass Transfer (Edited by Hetsroni, G., Sideman, S. & Hartnett, J. P.) Vol. 6, pp. 207-234. Pergamon, Oxford, (1972).

57. Chu, K. J., and Dukler, A. E., "Statistical Characteristics of Thin, Wavy Films," A.I.Ch.E. J., 20, 695-706, (1974).

58. Lecroart, H. and Lewi, J., "Mesures locales et leur interpretation statistique pour un ecoulement diphasique a grande vitesse et taux de vide," Societe Hydrotechnique de France, Douziemes journees de l'Hydraulique, Paris, 1972, Question IV, Rapport 7.

59. Lecroart, H. and Porte R., "Electrical Probes for Study of Two-Phase Flow at High Velocity," Presented at the Interna. Symposium on Two-Phase Systems, Haifa, Israel, (1972).

60. Wamsteker, A.J.J. et al., "The Application of the Impedance Method for Transient Void Fraction Measurement and Comparison with the X-ray Attenuation Technique," EURAEC-1109, June 1964.

61. Leung, J., The Occurrence of Critical Heat Flux During Blowdown with Flow Reversal, M.Sc. Thesis, Northwestern University, Evanston, Illinois, (1976).

62. Cimorelli, L., and Evangelisti, R., "The Application of the Capacitance Method for Void Fraction Measurement in Bulk Boiling Conditions," Int. J. Heat Mass Trans., 10, pp277, (1967).

63. Bencze, I. and Oerbeck, I., "Development and Application of an Instrument for Digital Measurement and Analysis of Void Using an AC Impedance Probe," KR-73, September 1964.

64. Oerbeck, I., "Impedance Void Meter," KR-32, November 1962.

65. Cimorelli, L., DiBartolomeo, and Premoli, A., "Void Fraction Measurement in a Boiling Channel Using the Impedance Method," RT-ING-(65) 7, Oct. 1965.

66. Cimorelli, L,. and Premoli, A., "Measurement of Void Fraction with Impedance Gage Technique," Energia Nucleare, 13, 1, 12, (1966).

67. Nielson, D. S., "Void Fraction Measurements in an Out-of-Pile High-Pressure Rig MK II-A by the Impedance Bridge Method," RISO-M-894, May 1969.

68. Hsu, Y. Y., Simon, F. F. and Grahm, R. W., "Application of Hot Wire Anemometry for Two-Phase Flow Measurement Such as Void Fraction and Slip Velocity," presented at the Two-Phase Flow Symposium at the Winter Annual ASME Meeting, Philadelphia, November 1963.

69. Jones, O. C. and Zuber, N., "Use of a Hot-Film Anemometer for Measurement of Two-Phase Void and Volume Flux Profiles in a Narrow Rectangular Channel," AIChE Sym. Ser., 74, 174, pp. 191-204, (1978).

70. Jones, O. C., "Preliminary Investigation of Hot Film Anemometer in Two-Phase Flow," TID-24104, November 1966.

71. Goldschmidt, V. and Eskmazi, S., "Two-Phase Turbulent Flow in a Plane Jet," ASME Paper No. 66-WA/APM-6, 1966.

72. Goldschmidt, V. and Householder, M. K., "The Hot Wire Anemometer as an Aerosol Droplet Size Sampler," Atmos. Environ., 3, 643, (1969).

73. Bragg, G. M. and Tevaarverk, J., "The Effect of a Liquid Droplet on a Hot Wire Anemometer Probe," Paper No. 2-2-19, presented at the First Symposium on Flow--Its Measurement and Control in Science and Industry, Pittsburgh, May 1971.

74. Delhaye, J. M., "Measurement of the Local Void Fraction Anemometer," CEA-R-3465(E), October 1968.

75. Delhaye, J. M., "Anemometer a Temperature Constante Etalonnage des Sondes a Film Chaude dans les Liquides," CENG Rapport TT No. 290, March 1968.

76. Delhaye, J. M., "Measure du Taux de Vide Local en Ecoulement Diphasique Eau-Air par un Anemometre a Film Chaud," CENG Rapport TT No. 79, October 1967.

77. Delhaye, J. M., "Theoretical and Experimental Results About Air and Water Bubble Boundary Layers," presented at the Novosibirsk Symposium, May 1968.

78. Delhaye, J. M., "Hot Film Anemometry in Two-Phase Flow," presented at the Symposium on Two-Phase Flow Instrumentation at the National Heat Transfer Conference, Minneapolis, August 1969.

79. Bergles, A.E., Roos, J.P., Bourne, J.G., "Investigation of Boiling Flow Regimes and Critical Heat Fluxes, Final Summary Report," Dynatech Corp. Report NYO-3304-13, 1968.

80. Abuaf, N., Swoboda, A. and Zimmer, G. A., "Reactor Safety Research Programs, Quarterly Progress Report," BNL-NUREG-50747, p. 175, 1977.

9. REFERENCES (Continued)

81. Abuaf, N., Feierabend, T.P., Zimmer, G.A., and Jones, O.C., "Radio Frequency (R-F) Prober for Bubble Size and Velocity Measurements," BNL-NUREG-50997, March 1979.

82. Abuaf, N., Feierabend, T.P., Zimmer, G.A., and Jones, O.C., "Radio Frequency (R-F) Prober for Bubble Size and Velocity Measurements," Rev. Sci. Inst., 50, 10, 1260-1263, Oct. 1979.

83. Fortescue, T., personal communication, 1978.

84. Marcus, B. D. and Dropkin, D., "Measured Temperature Profiles Within the Superheated Boundary Layer Above a Horizontal Surface in Saturated Nucleate Pool Boiling of Water," J. Heat Transfer, 87C, 333-341, (1965).

85. Bonnet, C. and Macke, E., "Fluctuations de temperature dans la paroi chauffante et dans le liquide au cours de l'ebullition nucleee," EUR 3162f, (1966).

86. Lippert, T. E. and Dougall, R. S., "A Study of the Temperature Profiles Measured in the Thermal Sublayer of Water, Freon-113, and Methyl Alcohol During Pool Boiling," J. Heat Transfer, 87C, 333-341, (1965).

87. Jacobs, J. and Shade, A. H., "Measurement of Temperatures Associated with Bubbles in Subcooled Pool Boiling," J. Heat Transfer, 91C, 123-128, (1969).

88. Van Stralen, S.J.D. and Sluyter, W. M., "Local Temperature Fluctuations in Saturated Pool Boiling of Pure Liquids and Binary Mixtures," Int. J. Heat Mass Transfer, 12, 187-198, (1969).

89. Stefanovic, N., Afgan, N., Pislar, V. and Jovanovic, L. J., "Experimental Investigation of the Superheated Boundary in Forced Convection Boiling," Heat Transfer, 5, Elsevier, Amsterdam, (1970).

90. Afgan, N., Jovanovic, L. J., Stefanovic, M. and Pislar, V., "An Approach to the Analysis of Temperature Fluctuation in Two-Phase Flow," Int. J. Heat Mass Transfer, 16, 187-194, (1973).

91. Afgan, N., Stefanovic, M., Jovanovic, L. J. and Pislar, V., "Determination of the Statistical Characteristics of Temperature Fluctuation in Pool Boiling," Int. J. Heat Mass Transfer, 16, 249-256, (1973).

92. Wiebe, J. R. and Judd, R. L., "Superheat Layer Thickness Measurements in Saturated and Subcooled Nucleate Boiling," J. Heat Transfer, 93C, 455-461, (1971).

93. Treschov, G. G., "Experimental Investigation of the Mechanism of Heat Transfer with Surface Boiling of Water," Teploenergetika, 3, 44-48, (1957).

94. Jiji, L. M. and Clark, J. A., "Bubble Boundary Layer and Temperature Profiles for Forced Convection Boiling in Channel Flow," J. Heat Transfer, 86C, 50-58, (1964).

95. Walmet, G. E. and Staub, F. W., "Electrical Probes for Study of Two-Phase Flows," Two-Phase Flow Instrumentation, edited by LeTourneau, B. W. and Bergles, A. E., pp. 84-101, ASME, (1969).

96. Barois, G., "Etude Experimentale de l'autovaporisation d'un Ecoulement Ascendant Adiabatique d'eau dans un Canal de Section Uniforme," These de Docteur-Ingenieur, Faculte des Sciences de l'Universite de Grenoble, (1969).

97. Van Paassen, C.A.A., "Thermal Droplet Size Measurements Using a Thermocouple," Int. J. Heat Mass Transfer, 17, 1527-1548, (1974).

98. Delhaye, J.M., Semeria, R., and Flamand, J.C., "Void Fraction, Vapor and Liquid Temperatures: Local Measurements in Two-Phase Flow Using a Microthermocouple," J. Heat Trans., 95C, pp365-370, (1973).

99. Delhaye, J.M., Semeria, R., and Flamand, J.C., "Mesure du Taux de Vide et des Temperatures du Liquid et de la Vapeur Ecoulement Diphasique Avec Changement de Phase a l;Aide d;un Microthermocouple," CEA-R4302, (1972).

100. Miller, N. and Mitchie, R. E., "Electrical Probes for Study of Two-Phase Flows," Two-Phase Flow Instrumentation (edited by LeTourneau, B. W. and Bergles, A. E.), pp. 82-88, ASME, (1969).

101. Miller, N. and Mitchie, R. E., "Measurement of Local Voidage in Liquid/Gas Two-Phase Flow Systems," J. Br. Nucl. Energy Soc., 9, 94-100, (1970).

102. Bell, R., Boyce, B. E. and Collier, J. G., "The Structure of a Submerged Impinging Gas Jet," J. Br. Nucl. Energy Soc., 11, 183-193, (1972).

103. Kennedy, T.D.A. and Collier, J. G., "The Structure of an Impinging Gas Jet Submerged in a Liquid," Multi-Phase Flow Systems, Inst. Chem. Engng. Symp. Ser. No. 38, II, Paper J4, (1974).

104. Hinata, S., "A Study on the Measurement of the Local Void Fraction by the Optical Fibre Glass Probe," Bull. J.S.M.E., 15, 1228-1235, (1972).

105. Danel, F. and Delhaye, J. M., "Sonde Optique pour Mesure du Taux de Presence Local en Ecoulement Diphasique," Mesures-Regulation-Automatisme, pp. 99-101, (1971).

106. Delhaye, J. M. and Galaup, J. P., "Measurement of Local Void Fraction in Freon-12 with a 0.1 mm Optical Fiber Probe," private communication (1975).

107. Abuaf, N., Jones, O.C., and Zimmer, G.A., "Response Characteristics of Optical Probes," ASME Preprint 78-WA/HT-3, August, 1978.

108. Abuaf, N., Jones, O. C., Jr. and Zimmer, G. A., "Optical Probe for Local Void Fraction and Interface Velocity Measurements," Rev. Sci. Instruments, 49, 8, 1090-1094, August, 1978.

109. Hsu, Y. Y., Ed., "Two Phase Flow Instrumentation Review Group Meeting," NUREG-0375 (1977).

110. White, D. A. and Tallmadge, J.A., "A Gravity Corrected Theory for Cylinder Withdrawal," AIChE J, 13, 4, pp. 745-750, 1967.

111. Tallmadge, J. A. and White, D. A., "Film Properties and Design Procedures in Cylinder Withdrawal," I&EC Process Design and Development, 7, 4, pp. 503-508, 1968.

112. White, D. A. and Tallmadge, J. A., "A Theory of Withdrawal of Cylinders from Liquid Baths," AIChE J, 12, 2, pp. 233-339, 1966.

113. Cravarolo, L. and Hassid, A., "Phase and Velocity Distribution in Two-Phase Adiabatic Dispersed Flow," CISE-R-98, August 1963.

114. Adorni, N., Alia, P., Cravarolo, L., Hassid, A. and Pedrocchi, E., "An Isokinetic Sampling Probe for Phase and Velocity Distribution Measurements in Two-Phase Flow Near the Wall of the Conduit," CISE-R-89, December 1963.

115. Truong Quang Minh and J. Huyghe, "Measurement and Correlation of Entrainment Fraction in Two-Phase, Two-Component, Annular Dispersed Flow," CENG Report No. TT-52, June 1965.

116. Moeck, E. O., "Measurement of Liquid Film Flow and Wall Shear Stress in Two-Phase Flow," Symposium on Two-Phase Flow Instrumentation, National Heat Transfer Conference, Minneapolis, August 1969.

117. Jannsen, E., "Two-Phase Flow and Heat Transfer in Multirod Geometries, Third Quarterly Progress Report April to July 1965," GEAP-4933, August 1965.

118. Hewitt, G. F., Kearsey, H. A., Lacy, P.M.C. and Pulling, D. J., "Burnout and Film Flow in the Evaporation of Water in Tubes," AERE-4864, March 1965.

119. Moeck, E. O., "Annular Dispersed Two-Phase Flow and Critical Heat Flux," AECL-3656, May 1970.

120. Hewitt, G. F. and Wallis, G. B., "Flooding and Associated Phenomena in Falling Film Flow in a Tube," AERE-R-4022, May 1963.

121. Hewitt, G. F., Kearsey, H. A., Lacy, P.M.C. and Pulling, D. J., "Burnout and Nucleation in Climbing Film Flow," AERE-R-4374, August 1963.

122. Hewitt, G. F., Lacy, P.M.C. and Nichols, B., "Transitions in Film Flow in a Vertical Tube," AERE-R-4614, April 1965.

123. Cousins, L. B., Denton, W. H. and Hewitt, G. F., "Liquid Mass Transfer in Annular Two-Phase Flow," AERE-R-4926, May 1965.

124. Butterworth, D., "Air-Water Climbing Film Flow in an Eccentric Annulus," AERE-R-5787, May 1968.

125. Singh, K., St. Pierre, C. C., Crago, W. A. and Moeck, E. O., "Liquid Film Flow Rates in Two-Phase Flow of Steam and Water at 1000 psia," AIChE J, 15, 1, 51, 1969.

126. Schraub, F. A., Simpson, R. L. and Jannsen, E., "Two-Phase Flow and Heat Transfer in Multirod Geometries: Air-Water Flow Structure Data for Round Tube, Concentric and Eccentric Annulus, and Nine-Rod Bundle," GEAP-5739, January 1969.

127. Staniforth, R., Stevens, G. F. and Wood, R. W., "An Experimental Investigation into the Relationship Between Burnout and Film Flow Rate in a Uniformly Heated Round Tube," AEEW-R-430, March 1965.

128. Adorni, N., Casagrande, I., Cravarolo, L., Hassid, A. and Silvestri, M., Experimental Data on Two-Phase Adiabatic Flow; Liquid Film Thickness, Phase and Velocity Distributions, Pressure Drops in Vertical Gas-Liquid Flow," CISE-R-35 (EUREAC-150), 1961.

129. Lahey, R. T., Jr., Shiralkar, B. S. and Radcliff, D. W., "Subchannel and Pressure Drop Measurements in a Nine-Rod Bundle for Diabatic and Adiabatic Conditions," GEP-13049, March 1970.

130. Schraub, F. A., "Isokinetic Sampling Probe Techniques Applied to Two-Component, Two-Phase Flow," ASME Paper No. 67-WA/FE-28, 1967. Also CEAP-5287, November 1966.

131. Todd, K. W. and Fallon, D. J., "Erosion Control in the Wet-Steam Turbine," Proc. I.M.E., 35, 180, 1965.

132. Jannsen, E., "Two-Phase Flow and Heat Transfer in Multirod Geometries: Second Quarterly Progress Report, January to April 1965," GEAP-4863, May 1965.

133. Wallis, G. B. and Steen, D. A., "Two-Phase Flow and Boiling Heat Transfer: Quarterly Progress Report for July to September 1963," NYO-10,488 October 1963.

134. Burick, R. J., Scheuerman, C. H. and Falk, A. Y., "Determination of Local Values of Gas and Liquid Mass Flux in Highly Loaded Two-Phase Flow," Paper No. 1-5-21 presented at the First Symposium on Flow--Its Measurements and Control in Science and Industry, Pittsburgh, May 1971.

135. Dussord, J. L. and Shapiro, A. H., "A Deceleration Probe for Measuring Stagnation Pressure and Velocity of a Particle-Laden Gas Stream," Jet Propulsion, p. 24, January 1958.

136. Ryley, D. J. and Kirkman, G. A., "The Concurrent Measurement of Momentum and Stagnation Enthalpy in a High Quality Wet Steam Flow," Paper No., 26, IME Thermodynamics and Fluid Mechanics Convention, Bristol, March 1968.

137. Schraub, F. A., "Isokinetic Probe and Other Two-Phase Sampling Devices: A Survey," presented at the Symposium on Two-Phase Flow Instrumentation, National Heat Transfer Conference, Minneapolis, 1969.

138. Shires, G. L. and Riley, P. J., "The Measurement of Radial Voidage Distribution in Two-Phase Flow by Isokinetic Sampling," AEEW-M-650, 1966.

139. Gill, L. E., Hewitt, G. F., Hitchon, J. W. and Lacy, P.M.C., "Sampling Probe Studies of the Gas Core in Annular Two-Phase Flow, Part 1; The Effect of Length on Phase and Velocity Distributions," Chem. Eng. Sci., 18, 525, 1963.

140. Preston, J. H., "Determination of Turbulent Skin Friction by Means of Pitot Tubes," J. Roy. Aero. Soc., 58, 109, 1954.

141. Patel, V. C., "Calibration of the Preston Tube and Limitations of its Use in Pressure Gradients," J. Fluid Mech., 23, 185, 1965.

142. King, C. W., "Measurement of Wall Shear Stress of a High Velocity Vapor Condensing in a Vertical Tube," PhD Thesis, University of Connecticut, 1970.

143. Jannsen, E., "Two-Phase Flow and Heat Transfer in Multirod Geometries; Eight Quarterly Progress Report, July to October 1966," GEAP-5300, November 1966.

144. Cravarolo, L., Giorgini, A., Hassid, A. and Pedrocchi, E., "A Device for the Measurement of Shear Stress on the Wall of a Conduit--Its Application in Mean Density Determination in Two-Phase Flow Shear Stress Data in Two-Phase Adiabatic Vertical Flow," CISE-R-82 (EURAEC-930), February 1964.

145. Rose, S. C., "Some Hydrodynamic Characteristics of Bubbly Mixtures Flowing Vertically Upwards in Tubes," ScD Thesis, MIT, September 1964.

146. Rose, S. C. and Griffith, P., "Flow Properties of Bubbly Mixtures," ASME Paper No. 65-HT-58, 1965.

147. Andeen, G. B. and Griffith, P., "The Momentum Flux in Two-Phase Flow," MIT-3496-1, October 1965.

148. Arnold, C. R. and Hewitt, G. F., "Further Developments in the Photography of Two-Phase Flow," AERE-R-5318, January 1967.

149. Cooper, K. D., Hewitt, G. F. and Pinchin, B., "Photography of Two-Phase Flow," AERE-R-4301, May 1963.

150. Hsu, Y. Y., Simoneau, F. J., Simon, F. F. and Grahm, R. W., "Photographic and Other Optical Techniques for Studying Two-Phase Flow," presented at the Symposium on Two-Phase Flow Instrumentation, National Heat Transfer Conference, Minneapolis, August 1969.

151. Lockart, R. W. and Martinelli, R. C., "Proposed Correlation of Data for Iso-Thermal Two-Phase, Two-Component Flow in Pipes," Chem. Eng. Progr. 44, 1944.

152. Hewitt, C. F., King, I. and Lovegrove, P. C., "Holdup and Pressure Drop Measurements in Two-Phase Annular Flow of Air-Water Mixtures," AERE-R-3764, June 1964.

153. Neal, L. G., "Local Parameters in Cocurrent Mercury-Nitrogen Flow," ANL-6625, January 1963.

154. Cravarolo, L. and Hassid, A., "Liquid Volume Fraction in Two-Phase, Adiabatic Systems," Energia Nucleare, 12, 11, 1965.

155. Petrick, M., "Two-Phase Air-Water Flow Phenomena," ANL-5787, March 1958.

156. Pike, R. W., Wilkinson, B., Jr., and Ward, H. C., "Measurement of the Void Fraction in Two-Phase Flow by X-ray Attenuation," AIChE J., 11, 5, 1965.

157. Jones, O.C., and Zuber, N., "The Interrelation Between Void Fraction Fluctuation and Flow Patterns in Two-Phase Flow," Int. J. Multiphase Flow, 2, 273-306, 1975.

158. Schrock, V. E. and Selph, F. B., "An X-ray Densitometer for Transient Steam Void Measurement," SAN-1005, March 1963.

159. Jones, O.C., "Determination of Transient Characteristics of an X-ray Void Measurement System for Use in Studies of Two-Phase Flow," KAPL-3859, February 1970.

160. Schroch, V. E., "Radiation Techniques in Two-Phase Flow Measurement," presented at the Symposium on Two-Phase Instrumentation, National Heat Transfer Conference, Minneapolis, August 1969.

161. Zuber, N., Staub, F. W., Bijwaard, G., and Kroeger, P. G., "Steady State and Transient Void Fraction in Two-Phase Flow Systems--Final Report for the Program on Two-Phase Flow Investigation," GEAP-5417, January 1967.

162. Hooker, H. H. and Popper, G. F., "A Gamma-Ray Attenuation Method for Void Fraction Determination in Experimental Boiling Heat Transfer Test Facilities," ANL-5766, November 1958.

163. Jones, O. C., "Procedural and Calculational Errors in Void Fraction Measurements by Particle or Photon Attenuation Techniques," KAPL-3361, October 1967.

164. Harms, A. A. and Forrest, C. F., "Dynamic Effects in Radiation Diagnosis of Fluctuating Voids," Nuc. Sci. Eng., 46, 408-413, 1971.

165. Harms, A. A. and Laratta, F.A.R., "The Dynamic-Bias in Radiation Interrogation of Two-Phase Flow," Int. J. Heat Mass Transfer, 16, 1459-1465, 1973.

166. Hancox, W. T., Forrest, C. F. and Harms, A. A., "Void Determination in Two-Phase Systems Employing Neutron Transmission," ASME Paper 72-HT-2, 1972.

167. Bestenbreur, T. P. and Spigt, C. L., "Study of Mixing Between Adjacent Channels in an Atmospheric Air-Water System," presented at the Two-Phase Flow Meeting at Winfrith, June 12-16, 1967. (See CONF-67065-6)

168. Martin, R., "Measurements of the Local Void Fraction at High Pressure in a Heating Channel," Nuc. Sci. Eng., 48, 125, 1972.

169. Spigt, C. L., Wamsteker, A.J.J. and von Vlaardingen, H. F., "Review of the Measuring, Recording and Analyzing Methods in Use in the Two-Phase Flow Programme of the Laboratory of Heat Transfer and Reactor Engineering at the Technological University of Eindhoven," Report WW016-R64 (EURATOM #III-17, Special TR#18), June 1964.

170. Smith, A. V., "A Fast Response Multi-Beam X-ray Absorpiton Technique for Identifying Phase Distributions During Steam-Water Blowdowns," J. Br. Nucl. Ener. Soc., 14, pp. 227-235, July 1975.

171. Yborrondo, Y. "Dynamic Analysis of Pressure Transducers and Two-Phase Flow Instrumentation," presented at the Third Water Reactor Safety Research Information Meeting, Washington, D.C., September 29-October 2, 1975.

172. Lassahn, G. D., Stephens, A. G., Taylor, J. D. and Wood, D. B., "X-Ray and Gamma-Ray Transmission Densitometry," presented at the International Colloquium on Two-Phase Flow Instrumentation, Idaho Falls, Idaho, June 11-14, 1979.

173. Abuaf, N., Zimmer, G. A., and Jones, O. C., private communication.

174. Zimmer, G. A., Wu, B.J.C., Leonhardt, W. J., Abuaf, N., and Jones, O. C., "Pressure and Void Distributions in a Converging-Diverging Nozzle with Non-Equilibrum Water Vapor Generation," BNL-NUREG-26003, April 1979.

175. Perkins, H. C., Jr., Yusuf, M., and Leppert, G., "A Void Measurement Technique for Local Boiling," Nuc. Sci. Eng., 11, 304, 1961.

176. Sha, W. T. and Bonilla, C. F., "Out-of-Pile Steam-Fraction Determination by Neutron-Beam Attenuation," Nuc. Appl., 1, 69, 1965.

177. Moss, R. A. and Kelly, A. J., "Neutron Radiographic Study of Limiting Planar Heat Pipe Performance," Int. J. of Heat and Mass Trans., 13, 3, 491, 1970.

178. Harms, A. A. and Forrest, C. F., "Dynamic Effects in Radiation Diagnosis of Fluctuating Voids," Nuc. Sci. Eng., 46, 408, 1971.

179. Harms, A. A., Lo, S., and Hancox, W. T., "Measurement of Time-Averaged Voids by Neutron Diagnosis," J. Appl. Phys., 42, 10, 4090 (1971).

180. Hancox, W. T., Forrest, C. F., and Harms, A. A., "Void Determination in Two-Phase Systems Employing Neutron Transmission," ASME Paper 72-HT-2, National Heat Transfer Conference, Denver, 1972.

181. Ornstein, H. L., "An Investigation of Turbulent Open Channel Flow Simulating Water Desalination Flash Evaporators," PhD Thesis, University of Connecticut, 1970.

182. Morrow, T. B. and Kline, S. J., "The Evaluation and Use of Hot-Wire and Hot-Film Anemometers in Liquids," Stanford University Report MD-25, 1971.

183. Hollasch, K. and Gebhart, B., "Calibration of Constant-Temperature Hot-Wire Anemometers at Low Velocities in Water With Variable Fluid Temperature," J. Heat Transfer, 94C, 17-22, 1972.

184. Hurt, J. C. and Welty, J. R., "The Use of a Hot-Film Anemometer to Measure Velocities Below 5 cm/sec in Mercury," J. Heat Transfer, 95C, 548-549, 1973.

185. Rosler, R. S. and Bankoff, S. G., "Large-Scale Turbulence Characteristics of a Submerged Water Jet," AIChE J, 9, 672-676, 1963.

186. Bouvard, M. and Dumas, H., "Application de la Methode du Fil Chaud a la Mesure de la Turbulence dans l'Eau," Houille Blanche, 3, 257-270, 1967.

187. Resch, F., "Etudes sur le Fil Chaud et le Film Chaud dans l'Eau," Houille Blanche, 2, 151-161, 1969.

188. Resch, F., "Etudes sur le Fil Chaud et le Film Chaud dans l'Eau," CEA-R3510, 1968.

189. Goldschmidt, V. W. and Eskinazi, S., "Diffusion de Particules Liquides dans le Champ Retardataire d'un Jet d'air Plan et Turbulent," Les Instabilites en Hydraulique et en Mecanique des Fluides, pp. 291-298. Societe Hydrotechnique de France, 8 emes journees de l'Hydraulique, Lille, France, 1964.

190. Goldschmidt, V. W. and Eskinazi, S., "Two-Phase Turbulent Flow in a Plane Jet," J. Appl. Mech., 33, 735-747, 1966.

191. Lackme, C., "Structure et Cinematique des Ecoulementes Diphasiques a Bulles," CEA-R3202, 1967.

192. Ginsberg, T., "Droplet Transport in Turbulent Pipe Flow," ANL-7694, 1971.

193. Goldschmidt, V. W., "Measurement of Aerosol Concentrations With A Hot-Wire Anemometer," J. Colloid Sci., 20, 617-634, 1965.

194. Goldschmidt, V. W. and Householder, M. K., "The Hot-Wire Anemometer as an Aerosol Droplet Size Sampler," Atmospheric Environment, 3, pp. 643-651, 1969.

195. Chuang, S. C. and Goldschmidt, V. W., "The Response of a Hot-Wire Anemometer to a Bubble of Air in Water," Turbulence Measurements in Liquids (edited by Patterson, G. K. and Zakin, J. L.), Univ. of Missouri, Rolla, Continuing Education Series, 1969.

196. Goldschmidt, V. W., Householder, M. K., Ahmadi, G., and Chuang, S. C., "Turbulent Diffusion of Small Particles Suspended in Turbulent Jets," Progress in Heat and Mass Transfer (edited by Hetsroni, G., Sideman, S., and Hartnett, J. P.), 6, pp. 487-508, Pergamon, Oxford, 1972.

197. Resch, F. J. and Leutheusser, J. H., "Le Ressaut Hydraulique; Mesures de Turbulence dans la Region Diphasique," Houille Blanche, 4, 279-293, 1972.

198. Resch, F. J., Leutheusser, H. J., and Alemu, S., "Bubbly Two-Phase Flow in Hydraulic Jump," J. Hydraul. Div. Am. Soc. Civ. Engrs., 100, No. HY1, Proc. Paper 10297, 137-149, 1974.

199. Ishigai, S., Nakanisi, S., Koizumi, T., and Oyabu, Z., "Hydrodynamics and Heat Transfer of Vertical Falling Liquid Films (Part I: Classification of Flow Regimes)," Bull. J.S.M.E., 15, 594-602, 1972.

200. Katarzhis, A. K., Kosterin, S. I., and Sheinin, B. I., "An Electric Method of Recording the Stratification of the Steam-Water Mixture," Izv. Akad. Nauk SSSR, 2, 132-136, A.E.R.E. Lib./Trans. 590, 1955.

201. Shiralkar, B. S., "Local Void Fraction Measurements in Freon-114 With a Hot-Wire Anemometer," NEDO-13158, General Electric Co., 1970.

202. Dix, G. E., "Vapor Void Fractions for Forced Convection With Subcooled Boiling at Low Flow Rates," PhD Thesis, University of California at Berkeley, 1971. Also General Electric Co., NEDO-10491, November 1971.

203. Shiralkar, B. S. and Lahey, R. T., Jr., "Diabatic Local Void Fraction Measurements in Freon-114 With a Hot-Wire Anemometer," ANS Trans., 15, No. 2, p. 880, 1972.

204. Hetsroni, G., Cuttler, J. M., and Sokolov, M., "Measurements of Velocity and Droplets Concentration in Two-Phase Flows," J. Appl. Mech., 36E, 334-335, 1969.

205. Subbotin, V. I., Sorokin, D. N., and Tsiganok, A. A., "Some Problems on Pool Boiling Heat Transfer," Heat Transfer, Vol 5, Elsevier, Amsterdam, 1970.

9. REFERENCES (Continued)

206. Petrick, M., and Swanson, B.S., "Radiation Attenuation Methods for Measuring Density in a Two-Phase Fluid," Rev. Sci. Inst., 29, 1079-1085, 1958.